Tending towards Non-fouling: A study of the interaction between proteins and surfaces prepared by radio frequency glow-discharge plasma

Marvin Mecwan

A dissertation

submitted in partial fulfillment of the

requirements for the degree of

Doctor of Philosophy

University of Washington

2019

Reading Committee:

Buddy Ratner, Chair

David Castner

Shaoyi Jiang

Program Authorized to Offer Degree:

Bioengineering

University of Washington

Abstract

Tending towards Non-fouling: A study of the interaction between proteins and surfaces prepared by radio frequency glow-discharge plasma

Marvin Magan Mecwan

Chair of the Supervisory Committee:
Professor Buddy Ratner
Departments of Bioengineering and Chemical Engineering

All proteins adsorb irreversibly onto surfaces and often results in denaturation, aggregation and loss of activity. This has serious implications not only for medical devices that are used clinically for the treatment of disease but also for the pharmaceutical industry that deals with handling, storage and delivery of protein-based drugs.

In this work, we explore radio frequency (RF) glow-discharge plasma technology as a method of creating non-fouling surfaces. We achieve this through two distinct strategies: a) prepare a highly-reactive surface initiators that could be used to grow HEMA polymer brushes via SI-ARGET ATRP, and b) create novel quasi-zwitterionic or mixed-charged surfaces that closely resemble the chemistry of zwitterionic polymers and therefore are capable of reducing protein adsorption.

In addition to preparing non-fouling surfaces to prevent protein adsorption, it is also equally important to properly evaluate the surface-protein interaction. This work explores and describes new protocols involving radiolabeling protein studies, radioimmunoassay and substrate-based direct ELISA to better understand the adsorption, retention and changes in biological activity of the protein once it comes in contact with a biomaterial surface, which further informs the biocompatibility of the surface.

Finally, we take the lessons learned from using RF glow-discharge plasma to create non-fouling surfaces and developing new protocols to study surface-protein interaction, and apply it to a real world application where we coat hypodermic syringes with a copolymer of HMDSO and MA to prevent protein adsorption while maintaining syringe lubricity. Overall, this research showcases the ability of RF glow-discharge plasma technology to create a variety of non-fouling surfaces that prevents protein adsorption and can be easily clinically translated for a variety of medical applications.

TABLE OF CONTENTS

List of Figures ……vi

List of Tables ……...x

Chapter 1. Highly-reactive haloester surface initiators for ARGET ATRP readily prepared by radio frequency glow-discharge plasma ……..……...1

1.1. Abstract ……..1

1.2. Introduction ……2

1.3. Experiment …..……..5

1.3.1. Plasma deposition and characterization of haloesters: M3BP, M2CP and E2FP ...5

1.3.1.1. Materials …….....5

1.3.1.2. Plasma polymerization of haloesters ……..5

1.3.1.3. Surface characterization ……..6

1.3.2. SI-ARGET ATRP reaction of HEMA using plasma deposited M3BP, M2CP, and E2FP as the surface initiator ……...8

1.3.2.1. Materials …….....8

1.3.2.2. Synthesis of HEMA polymer brushes ……....8

1.3.2.3. Surface characterization ……..8

1.4. Results and Discussion ……..9

1.5. Conclusions ……..23

1.6. Acknowledgements ……..24

1.7. Supplemental Section …….....25

Chapter 2. Quasi-zwitterionic surface coatings prepared by radio frequency glow-discharge plasma reduce protein adsorption ……..……...……...…30

2.1. Abstract ……30

2.2. Introduction ……..31

2.3. Experiment …….....33

2.3.1 Plasma deposition, surface characterization and protein studies on quasi-zwitterionic surface coatings ……...33

2.3.1.1 Materials ……...33

2.3.1.2 Plasma polymerization ……..33

2.3.1.3 Surface characterization ……35

2.3.1.4 I-125 radiolabeled protein studies ……36

2.3.1.5 Cytotoxicity studies ……..37

2.3.2 Plasma deposition and protein studies on a mini-library of quasi-zwitterionic surface coatings ……...…38

2.3.2.1 Materials …….....38

2.3.2.2 Plasma polymerization ……..38

2.3.2.3 Protein iodination using ICl method ……40

2.3.2.4 I-125 radiolabeled HSA protein adsorption on MA-DMAA family of quasi-zwitterionic coatings ……...40

2.3.2.5 I-125 radiolabeled HSA protein adsorption (competitive binding with Fg) on MA-2VP family of quasi-zwitterionic coatings ……...41

2.3.2.6 Substrate-based direct ELISA on AA-AAmine family of quasi-zwitterionic coatings ……41

2.4. Results and Discussion ……42

2.5. Conclusions ……58

2.6. Acknowledgements ……59

Chapter 3. Radio frequency glow-discharge polyether and fluoropolyether plasma coatings for the prevention of IgG protein adsorption ……60

3.1. Abstract ……60

3.2. Introduction ……61

3.3. Experiment ……63

3.3.1. Plasma deposition and characterization of biomaterial surfaces ……63

3.3.1.1. Materials ……63

3.3.1.2. Plasma polymerization of TG, AA, C3F6 and C3F6O ……63

3.3.1.3. Surface characterization ……65

3.3.2. I-125 radiolabeled protein studies and radioimmunoassay ……66

3.3.2.1. Materials ……66

3.3.2.2. Protein iodination using ICl method ……66

3.3.2.3. I-125 radiolabeled bovine IgG protein adsorption and retention ……67

3.3.2.4. Radioimmunoassay using goat anti-bovine IgG (unconjugated) ……67

3.3.3. Substrate-based direct ELISA ……68

3.3.3.1. Materials ……68

3.3.3.2. Substrate-based direct ELISA using goat anti-bovine IgG (HRP conjugate) ……...69

3.4. Results and Discussion ……...……70

3.5. Conclusions ……...…...80

3.6. Acknowledgements ……...……...80

Chapter 4. Highly-reactive haloester surface initiators for ARGET ATRP readily prepared by radio frequency glow-discharge plasma ……..…….……....82

4.1. Abstract ……82

4.2. Introduction ……....83

4.3. Experiment …….....85

4.3.1. Plasma deposition and characterization of MA, HMDSO, HMDSO-MA and TG surface coatings ……...….85

4.3.1.1. Materials ……...85

4.3.1.2. Plasma polymerization ……..85

4.3.1.3. Surface characterization ……....88

4.3.1.4. Water contact angle ……...89

4.3.2. I-125 radiolabeled protein studies ……89

4.3.2.1. Materials ……...89

4.3.2.2. Protein iodination using ICl method ……90

4.3.2.3. I-125 radiolabeled bovine IG protein adsorption and retention ……90

4.3.3. Syringe glide force testing ……91

4.3.3.1. Plasma polymerization …….....91

4.3.3.2. Glide force measurements using INSTRON ……91

4.4. Results and Discussion ……93

4.5. Conclusions ……102

4.6. Acknowledgements ……103

5. Bibliography ……104

6. Appendix ……...111

LIST OF FIGURES

Figure 1.1. Schematic representation of the process to grow PHEMA polymer brushes via SI-ARGET ATRP from plasma polymerized haloester surfaces. We first create a surface rich in either Br, Cl or F by plasma depositing haloesters onto glass coverslips. This is followed by placing the plasma polymerized haloester coverslips into an ARGET ATRP solution in excess of HEMA to grow PHEMA brushes …….....4

Figure 1.2. Representative XPS survey scans and corresponding monomer chemical structures (inset) of plasma polymerized (A) M3BP (B) M2CP (C) E2FP and (D) CEMA on glass coverslips. Major elemental peaks are labeled in each survey scan ……10

Figure 1.3. Representative high-resolution spectra of the C1s peak (black envelope) and corresponding monomer chemical structure (inset) of plasma polymerized (A) M3BP (B) M2CP (C) E2FP and (D) CEMA on glass coverslips. Fitted peaks are labeled to correspond to different bonding environments within each chemical structure ……..11

Figure 1.4. HEMA polymer brush coating thickness grown via SI-ARGET ATRP on plasma polymerized M3BP, M2CP, E2FP and CEMA surface coatings. All samples were dry during thickness measurements (n = 4) ……14

Figure 1.5. Representative ToF-SIMS spectra of HEMA polymer brushes grown on plasma polymerized (C) M3BP (D) M2CP (E) E2FP and (F) CEMA surfaces via SI-ARGET ATRP. A glass disc without surface initiator is used as a negative control (A), while a PHEMA hydrogel was used as positive control (B). Positive polarity spectra were acquired in high mass resolution mode with Bi^{3+} primary ion species over a 0-200m/z mass range for HEMA. Major peaks associated with HEMA are highlighted in each spectrum, the molecular formula and normalized intensities are displayed in Supplemental Table S1.2 ……21

Figure S1.1. ToF-SIMS relative intensity of Br_x species. ToF-SIMS relative peak intensities (normalized to total counts) of A) Br B) Br_2 C) Br_3 and D) Br_4. It should be noted that when detected, the intensity of the Br_4 peak was very low. Data from 2 replicates of each sample type are shown (except for the control which only contains 1 sample). The bar height represents the average relative intensity and the error bars show the standard deviation (n=4, except for the control n=5). The samples are ordered from left to right, plasma polymerized M3BP, drop-coated M3BP control, plasma polymerized M3BP after methanol soak, and extract (methanol wash solution from plasma polymerized M3BP samples). The Br_4 signal from the control is an artifact of the background noise in that region and is not from Br_4 ……25

Figure S1.2. Lack of HEMA peaks on plasma polymerized haloester coatings in the absence of copper (II) bromide. Representative ToF-SIMS spectra of HEMA polymer brushes grown on plasma polymerized (C) M3BP (D) M2CP (E) E2FP and (F) CEMA surfaces via surface initiated ARGET ATRP in the absence of $CuBr_2$ for 2 h. No major peaks from pHEMA can be seen in these treatment groups indicating that no pHEMA chain growth has occurred. Since $CuBr_2$ is crucial as

a catalyst for the ARGET ATRP reaction these results suggest that we are growing HEMA polymer brushes via SI ARGET ATRP reaction. A pHEMA hydrogel was used as positive control (A) while a glass disc without surface initiator is used as a negative control (B). Peak intensities are normalized to the total intensity of the spectra. Major positive secondary ions are labelled. Spectra were taken in triplicate from 3 sample regions over a 500 x 500 micron analysis area, maintain the primary ion dose density below $2x10^{12}$ ions/cm^2 with Bi_3^+ species ……..28

Figure S1.3. Lack of HEMA peaks on plasma polymerized fluoro coatings in the presence as well as in the absence of CuBr$_2$. Representative ToF-SIMS spectra of HEMA polymer brushes grown on plasma polymerized C3F6 surfaces via surface initiated ARGET ATRP in the (A) presence and (B) absence of $CuBr_2$ for 2 h. No major peaks from pHEMA can be seen in these treatment groups indicating that no pHEMA chain growth has occurred. The results from this suggest that plasma polymerized E2FP coatings is unique in its ability to grow HEMA polymers brushes compared to other plasma polymerized fluoro surfaces. A pHEMA hydrogel was used as positive control (A). Peak intensities are normalized to the total intensity of the spectra. Major positive secondary ions are labelled. Spectra were taken in triplicate from 3 sample regions over a 500 x 500 micron analysis area, maintain the primary ion dose density below $2x10^{12}$ ions/cm^2 with Bi_3^+ species ……29

Figure 2.1. Custom-built plasma reactor setup with two inlets which allows for the controlled flow of two monomers into the plasma chamber using vernier caliper valves ……..35

Figure 2.2. Representative XPS survey scans and corresponding monomer chemical structures (inset) of plasma polymerized (A) AA (B) AAmine (C) DMAA (D) AA:AAmine 1:1 (E) AA:AAmine 1:2 (F) AA:AAmine 2:1 and (G) AA:DMAA 1:1 on glass coverslips. Major elemental peaks are labeled in each survey scan ……44

Figure 2.3. Representative high-resolution spectra of the C1s peak (black envelope) and corresponding monomer chemical structure (inset) of plasma polymerized (A) AA (B) AAmine (C) DMAA (D) AA:AAmine 1:1 (E) AA:AAmine 1:2 (F) AA:AAmine 2:1 and (G) AA:DMAA 1:1 on glass coverslips. Fitted peaks are labeled to correspond to different bonding environments within each chemical structure ……..46

Figure 2.4. Amount of bovine IgG adsorbed onto plasma polymerized quasi-zwitterionic surface coatings AAc:AAmine 2:1, AAc:AAm 1:2, DMAA, AA:DMAA 1:1 and glass controls after 2 h in a 0.1 mg/mL bovine IgG as determined by I-125 radiolabeling method ……48

Figure 2.5. MTT Cell Viability assay at 24 h (A) and LIVE/DEAD cell staining at 48 h of (B) TCPS control (C) Latex control, and plasma polymerized (D) AA (E) AAmine (F) AA:AAmine 1:1 ……..49

Figure 2.6. Amount of HSA adsorbed to plasma polymerized MA, DMAA, MA:DMAA 1:1, MA:DMAA 1:2, MA:DMAA 2:1, MA:DMAA 1:3, MA:DMAA 3:1 and glass control after 2 h in a 0.3 mg/mL HSA solution in CPBSzI as determined by I-125 radiolabeling method ……51

Figure 2.7. Amount of HSA competitively adsorbed to plasma polymerized MA, 2VP, MA:2VP 1:1, MA:2VP 1:1.5 and MA:2VP 1.5:1 after 2 h in a binary solution of HSA: 0.3 mg/mL and Fg: 0.03 mg/mL in cPBSzI as determined by I-125 radiolabeling method …….52

Figure 2.8. Amount of active IgG adsorbed to plasma polymerized AA, AAmine, AA:AAmine 1:1, AA:AAmine 1:2 and AA:AAmine 2:1 after 2 h in a 0.1 mg/mL bovine IgG solution in cPBS as determined by substrate-based ELISA ……..53

Figure 2.9. Amount of HSA adsorbed to plasma polymerized MA, DMAA, MA:DMAA 1:1, MA:DMAA 1:2, MA:DMAA 2:1, MA:DMAA 1:3, MA:DMAA 3:1 and glass control after 2 h in a 0.3 mg/mL HSA solution in CPBSzI as determined by I-125 radiolabeling method, sorted and plotted against the "ratio of charge" ……...56

Figure 2.10. Amount of HSA competitively adsorbed to plasma polymerized MA, 2VP, MA:2VP 1:1, MA:2VP 1:1.5 and MA:2VP 1.5:1 after 2 h in a binary solution of HSA: 0.3 mg/mL and Fg: 0.03 mg/mL in cPBSzI as determined by I-125 radiolabeling method, sorted and plotted against the "ratio of charge" ……...57

Figure 2.11. Amount of active IgG adsorbed to plasma polymerized AA, AAmine, AA:AAmine 1:1, AA:AAmine 1:2 and AA:AAmine 2:1 after 2 h in a 0.1 mg/mL bovine IgG solution in cPBS as determined by substrate-based ELISA, sorted and plotted against the "ratio of charge" ……58

Figure 3.1. Custom-built plasma reactor setup for the plasma polymerization of monomers ….64

Figure 3.2. Representative XPS survey scans and corresponding monomer chemical structures (inset) of plasma polymerized (A) AA (B) TG (C) C3F6 and (D) C3F6O. Major elemental peaks are labeled in each survey scan ……..72

Figure 3.3. Representative high-resolution spectra of the C1s peak and corresponding monomer chemical structure (inset) of plasma polymerized (A) AA (B) TG (C) C3F6 and (D) C3F6O. Fitted peaks are labeled to correspond to different bonding environments within each chemical structure ……73

Figure 3.4. Amount of IgG adsorbed to plasma polymerized AA, TG, C3F6 and C3F6O on glass coverslips and SS substrate after 2 h in a 0.1 mg/mL bovine IgG solution as determine I-125 radiolabeling method …….75

Figure 3.5. Amount of IgG retained on plasma polymerized AA, TG, C3F6 and C3F6O on glass coverslips and SS substrate after overnight elution with 2% SDS as determined by I-125 radiolabeling method …….76

Figure 3.6. The ratio of tagged goat anti-bovine IgG to tagged bovine IgG adsorbed to the surface of plasma polymerized TG, AA, C3F6 and C3F6O on glass coverslips and SS substrates as determined by radioimmunoassay …….77

Figure 3.7. The ratio of absorbance read at 450 nm using substrate-based direct ELISA to the amount of tagged bovine IgG adsorbed determined by radioimmunoassay to the surface of plasma polymerized TG, AA, C3F6 and C3F6O on glass coverslips and SS substrates ……78

Figure 3.8. The percentage reduction in bovine IgG protein activity after a residence time of 7 d on the surface of plasma polymerized TG, AA, C3F6 and C3F6O on glass coverslips and SS substrates as determined by substrate-based direct ELISA ……79

Figure 4.1. Custom-built plasma reactor setup with two inlets which allows for the controlled flow of two monomers into the plasma chamber using vernier caliper valves ……..86

Figure 4.2. Custom-built syringe testing fixture for use with the INSTRON to measure the syringe glide force ..……92

Figure 4.3. Representative XPS survey scans and high-resolution spectra of the C1s peak (black envelope) and corresponding monomer chemical structure (inset) of plasma polymerized (A) and (B) MA; (C) and (D) HMDSO; and (E) and (F) HMDSO-MA on glass coverslips. Fitted peaks are colored to correspond to carbons in different chemical environments ……..95

Figure 4.4. Amount of bovine IgG adsorbed onto plasma polymerized MA, HMDSO, HMDSO-MA, TG and dip-coated PDMS samples after 2 h in a 0.1 mg/mL bovine IgG solution in different pH conditions (acidic, neutral and basic) as determined by I-125 radiolabeling method ……..97

Figure 4.5. Amount of bovine IgG retained on plasma polymerized MA, HMDSO, HMDSO-MA, TG and dip-coated PDMS samples in different pH conditions (acidic, neutral and basic) after overnight elution with 2% SDS as determined by I-125 radiolabeling method ……...98

Figure 4.6. Amount of bovine IgG adsorbed onto plasma polymerized MA, HMDSO, HMDSO-MA, TG and dip-coated PDMS samples after 2 h in a 0.1 mg/mL bovine IgG solution in different pH conditions (acidic, neutral and basic) in the presence of PS80 as determined by I-125 radiolabeling method ……...…100

Figure 4.7. Amount of bovine IgG retained onto plasma polymerized MA, HMDSO, HMDSO-MA, TG and dip-coated PDMS samples in different pH conditions (acidic, neutral and basic) in the presence of PS80 after overnight elution with 2% SDS as determined by I-125 radiolabeling method . ……..……..101

Figure 4.8. Syringe peak glide force measurements of plasma polymerized MA, HMDSO, HMDSO-MA, TG and untreated control syringes at room temperature in both dry and wet conditions ……...102

LIST OF TABLES

Table 1.1. Summary of surface elemental composition of plasma polymerized M3BP, M2CP, E2FP and CEMA surface coatings as determined by survey scans obtained from XPS (n = 3) …16

Table 1.2. Surface elemental compositions by XPS (n = 3) of plasma polymerized M3BP, M2CP, E2FP and CEMA surface coatings after being in ARGET ATRP solution for 5, 15, 30, 60 and 120 min ……17

Table S1.1. Location of highest relative intensity C_xH_y peaks. Major positive secondary ion peaks on the surface of plasma polymerized M3BP and drop-coated M3BP. 'x' denotes which sample showed the highest relative intensity for the given peak. If 'x' is in both columns then the relative intensity was about equal for both samples (n = 18 spectra for plasma polymerized sample, n = 5 for drop coated control) ……26

Table S1.2. Major positive secondary ion peaks for PHEMA control and HEMA polymer brushes grown on plasma polymerized M3BP, M2CP, E2FP and CEMA surface coatings via SI-ARGET ATRP. Major peaks from PHEMA standard spectra that appear on ARGET ATRP surfaces are outlined in red ……27

Table 2.1. Mini-library of quasi-zwitterionic surface coating compositions prepared by varying the ratio of vapor pressures of the monomers introduced into the plasma reactor ……39

Table 2.2. Summary of surface elemental composition of plasma polymerized quasi-zwitterionic surface coatings as determined by survey scans obtained from XPS ……45

Table 2.3. Summary of chemical bonding environments of plasma polymerized quasi-zwitterionic surface coatings as determined by high-resolution C1s scans obtained from XPS. The ratio of bulk COO peak at ~289 eV to the bulk CN/CO peak at ~287 eV was used as a gross indication of surface charge. As the ratio increased the amount of negative charge on the surface also increased relative to the positive charge ……55

Table 3.1. Summary of the plasma treatment parameters used for the plasma deposition of AA, TG, C3F6 and C3F6O onto substrates ……..65

Table 3.2. Summary of surface elemental composition of plasma polymerized AA, TG, C3F6 and C3F6O surface coatings as determined by survey scans obtained from XPS ……71

Table 4.1. Summary of surface elemental composition of plasma polymerized MA, HMDSO, HMDSO-MA and TG surface coatings as determined by survey and hi-res scans obtained from XPS (n = 3) ……96

ACKNOWLEDGEMENTS

I would like to take this opportunity to gratefully acknowledge the many people who have been instrumental in my journey through graduate school and towards the completion of my dissertation. Special thanks to my advisor, Prof. Buddy D. Ratner, for his support and guidance during my graduate education. He gave me the independence to critically think outside the box when presented with a problem and allowed me to become involved with a diverse group of research projects in the lab. Through this exposure, I was able to learn more about myself and become confident in my abilities as a researcher. I would also like to thank my dissertation committee members, Prof. David Castner, Prof. Shaoyi Jiang and Prof. Thomas Horbett for their invaluable feedback and advice as I was laying out the groundwork for my dissertation. Additionally, I would like to sincerely thank Prof. Adam Warren who served as my Graduate School Representative (GSR). I appreciate his availability on such short notice and dedication to fulfilling the role of GSR with rigor, as well as being a good friend over the past several years.

My deep gratitude also goes to the many people in various labs who have contributed their time, effort, scientific feedback, and have put up with me during my graduate work. Most important of them all is Winston Ciridon. I wholeheartedly admire his extraordinary commitment to training me to understand and use the plasma reactor, and to help me troubleshoot the system anytime it gave up on me. He has been absolutely crucial to my graduate work experience in the lab and I could not imagine completing my dissertation without him. I would also like to thank our two lab managers over the years, Colleen Irvin and Sharon Creason, for their efforts in supporting me and my research, and making sure that the lab ran smoothly. For some odd reason

I constantly butted heads with both of them (mainly due to differences in work ethics), but we always managed to work out our differences in the end. My honest gratitude also goes out to a number of current and past Ratner lab members: Dr. Alex Chen, Dr. Anna Galperin, Dr. Jeanette Stein, Dr. Alaina Floyd, Le Zhen, Dr. Razieh Khalifehzadeh, Julia King, Prabhleen Kaur and many more. Their positive criticism, technical assistance and helpful discussions pertaining to science and otherwise, in and out of lab, holds immense value to me and really made me feel part of a strong and supportive work family. I also wish to acknowledge my close peers in the bioengineering program Dr. Anna Blakney, Amanda Sudduth and Mallory Monahan for never failing to be their true self and constantly inspiring me.

I would like to express my sincere appreciation to my many friends that I've made since moving to Seattle for their love and support through all of my graduate tribulations and triumphs. Going into graduate school I knew I wanted a good work-life balance, and my friends really helped me achieve that; they uplifted me when I was down and celebrated my achievements with me, and kept me sane throughout the process.

Finally, I would like to thank my family. Their encouragement, sacrifices, devotion and patience is the reason I have been able to pursue the education that I desired. Thank you for everything.

DEDICATION

To my family, chosen and biological, for all their love and support.

And to my most handsome canine partner, Darth “Genghis” Jones.

Chapter 1

HIGHLY-REACTIVE HALOESTER SURFACE INITIATORS FOR ARGET ATRP READILY PREPARED BY RADIO FREQUENCY GLOW DISCHARGE PLASMA.

Marvin M. Mecwan,[1] Michael J. Taylor,[1, 3] Daniel J. Graham,[1, 3] and Buddy D. Ratner[1, 2]

1 Department of Bioengineering, University of Washington, Seattle, WA 98195

2 Department of Chemical Engineering, University of Washington, Seattle, WA 98195

3 NESAC/BIO, University of Washington, Seattle, WA 98195

1.1 ABSTRACT

New surface initiators for ARGET ATRP (activators regenerated by electron transfer atomic transfer radical polymerization) have been prepared by the plasma deposition of haloester monomers. Specifically, methyl 3-bromopropionate (M3BP), methyl 2-chloropropionate (M2CP), and ethyl 2-fluoropropionate (E2FP) were plasma deposited onto glass discs using RF glow discharge plasma. This technique creates surface coatings that are resistant to delamination and rich in halogen species making them good candidates for surface initiators for ARGET ATRP. Of all the plasma polymerized surface coatings, M3BP showed the highest halogen content and was able to grow 2-hydroxyethyl methacrylate (HEMA) polymer brushes on its surface via ARGET ATRP in as little as 15 min as confirmed by XPS (X-ray photoelectron spectroscopy). Surprisingly, E2FP, a fluoroester, was also able to grow HEMA polymer brushes despite fluorine being a poor leaving group for ARGET ATRP. The versatility of RF glow discharge plasma offers a clear advantage over other techniques previously used to immobilize ARGET ATRP surface initiators.

1.2 INTRODUCTION

The ability to modify surfaces with thin polymeric films allows one to tailor properties such as wettability,[1] biocompatibility,[2] biocidal activity,[3] adhesion,[4] and adsorption[5]. Surface initiated atom transfer radical polymerization (SI ATRP) is one such technique that has become a powerful tool for the preparation of functional surfaces and interfaces to match the desired needs of a specific biomedical application.[6] Using this technique researchers have been able to graft various polymers, such as polystyrene,[7] poly(methyl methacrylate) (PMMA),[8] poly(oligoethyleneglycol methacrylate),[9] poly(hydroxyethyl methacrylate) (PHEMA),[10] poly(N-isopropyl acrylamide),[11] poly(carboxybetaine methacrylate),[12,13] poly(sulfoxybetaine methacrylate),[12,14] and many other polymers onto various surfaces.[15]

One major drawback of ATRP is that it requires inert atmospheric conditions as a small amount of oxygen causes Cu(I) to oxidize to Cu(II) which results in a significant reduction in polymerization rate.[16] In order to overcome this, activators regenerated by electron transfer atomic transfer radical polymerization (ARGET ATRP) use a reservoir of reducing agent such as ascorbic acid[17] in the reaction mixture which reduces Cu(II) to Cu(I) in situ. The benefits of ARGET ATRP over conventional ATRP makes it a particularly attractive system for surface initiated polymerization of polymer brushes, such as PMMA[18] and PHEMA[19] on a variety of substrates.

The composition and density of surface initiator are important parameters that determine the grafting density and thickness of the grafted polymer.[20] In order to graft a polymer from a surface via SI ATRP or SI ARGET ATRP, a halogen is required to initiate the reaction. Bromoester based initiators such as bromoisobutyryl bromide (BIBB) have often been used to

modify the surface to act as initiators for the SI ATRP reaction.[7,12,21,22] Some researchers have also used alpha methyl bromopropionate (MBP) as an effective initiator to graft polymer chains.[23,24]

RF glow discharge plasma polymerization has historically been used to create uniform thin polymer films that are strongly bound to surfaces.[25–27] The Badyal group have used pulsed plasma polymerization of 4-vinylbenzyl chloride[28,29] and 2-bromoethyl acrylate[28] to prepare initiator nanofilms for use in ATRP. Several other research groups have immobilized ATRP initiators by plasma polymerizing bromoesters such as allyl-2-bromo-2-methylpropionate[30] and ethyl α-bromoisobutyrate[31,32] onto substrates. Additionally, our lab has previously plasma polymerized 2-chloroethyl methacrylate (CEMA) as a surface initiator in order to synthesize and pattern surfaces with poly[(oligoethylene glycol) methyl methacrylate] (POEGMA) polymer brushes grown by SI ATRP[33].

In this paper we explore ARGET ATRP surface initiators that were prepared using a robust one step, solvent-free synthesis method using RF glow discharge plasma polymerization of haloesters, specifically: methyl-3-bromopropionate (M3BP), methyl-2-chloropropionate (M2CP), and ethyl-2-fluoropropionate (E2FP). Once prepared, we used the plasma polymerized haloester surface as a surface initiator for SI-ARGET ATRP synthesis of HEMA as proof of concept (Figure 1.1). To the best of our knowledge, this is the first time that chloro- and fluoroesters have been plasma polymerized on surfaces and used as surface initiators for ARGET ATRP synthesis of polymer brushes.

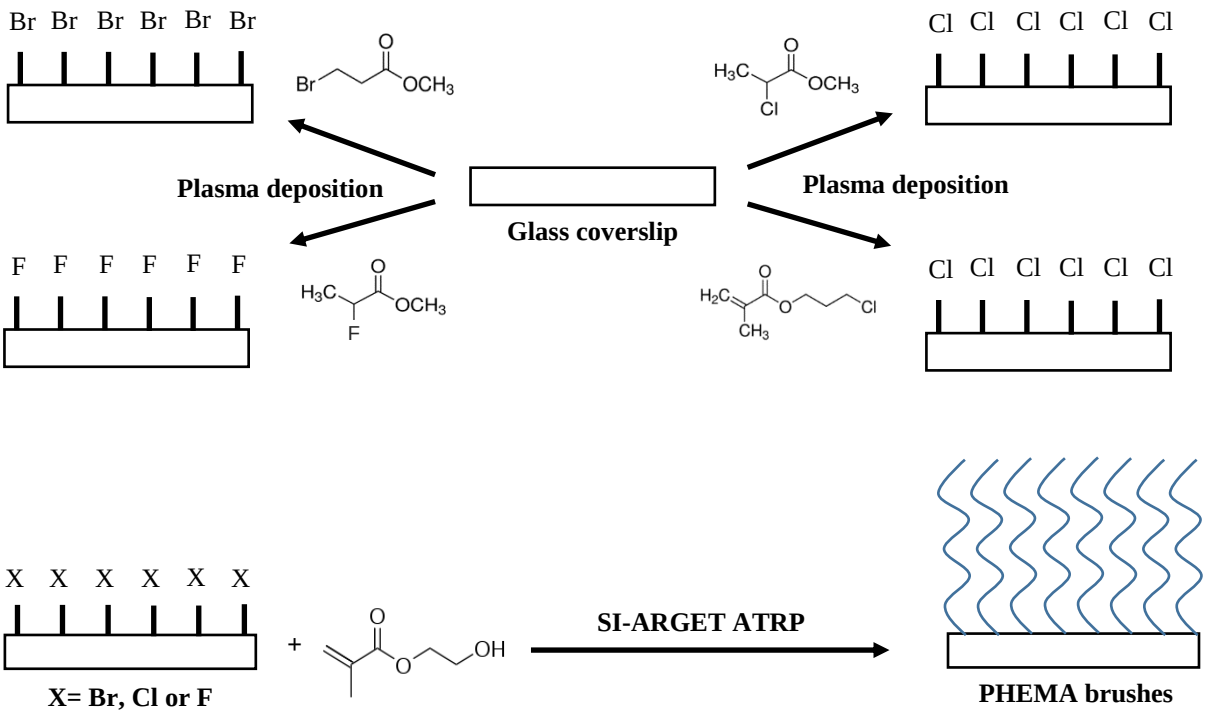

Figure 1.1. Schematic representation of the process to grow PHEMA polymer brushes via SI-ARGET ATRP from plasma polymerized haloester surfaces. We first create a surface rich in either Br, Cl or F by plasma depositing haloesters onto glass coverslips. This is followed by placing the plasma polymerized haloester coverslips into an ARGET ATRP solution in excess of HEMA to grow PHEMA brushes.

1.3 EXPERIMENT

1.3.1 Plasma deposition and characterization of haloesters: M3BP, M2CP and E2FP

1.3.1.1 Materials

8mm glass coverslips were purchased from Knitell Glass (Cat. No. G401-08). Methyl 3-bromopropionate (M3BP) was purchased from Sigma-Aldrich (Cat. No. 3395-91-3), Methyl 2-chloropropionate (M2CP) was purchased from Alfa Aesar (Cat. No. A18541), Ethyl 2-fluoropropionate (E2FP) was purchased from TCI America (Cat. No. 349-43-9), and 2-chloroethyl methacrylate (CEMA) was purchased from Pfaltz & Bauer (Cat. No. 1888-94-4). All organic solvents were purchased from Fisher Scientific.

1.3.1.2 Plasma polymerization of haloesters

Prior to plasma deposition, 8mm glass coverslips were placed in a sample holder within a glass container and ultrasonicated in a water bath for two 10 min cycles each in methylene chloride, followed by acetone and then methanol. The glass samples were then air-dried in a fume hood.

Plasma polymerization of haloesters was carried out in a custom-built plasma reactor setup based on the design reported in Lopez et al.[34] Cleaned glass coverslips were loaded in the plasma reactor and positioned in between the powered and grounded electrodes (100 mm apart), and a mechanical pump was used evacuate the reactor to the desired base pressure in the low 10^{-3} Torr range. A liquid nitrogen cooled cold trap between the vacuum pump and the reactor was used to condense organic materials. The powered electrode was connected to a 13.56 MHz radio frequency power source and an automatic impedance matching network. The coverslips were

first etched in argon gas for 10 min at 40W while maintaining a pressure of 250mT and then plasma coated with a methane deposition at 80W for 5 min at a pressure of 140mT. This plasma-deposited methane layer generated at high plasma power has been found to allow plasma coatings to strongly adhere to the substrate, thus preventing delamination. Following this, the coverslips were coated with the haloester of choice. In brief, a flask containing approximately 20mL of either M3BP, M2CP or E2FP was connected to a caliper valve and was used to control the monomer delivery rate into the plasma reactor. The coverslips were coated for 1 min at 80 W in order to form an adhesion promoting layer, after which the power was lowered to 10 W for 10 min, while maintaining a pressure of 150 mT for the monomer throughout the plasma deposition process. Finally, samples were quenched under M3BP, M2CP or E2FP vapor for 5 min before retrieving them.

CEMA plasma deposited glass coverslips were used as a positive control for all experiments and were prepared by a modified protocol as described by Hucknall et al.[33] Following the argon etching process, and methane plasma deposition, glass coverslips were coated with CEMA for 1 min at 80 W and for 10 min at 10 W, followed by quenching for 5 min. A pressure of 150 mT was also maintained for CEMA throughout the process.

1.3.1.3 Surface characterization

X-ray photoelectron spectroscopy (XPS) was performed on all plasma polymerized glass disc samples on a Surface Science Instruments S-Probe equipped with a monochromatic Al Kα source and a low energy electron flood gun for charge neutralization. X-ray analysis for these acquisitions was in a circle approximately 800 μm across. Pressure in the analytical chamber during spectral acquisition was less than 5×10^{-9} Torr. Low-resolution survey scans were

obtained from 0 to 1100 eV with a 1 eV step size and pass energy of 150 eV. High resolution C 1s scans were obtained from 270 to 290 eV with a 0.065 eV step size and pass energy of 50 eV. The spectra were analyzed off line with Service Physics Hawk version 7 data analysis software to calculate the elemental compositions from peak areas and to peak fit high resolution spectra. All binding energies were calibrated with reference to the aliphatic carbon at C 1s = 285.0 eV. A Shirley background was used for all spectra.

Furthermore, in order to test the robustness of the plasma polymerized surfaces, samples were placed in a glass disc holder and soaked in methanol for 2 h. The samples were then air-dried in a chemical hood and analyzed via XPS.

Additionally, plasma polymerized M3BP surface coatings were analyzed using time-of-flight secondary ion mass spectroscopy (ToF-SIMS) (IONTOF TOF.SIMS 5 spectrometer) using a 25 keV Bi_3^+ cluster ion source in the pulsed mode, and was compared to M3BP that was drop coated onto silicon wafer and air-dried. Plasma polymerized M3BP surface coatings were also soaked in methanol for 2 h, and the surface coatings post methanol soak as well as the extract from the methanol soak were analyzed using ToF-SIMS. Spectra were acquired for both positive and negative secondary ions over a mass range of m/z = 0 to 850. The ion source was operated with at a current of 0.17 pA. Secondary ions of a given polarity were extracted and detected using a reflectron time-of-flight mass analyzer. Spectra were acquired using an analysis area of 100 micron x 100 micron. The primary ion dose for each spectrum was $8.7x10^{11}$ ion/cm^2. Positive ion spectra were calibrated using the CH_3^+, $C_2H_3^+$, and $C_3H_5^+$ peaks. The negative ion spectra were calibrated using the CH^-, OH^-, C_2H^-, C_4H^-, and Br_2^- peaks. Calibration errors were kept below 25 ppm. Mass resolution ($m/\Delta m$) for a typical spectrum was between 5000 to 6000 for m/z = 27 (pos) and between 4500 to 6000 for m/z = 25 (neg).

1.3.2 SI-ARGET ATRP reaction of HEMA using plasma deposited M3BP, M2CP, and E2FP as the surface initiator

1.3.2.1 Materials

HEMA (ophthalmic grade) was purchased from Polysciences, Inc. (Cat. No. 04675). L-Ascorbic acid (Cat. No. A5960), tris(2-pyridylmethyl)amine (Cat. No. 723134), and copper (II) bromide (Cat. No. 221775) were all purchased from Sigma-Aldrich.

1.3.2.2 Synthesis of HEMA polymer brushes

To grow HEMA brushes on M3BP, M2CP, E2FP and CEMA plasma deposited surfaces, we modified a protocol provided by Paterson et al.[19] A solution prepared from HEMA (2mL, 16.4 mmoL), methanol (1.5 mL), stock solutions of $CuBr_2$/TPMA (44 µL, 0.84 µmoL $CuBr_2$, 4.2 µmoL TPMA), and L-ascorbic acid (460 µL of 25 mg/mL of ascorbic acid in methanol) in a round bottom Schlenk flask was degassed by five freeze-pump-thaw cycles and the flask was backfilled with nitrogen. The solution was then pipetted into a 50 mL falcon tube containing a sample holder with the plasma polymerized substrates, capped, and then allowed to polymerize at ambient room temperature. After the desired polymerization time (5 min, 15 min, 30 min, 1 h and 2 h), the glass disc holder containing the samples were removed and subsequently rinsed five times with 50% v/v methanol in water, and dried in air in a chemical hood. Clean glass discs were used as negative controls.

1.3.2.3 Surface characterization

The polymer brush surface synthesized by SI-ARGET ATRP were analyzed using XPS as well as ToF-SIMS as described in Section 1.3.1.3.

Additionally, the thickness of the polymer brushes synthesized by SI-ARGET ATRP were determined by profilometry on a Bruker DektakXT Stylus Profiling system with a 2 µm stylus. Scratches were created on the surfaces using a razor blade and the profile across the scratch was used to determine polymer brush thickness. All samples were dry at the time of thickness measurement.

1.4 Results and Discussion

In most previous work, substrates modified with polymer brushes are limited to materials such as gold, silicon and metal oxides that support the formation of self-assembled monolayers (SAM) that present ATRP initiators.[35,36] However, surfaces of many technologically relevant materials, such as glass, plastics and metals do not support SAM formation. To overcome this limitation, we used glow discharge RF plasma for deposition of a surface initiator onto glass disc substrates to initiate SI-ARGET ATRP of HEMA. We chose glow discharge RF plasma because it is capable of functionalizing a surface with halogen precursors independent of substrate material.

XPS was used to assess the functionalization of glass coverslips with the surface initiators. The survey scans seen in Figure 1.2, and summarized in Table 1.1, provide information on the overall surface chemical composition before and after methanol wash. We observed that the bromine content in plasma polymerized M3BP coatings, 33 atomic % Br, was significantly higher than the expected amount of bromine (14 atomic % Br) based on the stoichiometry of the compound. Conversely, the chlorine and fluorine content in plasma polymerized M2CP and E2FP coatings were much lower than expected—4 atomic % Cl vs the expected 14 atomic % Cl in M2CP and 3 atomic % F vs the expected 14 atomic % F in E2FP.

For the plasma polymerized CEMA coatings we found that the overall chemical composition matched the expected composition reasonably well.

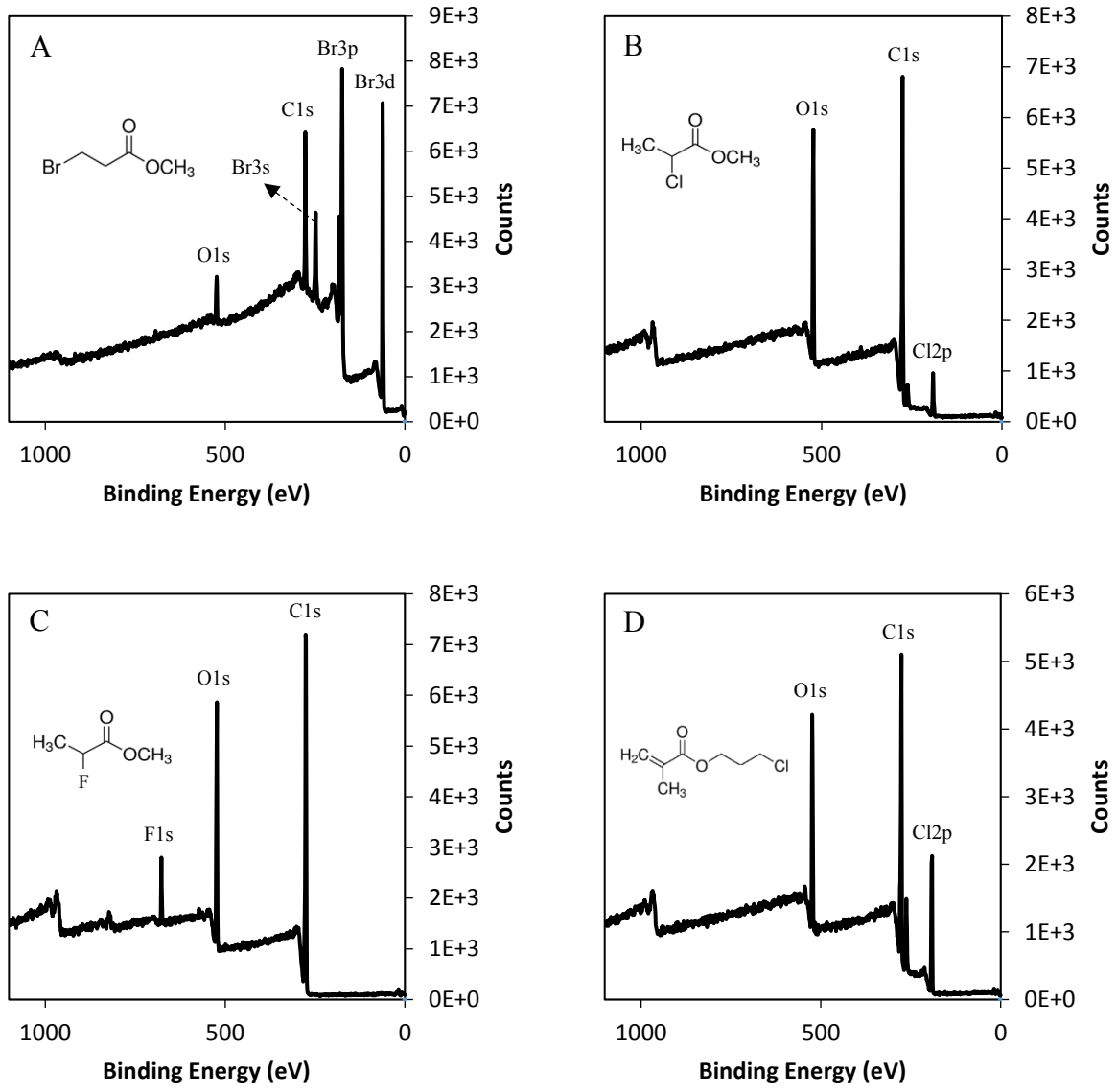

Figure 1.2. Representative XPS survey scans and corresponding monomer chemical structures (inset) of plasma polymerized (A) M3BP (B) M2CP (C) E2FP and (D) CEMA on glass coverslips. Major elemental peaks are labeled in each survey scan.

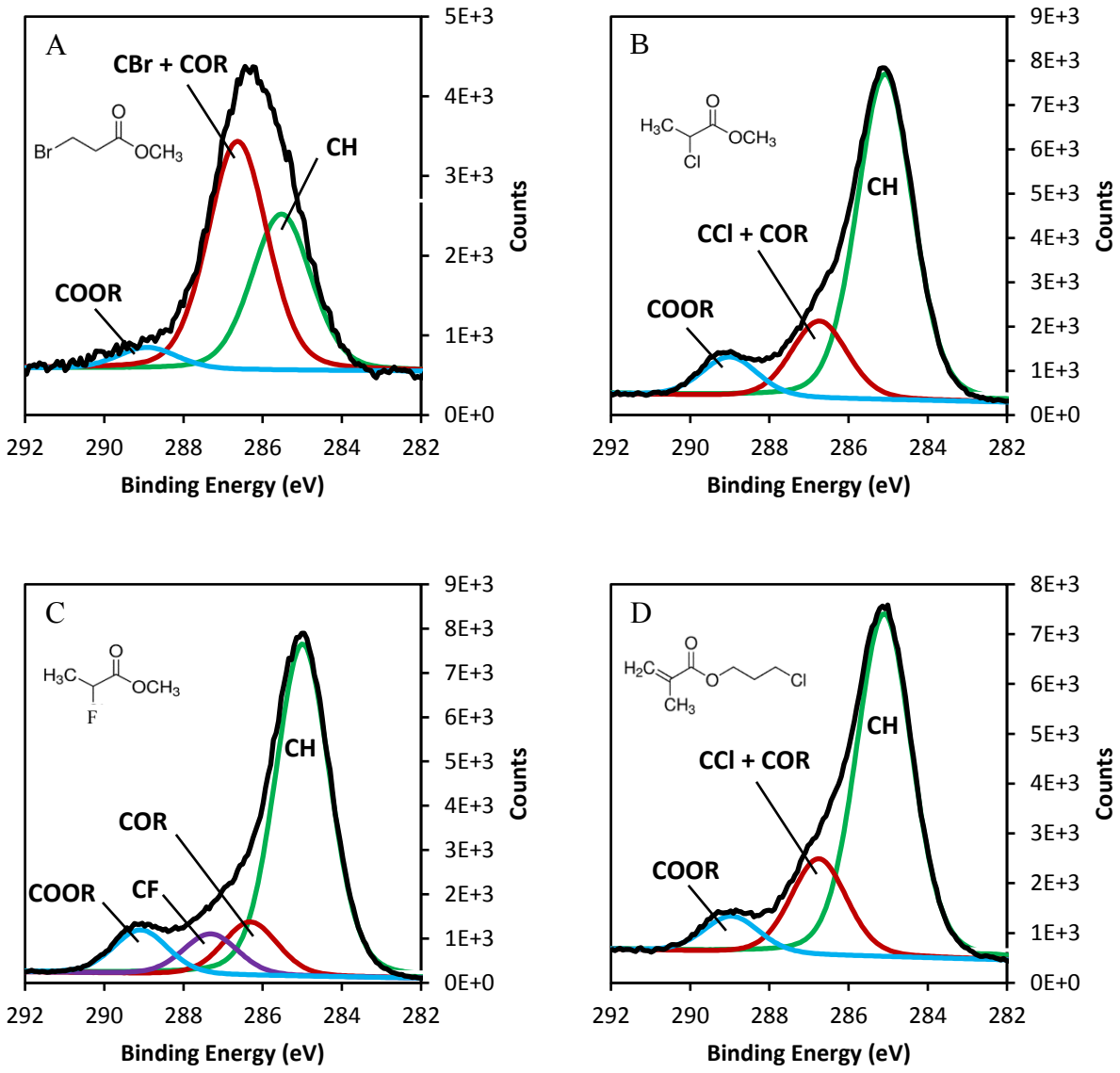

Figure 1.3. Representative high-resolution spectra of the C1s peak (black envelope) and corresponding monomer chemical structure (inset) of plasma polymerized (A) M3BP (B) M2CP (C) E2FP and (D) CEMA on glass coverslips. Fitted peaks are labeled to correspond to different bonding environments within each chemical structure.

High resolution C 1s spectra (Figure 1.3) provide insight into the chemical bonding environment of carbon. In Table 1.1, we compare the observed contributions of each chemical state of carbon to the expected contributions based on the stoichiometric ratios present in each chemical structure. As seen in Figure 1.3, the shape and features of the high-resolution C1s peak of the M3BP, M2CP and CEMA plasma polymerized coatings were fitted with three width-constrained peaks corresponding to three different bonding environments: CH_y at 285 eV, C—X (where X is either Br, Cl) and C—OR both at ~286.5 eV, and COOR at 289 eV.[37] Similarly, four width-constrained peaks were used to fit the high-resolution C1s peak of E2FP plasma polymerized coatings: CH_y at 285.0 eV, C—OR at 286.5 eV, C—F at 287.5 eV and COOR at 289 eV.[37] It should be noted that all XPS spectra were shifted ~9.3 eV so that the hydrocarbon peak could align at 285.0 eV (charging binding energy correction).

In the case of plasma polymerized M2CP and E2FP coatings, the observed contribution of the corresponding halogen is less than expected. On the other hand, the amount of Br seen on plasma polymerized M3BP coatings is significantly higher (~230 %) than what is stoichiometrically expected. This confounding result is the outcome of a complex reaction and can be attributed to radical chemical reactivity, concentration of species in the gas phase, transport to the surface from the gas phase and the probabilities for surface reaction. However, it is outside the scope of this paper to develop a complete mass transport-reaction model to explain the chemical observations. Furthermore, from the high-resolution C1s spectra of plasma polymerized M3BP we observe nearly 56% of the total signal from C—Br and C—OR which suggests that the surface of plasma polymerized M3BP coatings are rich in CBr_x species.

XPS was also used to evaluate whether the plasma polymerized coatings delaminate or change after soaking in methanol (Table 1.1). Importantly, after the methanol wash, no elemental peaks associated with glass discs (specifically silicon) were observed. This indicates that the plasma polymerized M3BP, M2CP, E2FP and CEMA coatings are stable and do not delaminate. Furthermore, the chlorine content on plasma polymerized M2CP and CEMA coatings increased slightly from 4.1 ± 0.2 % to 7.3 ± 0.6 %, and 8.5 ± 0.6 % to 10.0 ± 0.3 % respectively, while the fluorine content on plasma polymerized E2FP coatings did not change significantly. These increases in the Cl signal suggest that there may be a gradient in Cl concentration through the depth of the M2CP and CEMA plasma coatings and that an overlayer of loosely bound, deposited material was removed by the solvent revealing an underlayer of the polymer network that has a higher concentration of Cl.

Interestingly, for plasma polymerized M3BP coatings the bromine content significantly reduced from 33.2 ± 0.1 % to 10.8 ± 1.0 % after the methanol wash. This significant reduction in Br after the methanol wash warranted further investigation. ToF-SIMS was used to investigate the surface of plasma polymerized M3BP samples before soaking and after soaking in methanol. In addition, we also analyzed the methanol extract and compared these to M3BP that was drop-coated onto silicon wafers and air-dried. From the ToF-SIMS data we observed that the plasma polymerized M3BP samples contained Br_x (x = 1-4) species whereas the drop-coated M3BP samples only contained Br and a small Br_2 signal. It should be noted that the exact structure of the bromine on the surface could not be determined from the Tof-SIMS data, however the presence of higher order Br_x species suggests polybromine compounds were present. Since the XPS composition data for the M3BP sample showed a significant amount of carbon and bromine with much lower amounts of oxygen, we also looked for the presence of Br_xC_y peaks.

Polybromide species though rare have been studied theoretically[38,39] and demonstrated experimentally.[40] It was noted that a series of peaks of the general formula of BrC_y^- (y = 1 to 12) were seen in the M3BP spectra along with Br_2C^- and $Br_2C_3^-$. All of these were minor peaks in the spectra suggesting either that they do not easily ionize, they are not stable ions or they are present in low levels at the surface. Since bromine has a unique isotopic pattern these peaks were confirmed by matching both their exact mass and isotopic pattern. No other $Br_xC_y^-$ peaks were found. In comparison only BrC^-, BrC_2^- and BrC_4^- were clearly seen in the drop-coated M3BP sample (see supplemental section Table S1.1). The presence of Br_xC_y peaks with y > 4 could be indicative of a highly crosslinked structure within the plasma deposited film. To further investigate this we looked at the relative intensity of hydrocarbon peaks between the plasma polymerized and drop coated M3BP samples. It was noted that the relative intensity of $C_xH_y^+$ peaks with y<x was higher on the plasma polymerized samples while the relative intensity of $C_xH_y^+$ peaks with y>x was higher on the controls (see supplemental Table S1.1). This further supports the hypothesis that the plasma polymerized sample is heavily crosslinked.

It was noted that the Br_4^- intensity was very small when detected. As expected, we also observed that the drop-coated M3BP samples preserved the structure of the monomer better than plasma polymerized M3BP samples. Furthermore, the M3BP samples soaked in methanol showed a significant reduction in all Br_x (x = 1-4) species and bromine signals [Br_x (x = 1-4)] were detected in their methanol wash. This data show that some bromine is lost from the surface after washing with methanol as was seen in the XPS data. It is likely that the majority of the bromine species lost were polybromine compounds as the relative intensity decrease of Br_x (x = 2-4) was greater than that of Br. These ToF-SIMS results can be found summarized in the supplemental section (Figure S1.1). Thus the results from XPS and ToF-SIMS suggest that the

plasma polymerized M3BP coatings are comprised of highly crosslinked C-Brx species as well as small branched polybromine species that have not been tied into the polymer network and are readily washed away during the methanol wash.

After characterization of plasma polymerized haloester surface coatings, their function as surface initiators for ARGET ATRP was assessed. To this end, as a proof of concept, we attempted to grow HEMA polymer brushes from the surface of these coating, and then characterized the surfaces using XPS, profilometry and ToF-SIMS. Surfaces analyzed included plasma polymerized M3BP, M2CP, E2FP and CEMA coatings soaked in ARGET ATRP solution for either 5 min, 15 min, 30 min, 1 h or 2 h.

Table 1.1. Summary of surface elemental composition of plasma polymerized M3BP, M2CP, E2FP and CEMA surface coatings as determined by survey scans obtained from XPS (n = 3).

Plasma coating		Before Methanol wash								
		Survey					C 1s			
		C	O	Br	Cl	F	Peak 1 CH	Peak 2 CX +/ COR X=Br/Cl	Peak 3 CF	Peak 4 COOR
M3BP	Observed	59.8 ± 0.6	7.0 ± 0.7	33.2 ± 0.1	-	-	38.6 ± 2.5	56.3 ± 2.6	-	5.1 ± 0.2
	Expected	57.1	28.6	14.3	-	-	25.0	50.0	-	25.0
M2CP	Observed	79.2 ± 1.4	16.6 ± 1.1	-	4.1 ± 0.2	-	72.2 ± 1.3	18.6 ± 1.0	-	9.3 ± 0.7
	Expected	57.1	28.6	-	14.3	-	25.0	50.0	-	25.0
E2FP	Observed	80.5 ± 1.6	16.7 ± 1.7	-	-	2.8 ± 0.2	71.3 ± 2.1	10.8 ± 0.5	9.2 ± 1.3	8.7 ± 1.1
	Expected	62.5	25	-	-	12.5	40.0	20.0	20.0	20.0
CEMA	Observed	78.0 ± 0.6	13.5 ± 0.1	-	8.5 ± 0.6	-	70.4 ± 1.8	22.0 ± 1.7	-	7.6 ± 0.1
	Expected	66.6	22.2	-	11.1	-	50	33.3	-	16.7

Plasma coating		After Methanol wash								
		Survey					C 1s			
		C	O	Br	Cl	F	Peak 1 CH	Peak 2 CX +/ COR X=Br/Cl	Peak 3 CF	Peak 4 COOR
M3BP	Observed	69.8 ± 0.5	19.5 ± 1.4	10.8 ± 1.0	-	-	61.5 ± 2.2	27.6 ± 1.9	-	10.9 ± 0.3
	Expected	57.1	28.6	14.3	-	-	25.0	50.0	-	25.0
M2CP	Observed	74.1 ± 0.4	18.6 ± 0.4	-	7.3 ± 0.6	-	64.5 ± 1.6	24.7 ± 1.3	-	10.8 ± 0.3
	Expected	57.1	28.6	-	14.3	-	25.0	50.0	-	25.0
E2FP	Observed	82.3 ± 0.7	15.2 ± 0.7	-	-	2.5 ± 0.0	70.4 ± 9.8	14.9 ± 8.3	8.8 ± 1.5	5.9 ± 0.1
	Expected	62.5	25	-	-	12.5	40.0	20.0	20.0	20.0
CEMA	Observed	77.0 ± 0.1	13.0 ± 0.3	-	10.0 ± 0.3	-	68.3 ± 0.4	24.9 ± 0.3	-	6.8 ± 0.1
	Expected	66.6	22.2	-	11.1	-	50	33.3	-	16.7

Table 1.2. Surface elemental compositions by XPS (n = 3) of plasma polymerized M3BP, M2CP, E2FP and CEMA surface coatings after being in ARGET ATRP solution for 5, 15, 30, 60 and 120 min.

Plasma coating	Reaction Time	Survey Scan				
		C	O	Br	Cl	F
M3BP	0 min	69.8 ± 0.5	19.5 ± 1.4	10.8 ± 1.0	-	-
	5 min	68.6 ± 1.1	27.8 ± 1.7	3.6 ± 2.1	-	-
	15 min	68.7 ± 0.9	31.3 ± 0.9	-	-	-
	30 min	68.9 ± 0.3	31.1 ± 0.3	-	-	-
	1 h	68.5 ± 0.8	31.5 ± 0.8	-	-	-
	2 h	68.3 ± 0.2	31.7 ± 0.2	-	-	-
M2CP	0 min	74.1 ± 0.4	18.6 ± 0.4	-	7.3 ± 0.6	-
	5 min	72.1 ± 0.2	22.3 ± 0.1	-	5.5 ± 0.1	-
	15 min	71.1 ± 0.8	27.1 ± 0.6	-	1.8 ± 0.2	-
	30 min	69.0 ± 0.6	31.0 ± 0.6	-	-	-
	1 h	68.8 ± 0.8	30.7 ± 0.8	-	0.5 ± 0.1	-
	2 h	68.3 ± 0.3	31.7 ± 0.3	-	-	-
E2FP	0 min	82.3 ± 0.7	15.2 ± 0.7	-	-	2.5 ± 0.0
	5 min	79.5 ± 5.5	18.7 ± 5.9	-	-	1.8 ± 0.4
	15 min	72.1 ± 0.3	27.0 ± 0.4	-	-	0.9 ± 0.2
	30 min	69.6 ± 0.5	30.4 ± 0.5	-	-	-
	1 h	69.3 ± 0.4	30.7 ± 0.4	-	-	-
	2 h	70.2 ± 1.6	29.8 ± 1.6	-	-	-
CEMA	0 min	77.0 ± 0.1	13.0 ± 0.3	-	10.0 ± 0.3	-
	5 min	71.9 ± 2.0	24.6 ± 2.5	-	3.5 ± 0.5	-
	15 min	75.5 ± 0.5	19.7 ± 0.5	-	1.8 ± 0.4	-
	30 min	70.6 ± 0.2	29.4 ± 0.2	-	-	-
	1 h	68.7 ± 0.4	31.1 ± 0.2	-	-	-
	2 h	69.5 ± 1.5	30.5 ± 1.5	-	-	-

A summary of the surface chemical composition after the ARGET ATRP reaction can be found in Table 1.2. In general, as the reaction time increases we observe a reduction in the amount of halogen on the surface of all plasma polymerized coatings. This result would suggest that the HEMA polymer brush is increasing in grafting density and/or polymer chain length which is why we notice a reduction in the concentration of the halogen on the surface as the ATRP reaction progresses. In all cases, by the 2 hr time point, the plasma polymerized coated surfaces only contain carbon and oxygen as seen in the survey scans (Table 1.2). Moreover, the high resolution C1s peaks of all plasma polymerized haloester coatings resembles that of HEMA polymer brushes and matches the C/O ratio expected for PHEMA (2/1) (data not shown). Particularly, plasma polymerized M3BP coatings are capable of growing HEMA polymer brushes that are at least 10 nm thick as rapidly as 15 min, whereas plasma polymerized M2CP, E2FP and CEMA coatings begin to grow HEMA polymer brushes that are at least 10 nm thick by 30 min. To the best of our knowledge, this is the fastest reported time for ARGET ATRP reaction of HEMA reported in literature. However, further experiments would be required to specifically measure kinetics and the reaction rates and compare them with other published studies.

As a negative control, we used clean glass coverslips and attempted to grow HEMA polymer brushes via SI-ARGET ATRP. XPS data showed that no polymer brush resulted from the SI-ARGET ATRP reaction even after being in solution for 5 h (data not shown). This is not surprising because a surface initiator that contains a halogen is necessary for the ARGET ATRP reaction to initiate and propagate.

Using profilometry we were able to determine the thickness of the HEMA polymer brushes at different points during the ARGET ATRP reaction (Figure 1.4). As expected, the

thickness of the HEMA polymer brush increases over time for all plasma polymerized haloester coatings. In all cases, except for E2FP, at the 2 hr time point we were able to grow films that were nearly 2 µm thick. Furthermore, we observed that the thickness of the HEMA polymer brushes on plasma polymerized E2FP surface initiators increases at a slower rate compared to M3BP and M2CP. It should also be noted that, as reaction time increases the surface of the HEMA polymer brushes grown on plasma polymerized surfaces changes from smooth to rough (data not shown). This resulted in the large standard deviation seen at longer reaction times.

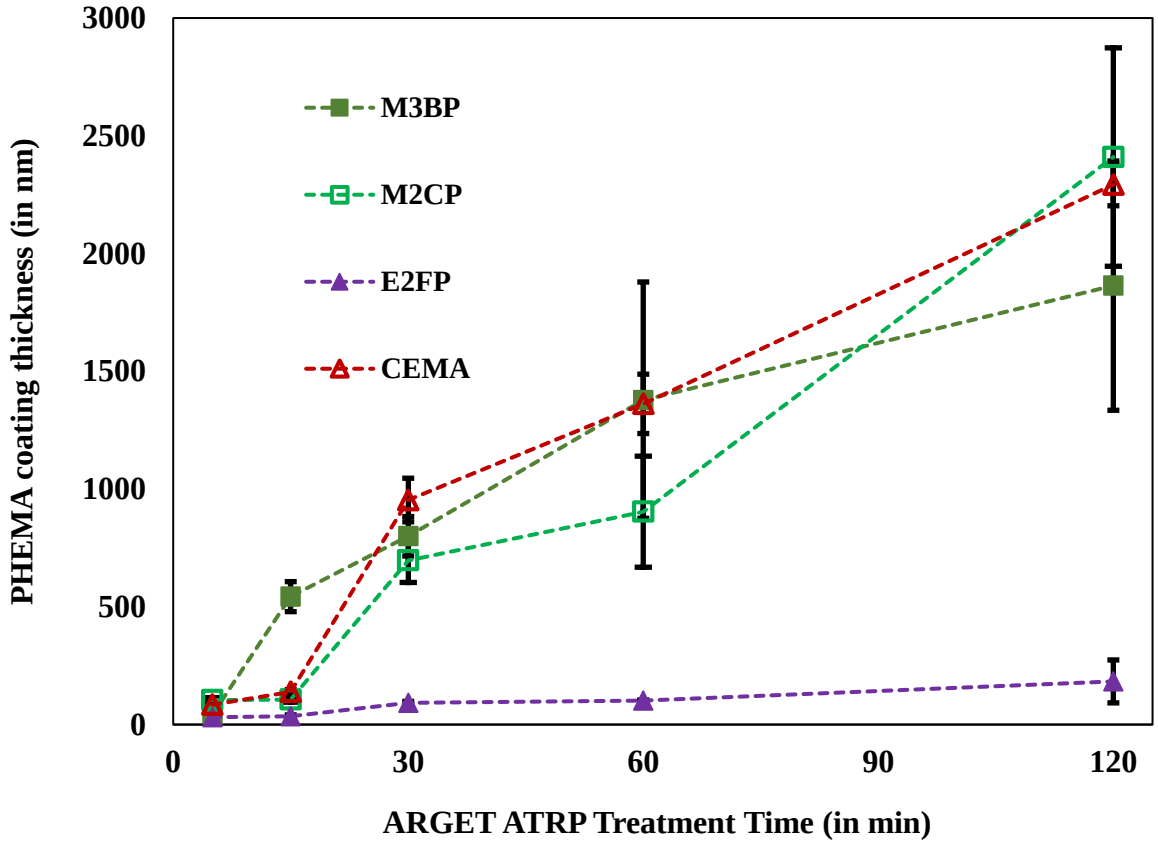

Figure 1.4. HEMA polymer brush coating thickness grown via SI-ARGET ATRP on plasma polymerized M3BP, M2CP, E2FP and CEMA surface coatings. All samples were dry during thickness measurements (n = 4).

ToF-SIMS was used to determine the presence of PHEMA on the plasma polymerized haloester surfaces following the ATRP reaction for 2 h. PHEMA produces a number of characteristic secondary ion fragments including the HEMA-OH monomer fragment at 113.06 m/z and the methacrylate fragment $C_4H_5O^+$ at 69.04 m/z.[41] A peak list for PHEMA was generated and can be seen in Supplemental Table S1.2. Positive ion spectra were then collected for the ATRP reaction surfaces with $CuBr_2$ (Figure 1.5). The characteristic PHEMA positive ions $C_2H_3O^+$, $C_2H_5O^+$, $C_3H_3O^+$, $C_4H_5O^+$, $C_8H_{11}^+$, $C_6H_9O_2^+$, $C_9H_{13}^+$ were detected for all plasma polymerized coatings after 2 h in the ATRP reaction (Figure 1.5).

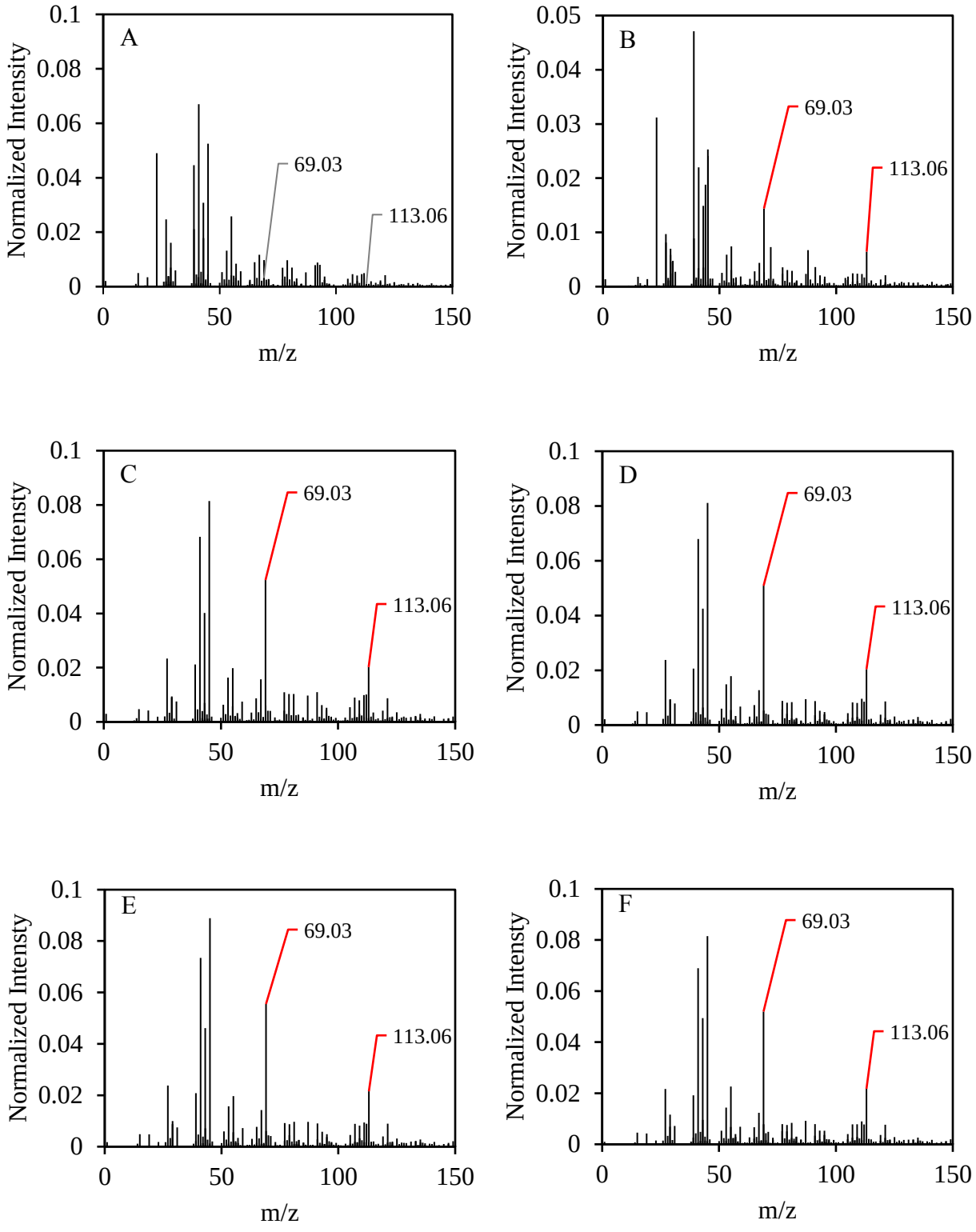

Figure 1.5. Representative ToF-SIMS spectra of HEMA polymer brushes grown on plasma polymerized (C) M3BP (D) M2CP (E) E2FP and (F) CEMA surfaces via SI-ARGET ATRP. A glass disc without surface initiator is used as a negative control (A), while a PHEMA hydrogel

was used as positive control (B). Positive polarity spectra were acquired in high mass resolution mode with Bi^{3+} primary ion species over a 0-200m/z mass range for HEMA. Major peaks associated with HEMA are highlighted in each spectrum, the molecular formula and normalized intensities are displayed in Supplemental Table S1.2.

Since fluorine is a poor leaving group, fluorine-based compounds are not used as surface initiators for ARGET ATRP reaction. Lanzalaco et al. have reported that F-based ATRP systems are less efficient compared to Br- and Cl- based systems.[42] For this reason, we were surprised to see that we were able to grow HEMA polymer brushes on the surface of plasma polymerized E2FP coatings as determined through profilometry and ToF-SIMS. This unexpected result led us to further investigate whether we are growing HEMA polymer brushes via SI-ARGET ATRP or through another reaction mechanism.

To this end, we placed plasma polymerized M3BP, M2CP, E2FP and CEMA in the ARGET ATRP reaction mixture in the absence of $CuBr_2$ for 2 h. As confirmed by ToF-SIMS, no PHEMA peaks were seen on any of these plasma polymerized M3BP, M2CP, E2FP and CEMA surface coatings (Supplemental Figure S1.2); the major peaks detected were mainly hydrocarbon chain fragments at 41.03 ($C_3H_5^+$), 43.05 ($C_3H_7^+$), and 55.05 m/z ($C_4H_7^+$). Since $CuBr_2$ is crucial as a catalyst for ARGET ATRP these results suggest that we are in fact growing HEMA polymer brushes via SI-ARGET ATRP.

To investigate the specificity of plasma polymerized E2FP coatings to initiate ARGET ATRP reaction, we also plasma polymerized hexafluoropropylene (C3F6) onto glass coverslips using a protocol previously described by Garrison et al.[43] and placed it in the ARGET ATRP reaction with or without $CuBr_2$ for 2 h. In both cases, ToF-SIMS verified that there were no HEMA polymer brushes on plasma polymerized C3F6 surface coatings with or without $CuBr_2$.

The results from the C3F6 experiments suggest that plasma polymerized E2FP coatings is unique in its ability to grow HEMA polymers brushes compared to other plasma polymerized fluoro surfaces. We hypothesize that the fluorine-carbon bonds in plasma polymerized E2FP coatings are weaker which allows the fluorine to participate in the ARGET ATRP reaction. The specific reaction mechanism, however, is currently unknown and warrants further investigation. This ToF-SIMS data can also be found summarized in the supplemental section (Figure S1.3).

1.5 Conclusions

The ability to control surface chemistry is critical for many applications. Though conceptually this appears simple, it is often difficult to directly modify the surface chemistry of some materials. In this work, we describe a straightforward method for the deposition of haloester monomers using RF glow discharge plasma that enables further surface modifications. Due to the versatility of RF glow discharge plasmas for surface modification, this process is scalable and can be applied to any surface of interest. We have also demonstrated that these surface coatings have high halogen contents and do not delaminate making them good candidates as surface initiators for ARGET ATRP reaction. As a demonstration of this process, we showed that all plasma polymerized haloester coatings can grow HEMA polymer brushes after 2 h in the ARGET ATRP HEMA solution. Specifically, plasma polymerized M3BP can grow HEMA polymer brushes within 15 min. Furthermore, even plasma polymerized E2FP (a fluoroester) was capable of growing HEMA polymer brushes. We believe that the methods described in this work have the potential to extend the use of HEMA coatings to a broad range of commercially interesting applications in the areas of biomedical devices, diagnostics, as well as cell and tissue engineering. Future studies will assess the efficacy of these haloester surface coatings to grow

other nonfouling zwitterionic coatings such as carboxybetaine methacrylate (CBMA) and sulfoxybetaine methacrylate (SBMA) via ARGET ATRP for various biomedical applications.

1.6 Acknowledgements

Funding was provided through the University of Washington Engineered Biomaterials program and by NESACBIO NIH Grant No. EB-002027. Part of this work was conducted at the Molecular Analysis Facility, a National Nanotechnology Coordinated Infrastructure site at the University of Washington which is supported in part by the National Science Foundation (grant ECC-1542101), the University of Washington, the Molecular Engineering & Sciences Institute, the Clean Energy Institute, and the National Institutes of Health.

1.7 SUPPLEMENTAL SECTION

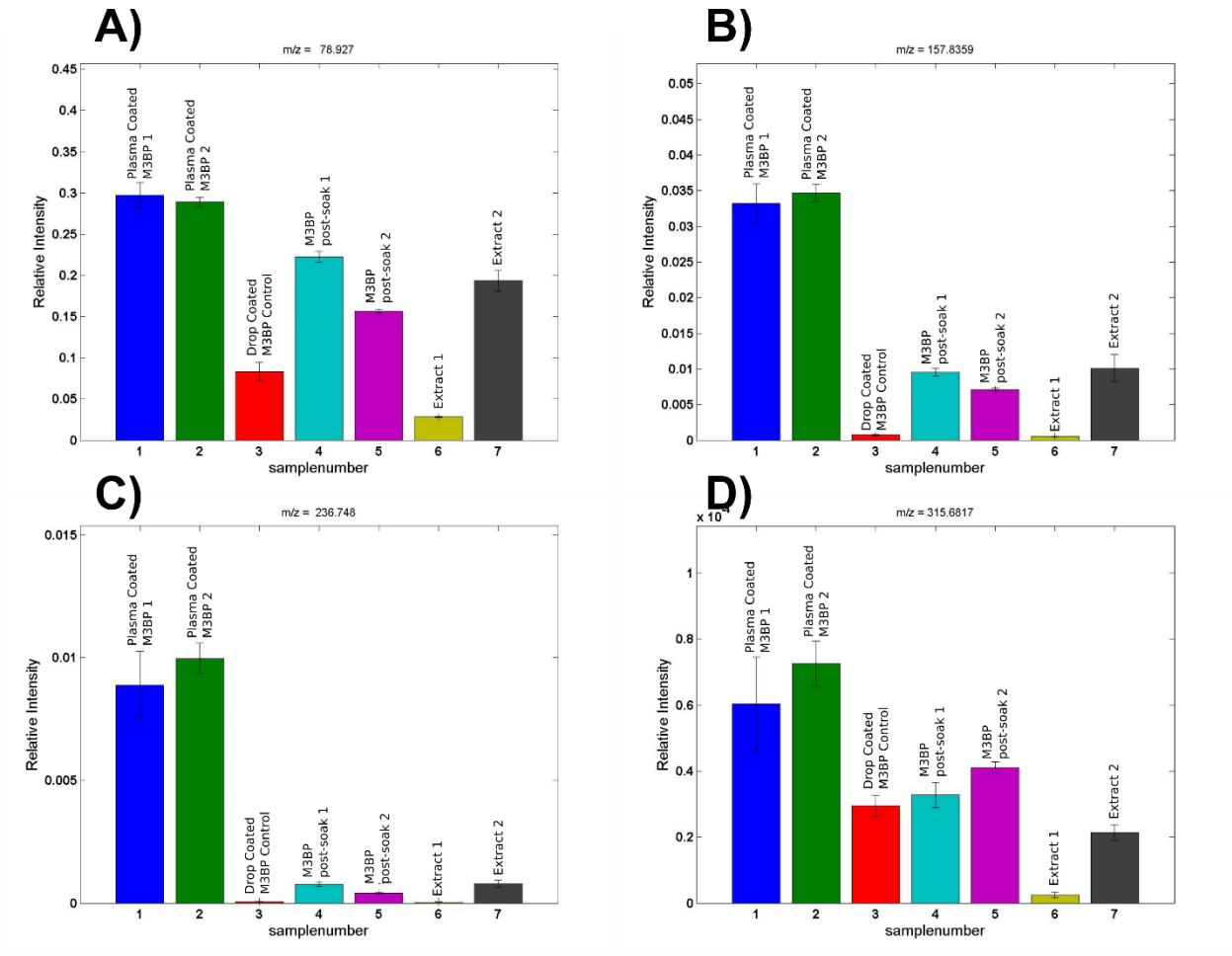

Figure S1.1. ToF-SIMS relative intensity of Br_x species. ToF-SIMS relative peak intensities (normalized to total counts) of A) Br B) Br_2 C) Br_3 and D) Br_4. It should be noted that when detected, the intensity of the Br_4 peak was very low. Data from 2 replicates of each sample type are shown (except for the control which only contains 1 sample). The bar height represents the average relative intensity and the error bars show the standard deviation (n=4, except for the control n=5). The samples are ordered from left to right, plasma polymerized M3BP, drop-coated M3BP control, plasma polymerized M3BP after methanol soak, and extract (methanol wash solution from plasma polymerized M3BP samples). The Br_4 signal from the control is an artifact of the background noise in that region and is not from Br_4.

Table S1.1. Location of highest relative intensity C_xH_y peaks. Major positive secondary ion peaks on the surface of plasma polymerized M3BP and drop-coated M3BP. 'x' denotes which sample showed the highest relative intensity for the given peak. If 'x' is in both columns then the relative intensity was about equal for both samples (n = 18 spectra for plasma polymerized sample, n = 5 for drop coated control).

CxHy	Plasma Polymerized M3BP	Drop Coated M3BP	CxHy	Plasma Polymerized M3BP	Drop Coated M3BP
C	x		C7H8		x
CH	x		C7H9		x
CH2	x		C7H11		x
CH3	x		C7H13		x
C2H	x		C7H14		x
C2H2	x		C8H	x	
C2H3		x	C8H2	x	
C2H4		x	C8H3	x	
C2H5		x	C8H4	x	
C3H	x		C8H5	x	
C3H2	x		C8H6	x	
C3H3	x	x	C8H7	x	
C3H5		x	C8H8	x	x
C3H7		x	C8H9		x
C4H	x		C8H10		x
C4H2	x		C8H11		x
C4H3	x		C8H13		x
C4H4	x	x	C8H14		x
C4H5		x	C9H	x	
C4H7		x	C9H2	x	
C4H9		x	C9H3	x	
C5H	x		C9H4	x	
C5H2	x		C9H5	x	
C5H3	x		C9H6	x	
C5H4	x		C9H7	x	
C5H5	x	x	C9H8	x	
C5H6		x	C9H9		x
C5H7		x	C9H10		x
C5H9		x	C10	x	
C6H	x		C10H	x	
C6H2	x		C10H2	x	
C6H3	x		C10H3	x	
C6H4	x		C10H4	x	
C6H5	x	x	C10H5	x	
C6H6	x	x	C10H6	x	
C6H7		x	C10H7	x	
C6H9		x	C10H8	x	

C6H11		x	**C10H9**	x	x
C6H13		x	**C10H10**	x	x
C7H	x		**C10H11**		x
C7H2	x		**C11**	x	
C7H3	x		**C11H**	x	
C7H4	x		**C11H2**	x	
C7H5	x		**C11H3**	x	
C7H6	x		**C11H4**	x	
C7H7		x	**C11H5**	x	
			C11H6	x	

Table S1.2. Major positive secondary ion peaks for PHEMA control and HEMA polymer brushes grown on plasma polymerized M3BP, M2CP, E2FP and CEMA surface coatings via SI-ARGET ATRP. Major peaks from PHEMA standard spectra that appear on ARGET ATRP surfaces are outlined in red.

			Intensity normalized to total counts					
Mass	**Structure**	**Accuracy (ppm)**	**PHEMA**	**Glass**	**CEMA**	**E2FP**	**M2CP**	**M3BP**
22.99	Na^+	2.25	0.031	0.049	0.002	0.001	0.000	0.009
27.98	Si^+	-7.30	0.161	0.004	0.000	0.000	0.000	0.000
43.02	$C_2H_3O^+$	9.02	0.015	0.026	0.043	0.041	0.038	0.028
45.03	$C_2H_5O^+$	12.16	0.024	0.045	0.071	0.086	0.074	0.053
55.02	$C_3H_3O^+$	-3.42	0.003	0.004	0.006	0.005	0.005	0.006
56.02	$C_3H_4O^+$	-5.41	0.001	< 0.001	0.002	0.002	0.002	0.001
57.03	$C_3H_5O^+$	9.69	0.002	0.002	0.004	0.003	0.003	0.003
61.03	$C_2H_5O_2^+$	-2.60	0.000	< 0.001	0.001	0.001	0.001	0.000
69.03	$C_4H_5O^+$	8.65	0.028	< 0.001	0.047	0.057	0.049	0.036
71.05	$C_4H_7O^+$	9.06	0.001	< 0.001	0.004	0.004	0.003	0.003
83.05	$C_5H_7O^+$	9.54	0.001	< 0.001	0.002	0.002	0.002	0.002
85.03	$C_4H_5O_2^+$	-7.56	0.001	< 0.001	0.002	0.002	0.002	0.001
87.04	$C_4H_7O_2^+$	-5.77	0.002	< 0.001	0.008	0.010	0.009	0.007
113.06	$C_6H_9O_2^+$	9.36	0.014	< 0.001	0.019	0.022	0.020	0.014

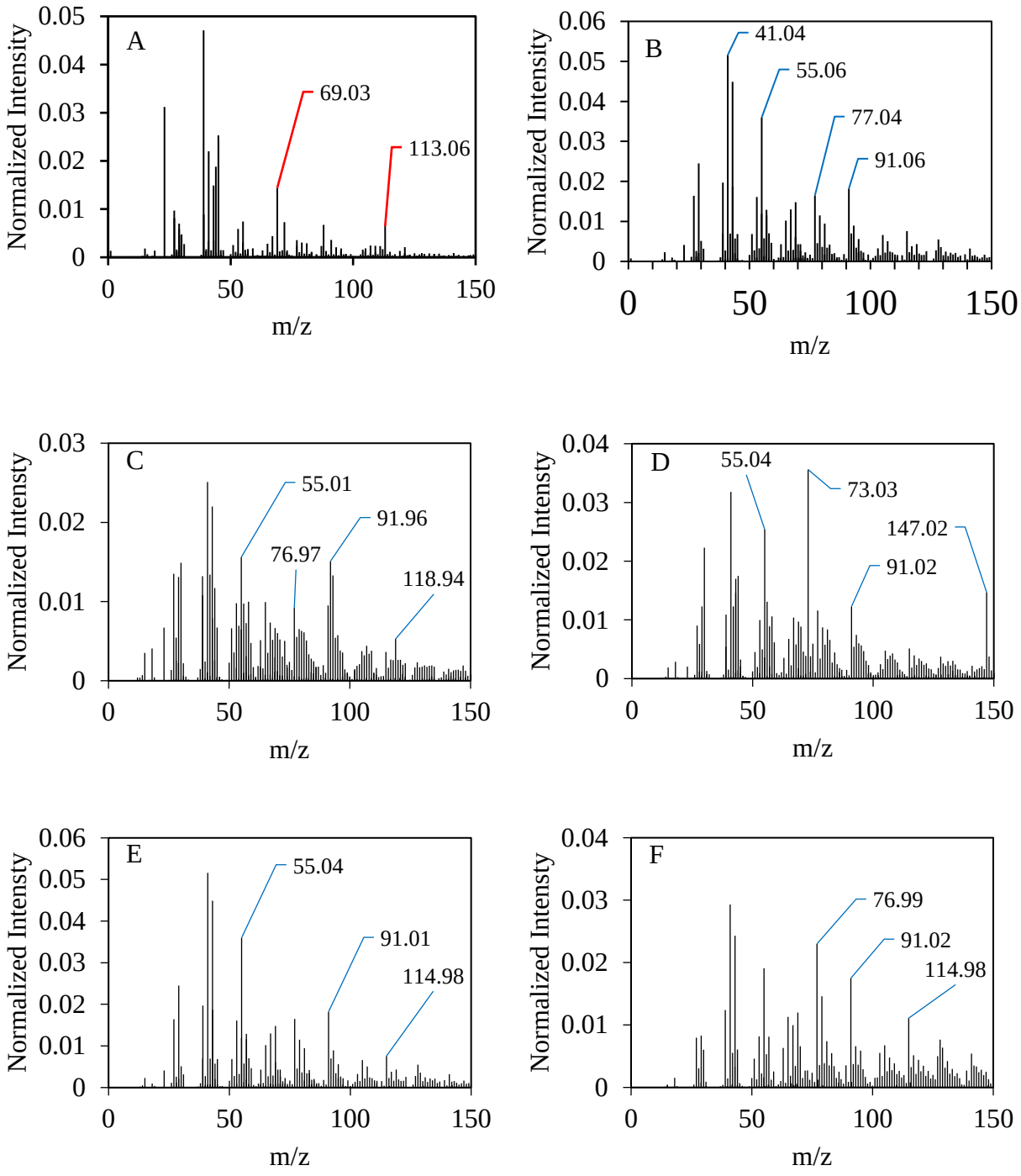

Figure S1.2. Lack of HEMA peaks on plasma polymerized haloester coatings in the absence of copper (II) bromide. Representative ToF-SIMS spectra of HEMA polymer brushes grown on plasma polymerized (C) M3BP (D) M2CP (E) E2FP and (F) CEMA surfaces via surface initiated ARGET ATRP in the absence of $CuBr_2$ for 2 h. No major peaks from pHEMA can be seen in these treatment groups indicating that no pHEMA chain growth has occurred. Since $CuBr_2$ is crucial as a catalyst for the ARGET ATRP reaction these results suggest that we are growing HEMA polymer brushes via SI ARGET ATRP reaction. A pHEMA hydrogel was used as positive control (A) while

a glass disc without surface initiator is used as a negative control (B). Peak intensities are normalized to the total intensity of the spectra. Major positive secondary ions are labelled. Spectra were taken in triplicate from 3 sample regions over a 500 x 500 micron analysis area, maintain the primary ion dose density below $2x10^{12}$ ions/cm^2 with Bi_3^+ species.

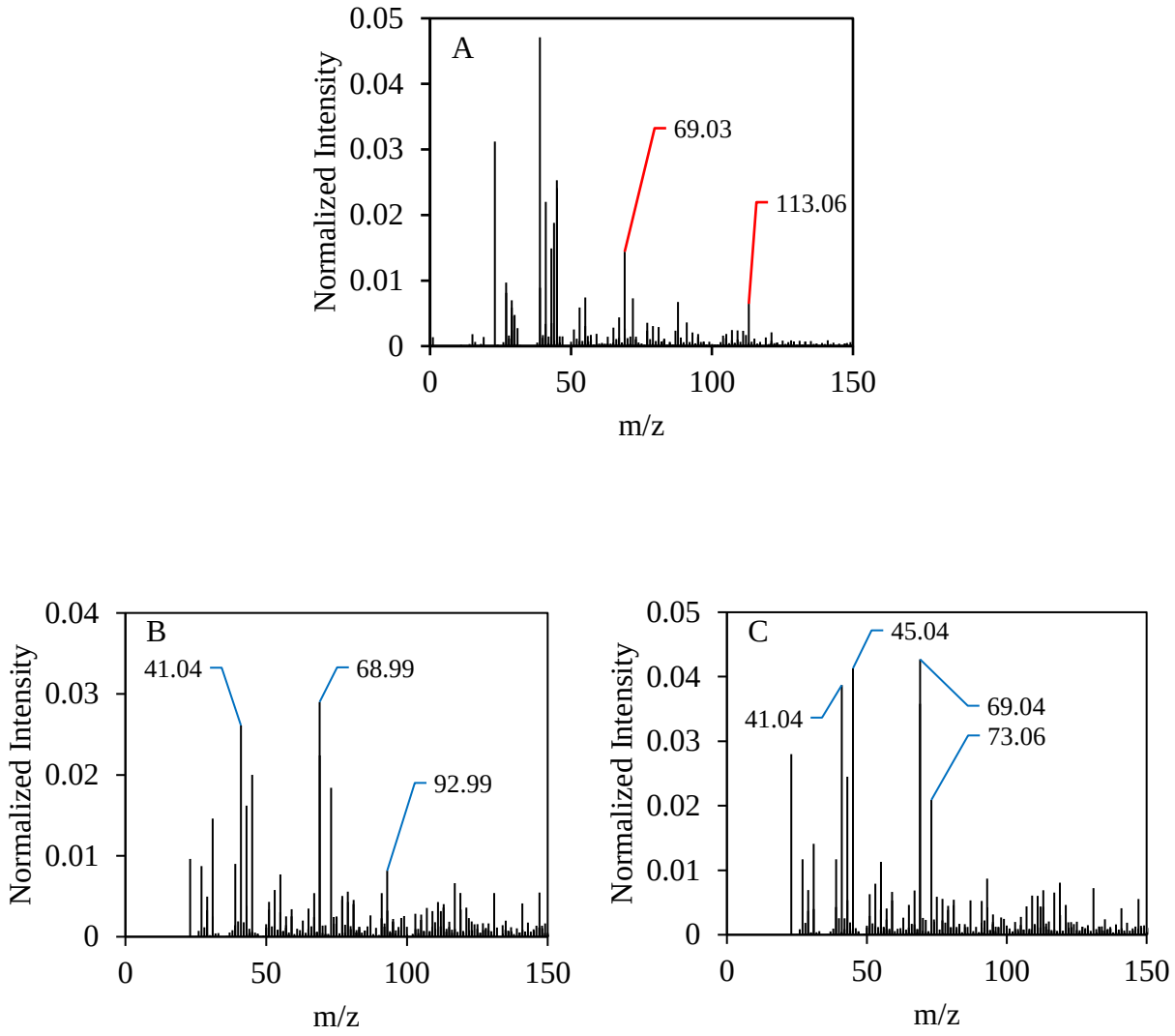

Figure S1.3. Lack of HEMA peaks on plasma polymerized fluoro coatings in the presence as well as in the absence of $CuBr_2$. Representative ToF-SIMS spectra of HEMA polymer brushes grown on plasma polymerized C3F6 surfaces via surface initiated ARGET ATRP in the (A) presence and (B) absence of $CuBr_2$ for 2 h. No major peaks from pHEMA can be seen in these treatment groups indicating that no pHEMA chain growth has occurred. The results from this suggest that plasma polymerized E2FP coatings is unique in its ability to grow HEMA polymers brushes compared to other plasma polymerized fluoro surfaces. A pHEMA hydrogel was used as positive control (A). Peak intensities are normalized to the total intensity of the spectra. Major positive secondary ions are labelled. Spectra were taken in triplicate from 3 sample regions over a 500 x 500 micron analysis area, maintain the primary ion dose density below $2x10^{12}$ ions/cm^2 with Bi_3^+ species.

Chapter 2

QUASI-ZWITTERIONIC SURFACE COATINGS PREPARED BY RADIO FREQUENCY GLOW-DISCHARGE PLASMA REDUCE PROTEIN ADSORPTION

Marvin M. Mecwan[1] and Buddy D. Ratner[1,2]

1 Department of Bioengineering, University of Washington, Seattle, WA 98195

2 Department of Chemical Engineering, University of Washington, Seattle, WA 98195

2.1 ABSTRACT

A majority of current arteriovenous (AV) vascular grafts for hemodialysis fail within one or two years of implantation. Zwitterionic polymers are non-fouling in nature and have great potential to be used in vascular grafts to prevent complications associated with stenosis and thrombosis. The authors describe a new technique for copolymerizing monomers with different charges to create quasi-zwitterionic or mixed-charge surfaces with low-fouling properties using radio frequency (RF) glow-discharge plasma. A mini-library of quasi-zwitterionic or mixed-charged were created using the following monomers in different ratios based on vapor pressure: methacrylic acid (MA) (-ve charge), acrylic acid (AA) (-ve charge), allylamine (AAmine) (+ve charge), N, N-dimethylallyamine (DMAA) (+ve charge), and 2-vinylpyridine (2VP) (+ve charge). I-125 rabiolabeled protein adsorption and substrate-based ELISA studies determined that all plasma polymerized quasi-zwitterionic surface coatings reduce protein adsorption compared to untreated controls. Specifically as the bulk ratio of COO peaks to CN/CO peaks (determined by hi-res C1s XPS spectra) increased, a decrease in protein adsorption was observed. This provides researchers with a new tool to fine tune mixed charge surfaces to achieve lower protein adsorption.

Furthermore, due to the versatility of RF glow discharge plasma, this process is scalable and can be used to coat the lumen surface of AV vascular graft and provide a low-fouling surface that would potentially prevent blood clots.

2.2 INTRODUCTION

End Stage Renal Disease (ESRD) is a growing concern worldwide and is expected to rise within the next decade.[44,45] In 2016, there were nearly 725,000 prevalent cases of ESRD within the United States alone and 63.1% of all ESRD patients received hemodialysis as a renal replacement therapy.[46] Vascular access or AV grafts is often needed for hemodialysis treatment which costs an average of $89,000 per patient annually in the United States, amounting to an annual hemodialysis cost of $42 billion in the US alone.[46] Furthermore, it has been reported that primary patency rates for AV grafts to be 40-50% at 1 year and about 26% at 18 months to 2 years,[47,48] and can result in re-hospitalization, more surgeries and sometimes even death of the patient.

One strategy to address this problem is to make the inner-lining of these vascular grafts non-fouling. RF glow-discharge plasma polymerization has historically been used to create uniform thin polymer films that are strongly bound to surfaces.[25–27] In the Ratner lab alone, RF glow-discharge plasma-treated surfaces have been used to create low fouling surfaces by the deposition of monomers such as tetraethylene glycol dimethyl ether or tetraglyme[34,49], and 2-hydroxyethyl methacrylate.[50] Due to the versatility of RF glow discharge plasma technology, this process is scalable and can be readily applied to any surface of interest with any geometry, such as AV grafts and other implants. Particularly, in one study, Cao et al. plasma treated polyethylene tubing with tetraglyme and were able to show unltralow fibrinogen adsorption and greatly reduced platelet adhesion in an ex vivo shunt sheep model.[51]

In recent years, zwitterionic materials such as poly(carboxybetaine) (pCB) and poly(sulfobetaine) (pSB) have been applied to a broad range of biomedical and engineering materials. Due to electrostatically induced hydration, surfaces coated with zwitterionic groups are highly resistant to nonspecific protein adsorption, bacterial adhesion, and biofilm formation.[52] Moreover, zwitterionic polymer hydrogels in mice have shown to resist foreign-body reaction.[53] For these reasons, zwitterionic materials are potentially good candidates for use in AV grafts. For successful plasma polymerization it is important that the monomer of interest be easily volatilized for introduction into the plasma reactor. Zwitterionic polymer precursors, such as carboxybetaine methacrylate (CBMA) and sulfobetaine methacrylate (SBMA), however, are solids with high boiling points which would not make them ideal for glow-discharge plasma treatment to coat AV graft lumen surfaces.

This study investigates the preparation of quasi-zwitterionic or mixed-charge surface coatings prepared by the simultaneous plasma deposition of a positively charged and negatively charged monomer, and its ability to act as a non-fouling surface was studied. Our monomers of choice for this research included: methacrylic acid (MA) (-ve charge), acrylic acid (AA) (-ve charge), allylamine (AAmine) (+ve charge), N, N-dimethylallyamine (DMAA) (+ve charge), and 2-vinylpyridine (2VP) (+ve charge). We hypothesize that these quasi-zwitterionic coatings or mixed-charge surfaces would lead to a new generation of surfaces that would resist nonspecific protein adsorption similar to zwitterionic polymers. To this end, we will be assessing the chemical composition and stability using X-ray photoelectron spectroscopy (XPS), the protein fouling characteristics using I-125 radiolabeling protein studies as well as substrate-based ELISA methods, and the cell cytotoxicity of NIH-3T3 mouse fibroblasts to assess the toxicology and cell compatibility of these surface coatings. Moreover, since RF plasma technology can coat almost

any type of surface at an industrial scale, this technology should be easily translatable to meet medical device industry needs for commercialization purposes.

2.3 EXPERIMENT

2.3.1 Plasma deposition, surface characterization and protein studies on quasi-zwitterionic surface coatings

2.3.1.1 Materials

8mm glass coverslips were purchased from Knitell Glass (Cat. No. G401-08). Allylamine (AAmine) (Cat. No. 145831), N, N-dimethylallylamine (DMAA) (Cat. No. 05937) and acrylic acid (AA) (Cat. No. 147230) were purchased from Sigma-Aldrich. All organic solvents were purchased from Fisher Scientific. For the radiolabeled protein studies, bovine IgG (Cat. No. I5506), sodium azide (Cat. No. S2002), and sodium iodide (Cat. No. 383112) were purchased from Sigma-Aldrich. Boric acid (Cat. No. A73-500), sodium phosphate monobasic (Cat. No. S369-500), and sodium hydroxide (Cat. No. S399-500) were purchased from Fisher Scientific. Sodium chloride crystals (Cat. No. SX0420-3) was purchased from EMD Millipore. Citric Acid, Monohydrate (Cat. No. 0115-01) was purchased from J.T. Baker. Iodine-125 radionuclide (Specific Activity: ~17Ci/mg, 10^{-5}M NaOH (pH 8-11)) was purchased from Perkin-Elmer (Cat. No. NEZ033A).

2.3.1.2 Plasma polymerization

Prior to plasma deposition, 8mm glass coverslips were placed in a sample holder within a glass container and ultrasonicated in a water bath for two 10 min cycles each in methylene

chloride, followed by acetone and then methanol. All samples were air-dried in a fume hood before use.

Plasma polymerization was carried out in a custom-built plasma reactor setup based on the design reported in Lopez et al[34] and was modified to have two inlets which allowed for the flow of two monomers into the plasma chamber (Figure 2.1). Cleaned glass coverslips were loaded in the plasma reactor and positioned in between the powered and grounded electrodes (100 mm apart), and a mechanical pump was used evacuate the reactor to the desired base pressure in the low 10^{-3} Torr range. A liquid nitrogen cooled cold trap between the vacuum pump and the reactor was used to condense organic materials. The powered electrode was connected to a 13.56 MHz radio frequency power source and an automatic impedance matching network. The coverslips were first etched in argon gas for 10 min at 40W while maintaining a pressure of 250 mT. Following that, substrates were either coated with AA, AAmine or DMAA for 1 min at 80 W in order to form an adhesion layer, after which the power was lowered to 10W for 10 min, while maintaining a pressure of 150 mT for the monomer throughout the plasma deposition process. Upon retrieval, samples were flipped, and the plasma treatment process was repeated with the same parameters to ensure uniform coatings on both sides of samples.

In order to form quasi-zwitterionic samples, a negatively charged monomer (AA) was connected to one inlet while a positively charged monomer (either AAmine or DMAA) was connected to the other inlet (Figure 2.1). Following the argon etching process, and methane plasma deposition, glass coverslips were coated with either equal vapor pressure parts of AAmine and AA (AA:AAmine 1:1) or DMAA and AA (AA:DMAA 1:1) or 2 parts AAmine and 1 part AA (AA:AAmine 1:2) or 1 part AAmine and 2 parts AA (AA:AAmine 2:1) and the

pressure was maintained at 150mT. The plasma polymerization parameters were exactly the same: 80W for 1 min, and 10W for 10 min, followed by quenching for 5 min. Samples were then flipped and the process was repeated on the opposite side.

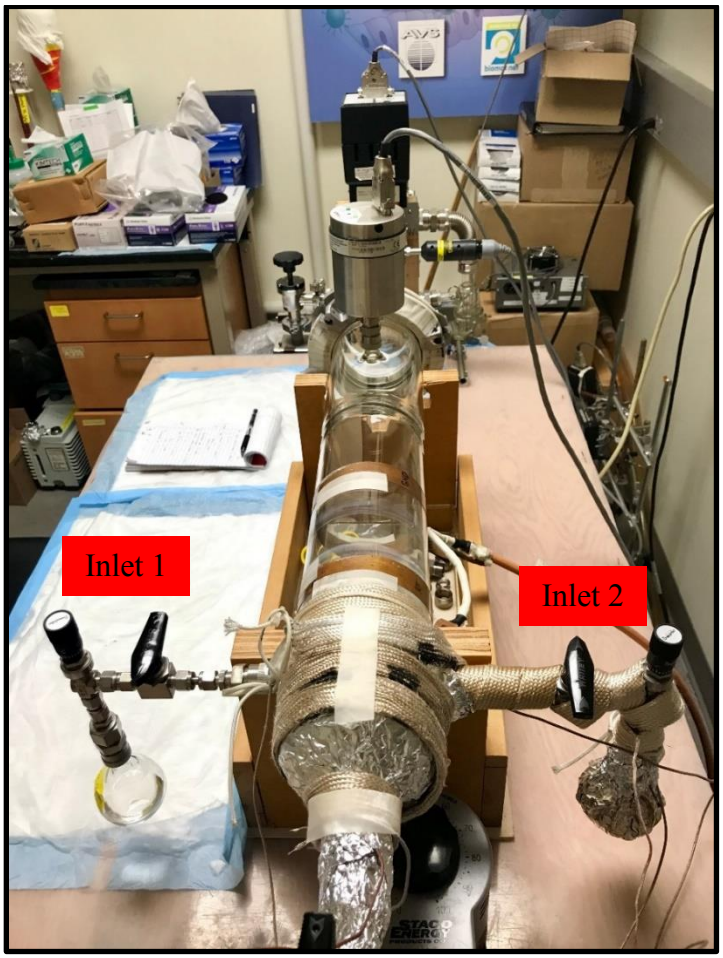

Figure 2.1. Custom-built plasma reactor setup with two inlets which allows for the controlled flow of two monomers into the plasma chamber using vernier caliper valves.

2.3.1.3 Surface characterization

X-ray photoelectron spectroscopy (XPS) was performed on all plasma polymerized glass disc samples on a Surface Science Instruments S-Probe equipped with a monochromatic Al Kα

source and a low energy electron flood gun for charge neutralization. X-ray analysis for these acquisitions was in a circle approximately 800 µm across. Pressure in the analytical chamber during spectral acquisition was less than 5 x 10^{-9} Torr. Low-resolution survey scans were obtained from 0 to 1100 eV with a 1 eV step size and pass energy of 150 eV. High resolution C 1s scans were obtained from 270 to 290 eV with a 0.065 eV step size and pass energy of 50 eV. The spectra were analyzed off line with Service Physics Hawk version 7 data analysis software to calculate the elemental compositions from peak areas and to peak fit high resolution spectra. All binding energies were calibrated with reference to the aliphatic carbon at C 1s = 285.0 eV. A Shirley background was used for all spectra.

2.3.1.4 I-125 radiolabeled protein studies

Bovine IgG was radiolabeled using the iodine monochloride (ICl) method modified by Horbett.[54] Briefly, 1mCi of Iodine-125 radionuclide was added to 0.5 mL 2x borate solution, to which 0.5 mL of ICl/NaCl mixture in a 2:1 ratio was added. Finally, 0.5 mL of a 10 mg/mL bovine IgG in a citrate phosphate buffered saline solution with sodium azide (cPBSz) was added and the iodination reaction was performed on ice for 20 min and then run through a size exclusion chromatography column. 40 fractions were collected to capture the labeled protein and free iodine peaks to evaluate iodination efficiency. The fractions from protein peaks were pooled together and run through a second chromatography column, repeating fraction collection and peak identification. Purified radiolabeled protein fractions were pooled together, placed in a lead pig, and frozen in -80^0C freezer until further use.

Prior to the protein adsorption studies, all quasi-zwitterionic plasma treated substrates (n=4) were soaked in 0.5mL cPBS solution with 10mM NaI (cPBSzI) for 30 min. For the

adsorption, the radiolabeled bovine IgG was thawed and then added to a 0.2 mg/mL solution of bovine IgG in cPBSzI to create “hot IgG” protein with an activity ~100 CPM/ng. 0.5 mL of the “hot IgG” protein was then added to each sample and allowed to adsorb for 2 h before rinsing three times with cPBSzI using a rinsing system. The samples were then transferred to a gamma counter tube and the radioactivity of each sample was then measured for 1 min along with protein standards using a Packard Cobra 2 Gamma Counter. Untreated glass coverslips were used as controls. Adsorption data were reported in ng/cm^2.

2.3.1.5 Cytotoxicity studies

NIH-3T3 mouse fibroblasts were used to determine if the quasi-zwitterionic plasma coatings were cytotoxic. Plasma treated samples (n=3) were placed in 24-well plates aseptically with 2 mL of complete growth medium (DMEM-high glucose + 1 v% L-glutamine + 1 v% antibiotic/antimycotic + 10 v% fetal bovine serum) and allowed to elute for 24 h at 37^{o}C. After 24 h of elution, 1 mL eluates were transferred from the plasma treated substrates to the sub-confluent cultured cells. MTT cell proliferation assay was performed at 24 h and LIVE/DEAD staining was performed at 48 h. For the MTT assay, samples were incubated with MTT reagent for 3 h at 37^{o}C. After incubation, cells were treated with MTT solvent for 15 min at room temperature, and absorbance was measured at 590 nm. For the LIVE/DEAD assay, sample wells were aspirated and the combined LIVE/DEAD assay reagents were added and allowed to incubate for 30 min at room temperature and then imaged using a fluorescence microscope. Tissue culture polystyrene (TCPS) was used a positive control and latex was used as a negative control.

2.3.2 Plasma deposition and protein studies on a mini-library of quasi-zwitterionic surface coatings

2.3.2.1 Materials

Methacrylic acid (MA) (Cat. No. 79-41-4) was purchased from Acros Organics. 2-vinylpyridine (2VP) (Cat. No. 100-69-6) was purchased from Sigma-Aldrich. Human fibrinogen (Fg) 100% clottable, plasminogen, von willebrand factor and fibronectin depleted (Cat. No. FIB 3) was purchased from Enzyme Research Laboratories.

2.3.2.2 Plasma polymerization

Plasma polymerization was carried out similar to the methods described in 2.3.1.2. The same reactor in Figure 2.1 was used for the plasma polymerization. Briefly, cleaned glass coverslips were loaded in the plasma reactor and positioned in between the powered and grounded electrodes (100 mm apart), and a mechanical pump was used evacuate the reactor to the desired base pressure in the low 10^{-3} Torr range. A liquid nitrogen cooled cold trap between the vacuum pump and the reactor was used to condense organic materials. The powered electrode was connected to a 13.56 MHz radio frequency power source and an automatic impedance matching network. The coverslips were first etched in argon gas for 10 min at 40W while maintaining a pressure of 250 mT. Following that, substrates were either coated with MA, AA, AAmine, DMAA and 2VP for 1 min at 80 W in order to form an adhesion layer, after which the power was lowered to 10W for 10 min, while maintaining a pressure of 150 mT for the monomer throughout the plasma deposition process. Upon retrieval, samples were flipped, and

the plasma treatment process was repeated with the same parameters to ensure uniform coatings on both sides of samples.

In order to form quasi-zwitterionic surface coatings, a negatively charged monomer (either AA or MA) was connected to one inlet while a positively charged monomer (either AAmine or DMAA or 2VP) was connected to the other inlet. Following the argon etching process glass coverslips were coated in the vapor pressure ratios laid out in Table 2.1 and the pressure was maintained at 150 mT. The plasma polymerization parameters were exactly the same: 80 W for 1 min, and 10W for 10 min, followed by quenching for 5 min. Samples were then flipped and the process was repeated on the opposite side.

Table 2.1. Mini-library of quasi-zwitterionic surface coating compositions prepared by varying the ratio of vapor pressures of the monomers introduced into the plasma reactor.

Quasi-zwitterionic surface coatings	Monomers (in vapor pressure parts)				
	MA	AA	AAmine	DMAA	2VP
MA:DMAA 1:1	1	-	-	1	-
MA:DMAA 1:2	1	-	-	2	-
MA:DMAA 2:1	2	-	-	1	-
MA:DMAA 1:3	1	-	-	3	-
MA:DMAA 3:1	3	-	-	1	-
AA:AAmine 1:1	-	1	1	-	-
AA:AAmine 1:2	-	1	2	-	-
AA:AAmine 2:1	-	2	1	-	-
MA:2VP 1:1	1	-	-	-	1
MA:2VP 1:1.5	1	-	-	-	1.5
MA:2VP 1.5:1	1.5	-	-	-	1

2.3.2.3 Protein iodination using ICl method

HSA was radiolabeled using the iodine monochloride (ICl) method modified by Horbett.[54] Briefly, 1mCi of Iodine-125 radionuclide was added to 0.5mL 2x borate solution, to which 0.5 mL of ICl/NaCl mixture in a 3:1 ration was added for bovine IgG and HSA respectively. Finally, 0.5 mL of a 10 mg/mL HSA in 1x borate solution (pH 8.0) was added and the iodination reaction was performed on ice for 20 min and then run through a size exclusion chromatography column. 40 fractions were collected to capture the labeled protein and free iodine peaks to evaluate iodination efficiency. The fractions from protein peaks were pooled together and run through a second chromatography column, repeating fraction collection and peak identification. Purified radiolabeled protein fractions were pooled together, placed in a lead pig, and frozen in -80^0 C freezer until further use.

2.3.2.4 I-125 radiolabeled HSA protein adsorption on MA-DMAA family of quasi-zwitterionic coatings

Prior to the protein adsorption studies, a family of MA-DMAA quasi-zwitterionic coatings, namely MA:DMAA 1:1, MA:DMAA 1:2, MA:DMAA 2:1, MA:DMAA 1:3, and MA:DMAA 3:1 (n = 4) were soaked in 0.75 mL cPBS solution with 10mM NaI (cPBSzI) for 30 min. For the adsorption, the radiolabeled HSA was thawed and then added to a 0.6 mg/mL solution of HSA in cPBSzI to create "hot HSA" protein with an activity ~100 CPM/ng. 0.75 mL of the "hot HSA" protein was then added to each sample and allowed to adsorb for 2 h before rinsing three times with cPBSzI using a rinsing system. The samples were then transferred to a gamma counter tube and the radioactivity of each sample was then measured for 1 min along with protein standards using a Packard Cobra 2 Gamma Counter. Untreated glass coverslips were

used as controls, while MA and DMAA plasma coated substrates were used as references. Adsorption data was reported in ng/cm^2.

2.3.2.5 I-125 radiolabeled HSA protein adsorption (competitive binding with Fg) on MA-2VP family of quasi-zwitterionic coatings

Prior to the protein adsorption studies, a family of MA-2VP quasi-zwitterionic coatings, namely MA:2VP 1:1, MA:2VP 1:1.5, and MA:2VP 1.5:1 (n = 4) were soaked in 0.75 mL cPBS solution with 10mM NaI (cPBSzI) for 30 min. For the adsorption, the radiolabeled HSA was thawed and then added to a binary solution containing both HSA (0.6 mg/mL) and Fg (0.06 mg/mL) in cPBSzI to create "hot binary HSA" protein with an activity ~100 CPM/ng. 0.75 mL of the "hot binary HSA" protein was then added to each sample and allowed to adsorb for 2 h before rinsing three times with cPBSzI using a rinsing system. The samples were then transferred to a gamma counter tube and the radioactivity of each sample was then measured for 1 min along with protein standards using a Packard Cobra 2 Gamma Counter. Untreated glass coverslips were used as controls, while MA and DMAA plasma coated substrates were used as references. Adsorption data was reported in ng/cm^2.

2.3.2.6 Substrate-based direct ELISA on AA-AAmine family of quasi-zwitterionic coatings

Prior to the substrate based ELISA study, a family of AA-AAmine quasi-zwitterionic coatings, namely AA:AAmine 1:1, AA:AAmine 1:2 and AA:AAmine 2:1 (n = 3) were soaked in 0.75 mL cPBS solution for 1 h. To this, 0.75 mL a 0.2 mg/mL solution of bovine IgG in cPBS was added to each sample and allowed to adsorb for 2 h before rinsing three times with wash

buffer. The samples were then blocked using 1 mL of 1x assay diluent, followed by rinsing three times with the wash buffer. Samples were transferred to new sample cups. 1 mg/mL solution of goat anti-bovine IgG conjugated with HRP was diluted 1:10,000 in 1x assay diluent, and 1 mL was then added to each sample and allowed to bind to the adsorbed bovine IgG on the surface for 30 min before rinsing five times with wash buffer. Samples were once again transferred to new sample cups and 1x TMB substrate was then added, allowed to incubate at room temperature for 2 min and the reaction was stopped using 0.5 mL of 1 N phosphoric acid. 150 μL of the yellow colored solution was then transferred to a clear 96 well plate and the absorbance of each well was read at 450 nm and the absorbance at 570 nm was subtracted from each well. Untreated glass coverslips were used as controls, while AA and AAmine plasma coated substrates were used as references. Absorbance data was reported in AU.

2.4 Results and Discussion

The goal of this research was to develop new surface coatings that would mimic the non-fouling properties of zwitterionic polymers and could be used to line the lumen of AV grafts and thus prevent thrombosis in the long run. To this end, we used RF glow-discharge plasma technology to prepare a range of quasi-zwitterionic plasma by copolymerizing a positively charged and a negatively charged monomer in different vapor pressure ratios. Once prepared, we then assessed the chemical composition, stability, protein adsorption and safety (toxicology) of these quasi-zwitterionic or mixed-charge surface coatings.

In order to test the feasibility of copolymerizing positive and negative charged monomers using RF glow-discharge plasma to create quasi-zwitterionic or mixed-charge surface coatings we used AA, AAmine and DMAA as our test monomers. XPS was used to assess the surface of

these plasma polymerized quasi-zwitterionic samples. The survey scans seen in Figure 2.2, and summarized in Table 2.2, provide information on the overall surface chemical composition. For these quasi-zwitterionic plasma polymerized coatings we found that the overall chemical composition matched the expected composition reasonably well (Table 2.2). It should, however, be noted that both AAmine and DMAA plasma coatings had small amounts of oxygen on the surface. Moreover, no peaks associated with the substrates were seen in the scans, which indicate that the plasma coatings were greater than 10nm in thickness, as this is the depth to which ESCA is able to analyze a surface. However, further experiments will need to be conducted to determine the thickness of the plasma coatings using either ellipsometry or profilometry.

High resolution C 1s spectra (Figure 2.3) provides insight into the chemical bonding environment of carbon. All plasma coatings showed characteristic shifts in the carbon peaks based on the chemical structure of the monomer. As seen in Figure 2.3 A-C, the shape and features of the high-resolution C1s peak of plasma polymerized AA, AAmine and DMAA allowed us to use two width-constrained peaks to fit the high resolution C1s peak corresponding to different bonding environments: CH (285eV) and COO (~289eV) for AA, and CH (285eV) and C—N (~287eV) for AAmine and DMAA. For the copolymers or quasi-zwitterionic surface coatings, the shape and features of the high-resolution C1s peak allowed us to use three width-constrained peaks corresponding to different bonding environments: CH (285eV), C—N and/or C—O (~287eV), and COO (~289eV) (Figure 2.3 D-G). The third peak seen in the high resolution spectra of the quasi-zwitterionic surface coatings is indication that the two initial monomers have copolymerized. It should also be noted that all XPS spectra were shifted so that the hydrocarbon peak could align at 285.0 eV (charging binding energy correction).

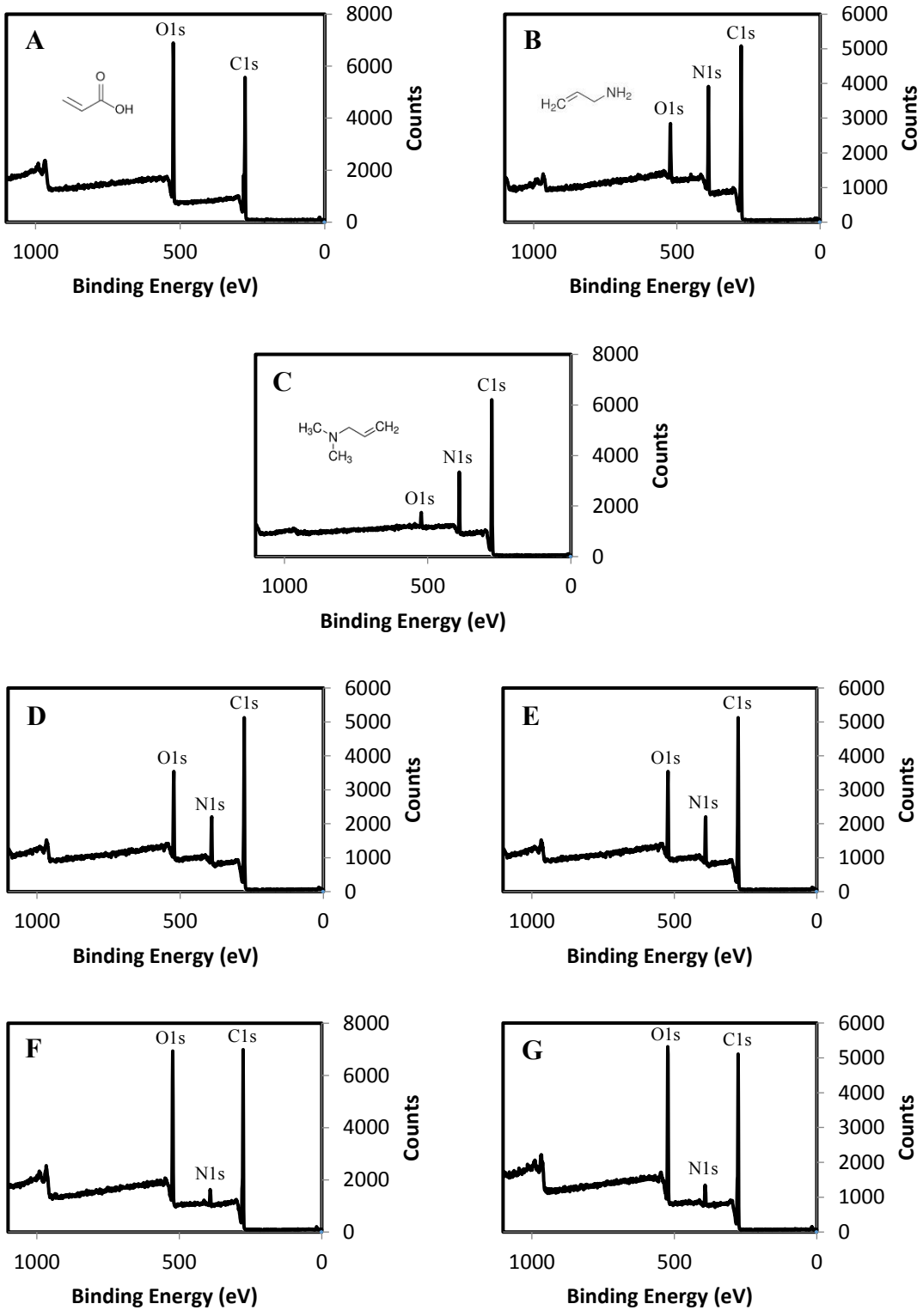
A
O1s
C1s
O
OH
8000
6000
4000
2000
0
Counts
1000
500
0
Binding Energy (eV)
B
C1s
N1s
O1s
H2C
NH2
6000
5000
4000
3000
2000
1000
0
Counts
1000
500
0
Binding Energy (eV)
C
C1s
H3C
N
CH3
CH2
N1s
O1s
8000
6000
4000
2000
0
Counts
1000
500
0
Binding Energy (eV)
D
C1s
O1s
N1s
6000
5000
4000
3000
2000
1000
0
Counts
1000
500
0
Binding Energy (eV)
E
C1s
O1s
N1s
6000
5000
4000
3000
2000
1000
0
Counts
1000
500
0
Binding Energy (eV)
F
O1s
C1s
N1s
8000
6000
4000
2000
0
Counts
1000
500
0
Binding Energy (eV)
G
O1s
C1s
N1s
6000
5000
4000
3000
2000
1000
0
Counts
1000
500
0
Binding Energy (eV)

Figure 2.2. Representative XPS survey scans and corresponding monomer chemical structures (inset) of plasma polymerized (A) AA (B) AAmine (C) DMAA (D) AA:AAmine 1:1 (E) AA:AAmine 1:2 (F) AA:AAmine 2:1 and (G) AA:DMAA 1:1 on glass coverslips. Major elemental peaks are labeled in each survey scan.

Table 2.2. Summary of surface elemental composition of plasma polymerized quasi-zwitterionic surface coatings as determined by survey scans obtained from XPS.

Plasma coating		Elemental Composition (%)		
		C	**O**	**N**
AA	Observed	**68.9**	**31.1**	**-**
	Expected	60	40	-
AAmine	Observed	**71.3**	**8.4**	**20.3**
	Expected	75	-	25
DMAA	Observed	**80.0**	**3.2**	**16.8**
	Expected	83.3	-	16.7
AA:AAmine 1:1	Observed	**71.0**	**18.9**	**10.2**
	Expected	66.7	22.2	11.1
AA:AAmine 1:2	Observed	**72.3**	**14.1**	**13.6**
	Expected	69.2	15.4	15.4
AA:AAmine 2:1	Observed	**71.9**	**23.7**	**4.4**
	Expected	64.3	28.6	7.1
AA:DMAA 1:1	Observed	**70.0**	**24.7**	**5.4**
	Expected	72.7	18.2	9.1

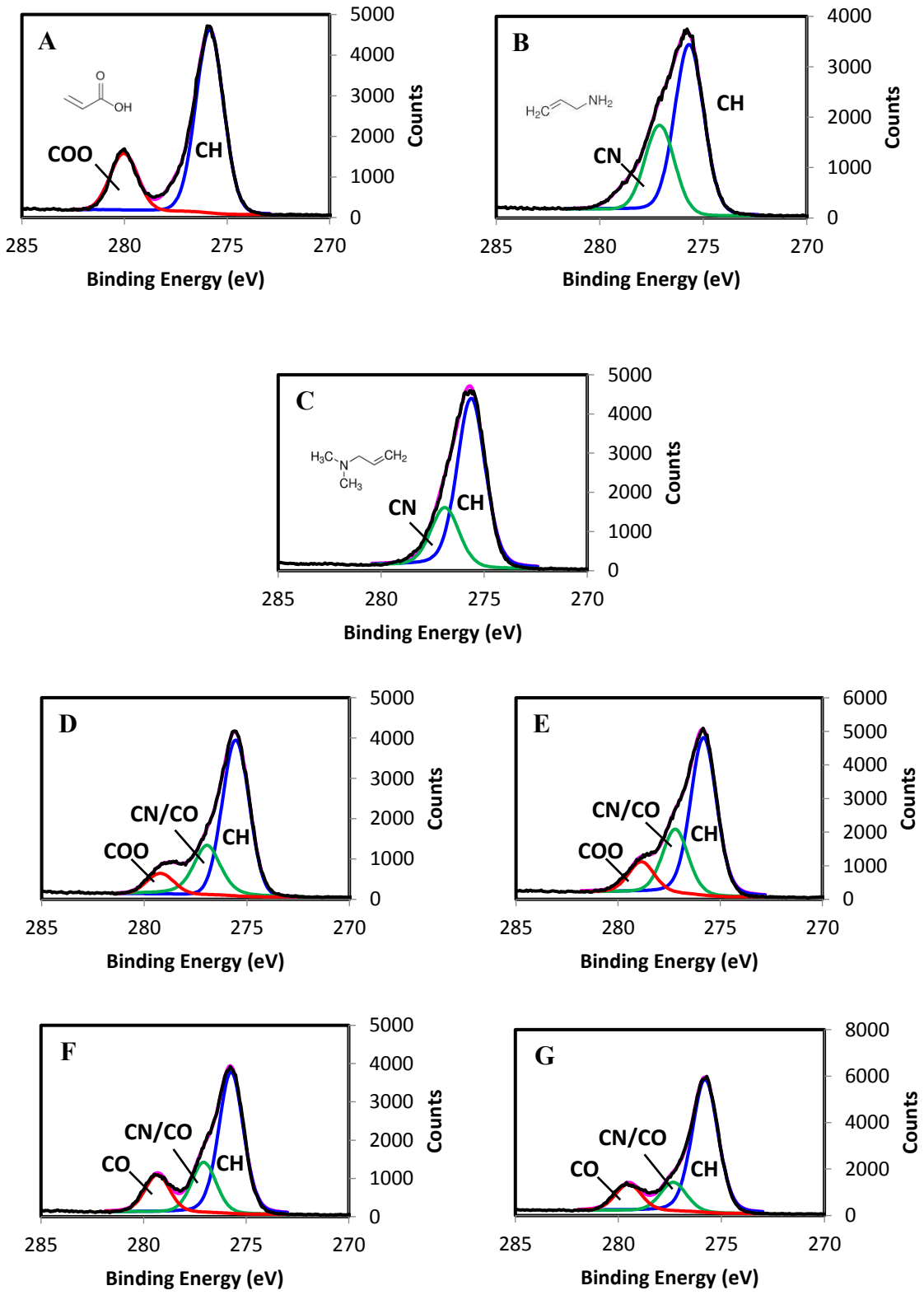

Figure 2.3. Representative high-resolution spectra of the C1s peak (black envelope) and corresponding monomer chemical structure (inset) of plasma polymerized (A) AA (B) AAmine

(C) DMAA (D) AA:AAmine 1:1 (E) AA:AAmine 1:2 (F) AA:AAmine 2:1 and (G) AA:DMAA 1:1 on glass coverslips. Fitted peaks are labeled to correspond to different bonding environments within each chemical structure.

In order to test the ability of these quasi-zwitterionic surface coatings to reduce protein adsorption, bovine IgG was used as a model protein, and was adsorbed to AA:AAmine 1:2, AA:AAmine 2:1, DMAA and AA:DMAA 1:1 for 2 h. Figure 2.3 depicts the results from the IgG protein adsorption study. As seen, all plasma polymerized quasi-zwitterionic coatings reduce bovine IgG protein adsorption compared to untreated glass controls. Of the quasi-zwitterionic surface coatings, AA:AAmine 2:1 and AA:DMAA 1:1 adsorb the least amount of IgG compared to AA:AAmine 1:2 and DMAA.

Finally, NIH-3T3 fibroblasts were used to determine whether plasma polymerized quasi-zwitterionic coatings were cytotoxic. For these studies we only assessed the cytotoxicity of AA, AAmine and AA:AAmine 1:1. As seen in Figure 2.5, for both MTT cell viability assay as well as LIVE/DEAD staining, this set of quasi-zwitterionic surface coatings performed better or comparable to the TCPS positive control.

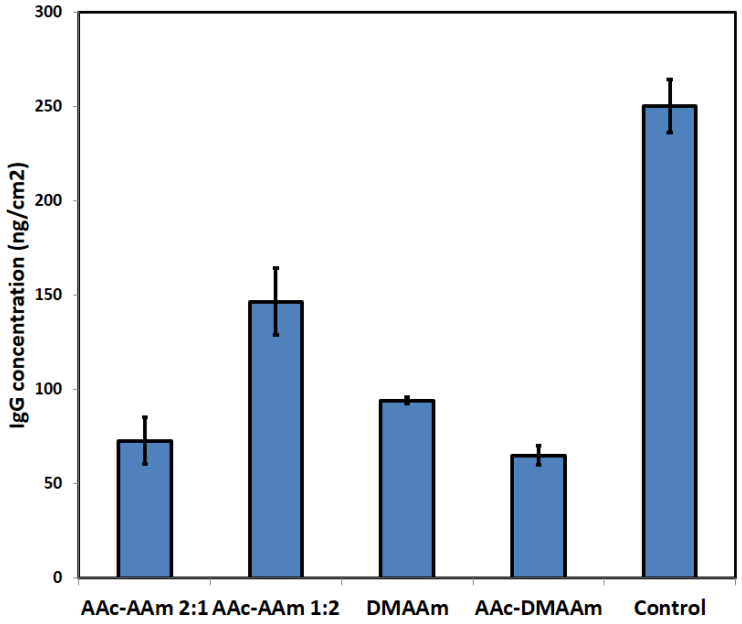

Figure 2.4. Amount of bovine IgG adsorbed onto plasma polymerized quasi-zwitterionic surface coatings AAc:AAmine 2:1, AAc:AAm 1:2, DMAA, AA:DMAA 1:1 and glass controls after 2 h in a 0.1 mg/mL bovine IgG as determined by I-125 radiolabeling method.

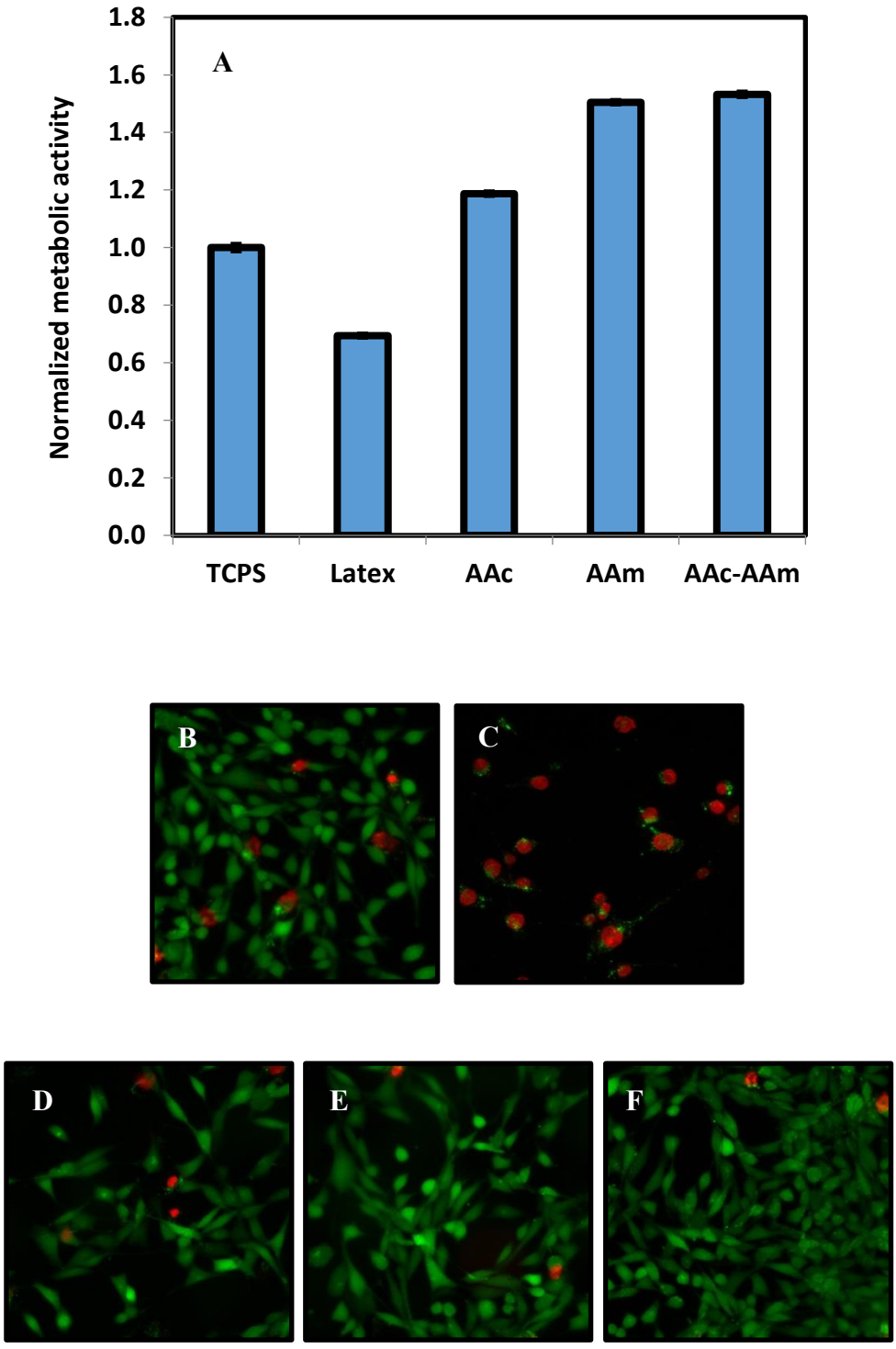

Figure 2.5. MTT Cell Viability assay at 24 h (A) and LIVE/DEAD cell staining at 48 h of (B) TCPS control (C) Latex control, and plasma polymerized (D) AA (E) AAmine (F) AA:AAmine 1:1.

These positive initial results led us to create a mini-library of quasi-zwitterionic surface coatings as laid out in Table 2.1 and to test their ability to reduce protein adsorption. We used a variety of protein studies to test different families of quasi-zwitterionic surface coatings. Figure 2.6 depicts the results from the HSA adsorption study on the family of MA-DMAA quasi-zwitterionic surface coatings. Figure 2.7 shows the results from the HSA competitive adsorption on the family of MA-2VP quasi-zwitterionic surface coatings in a binary solution with HAS and Fg. And finally, Figure 2.8 illustrates the results from the IgG protein activity on the family of AA-AAmine quasi-zwitterionic surface coatings. Since these three protein experiments are distinct, no direct comparison can be made between them. We do notice that in each of these protein studies there is one or two quasi-zwitterionic or mixed-charge surface coating which reduces protein adsorption better than all other treatment groups. However, no obvious trends are seen.

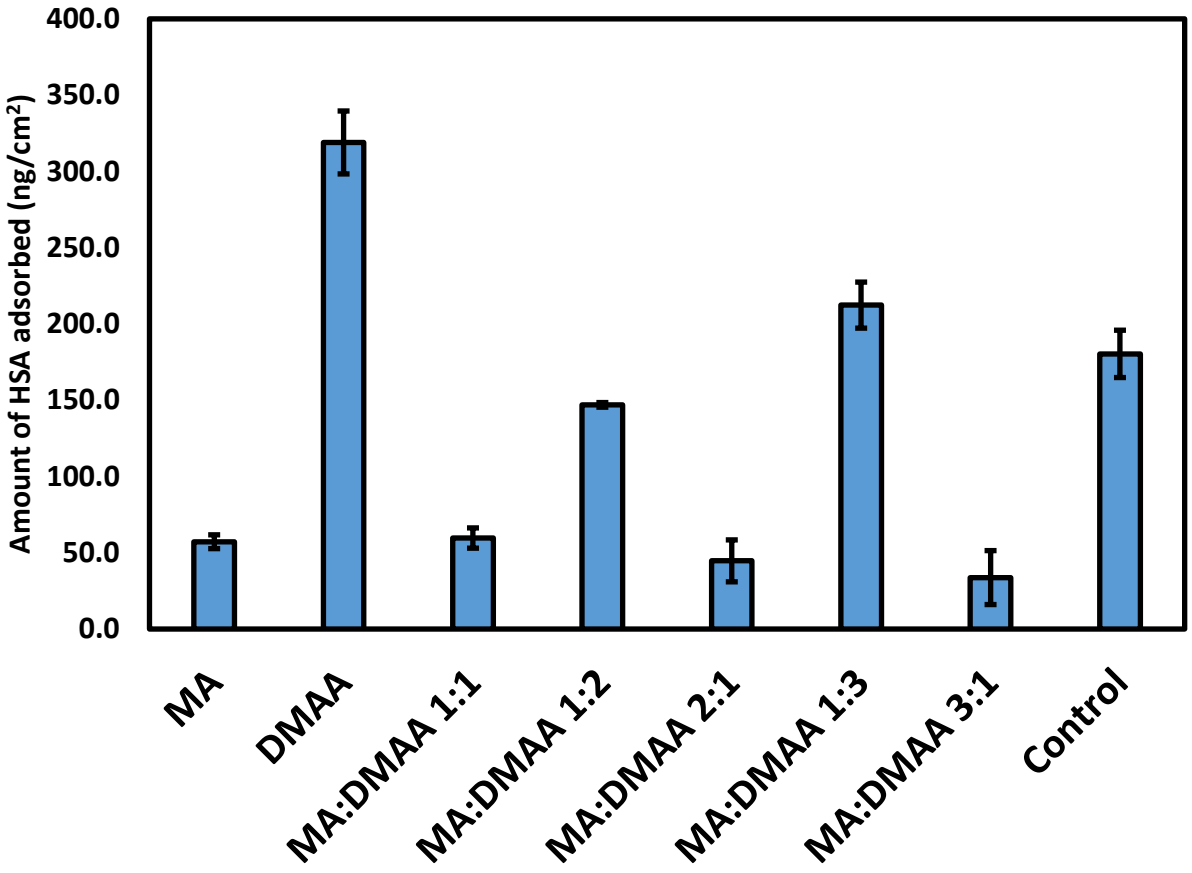

Figure 2.6. Amount of HSA adsorbed to plasma polymerized MA, DMAA, MA:DMAA 1:1, MA:DMAA 1:2, MA:DMAA 2:1, MA:DMAA 1:3, MA:DMAA 3:1 and glass control after 2 h in a 0.3 mg/mL HSA solution in CPBSzI as determined by I-125 radiolabeling method.

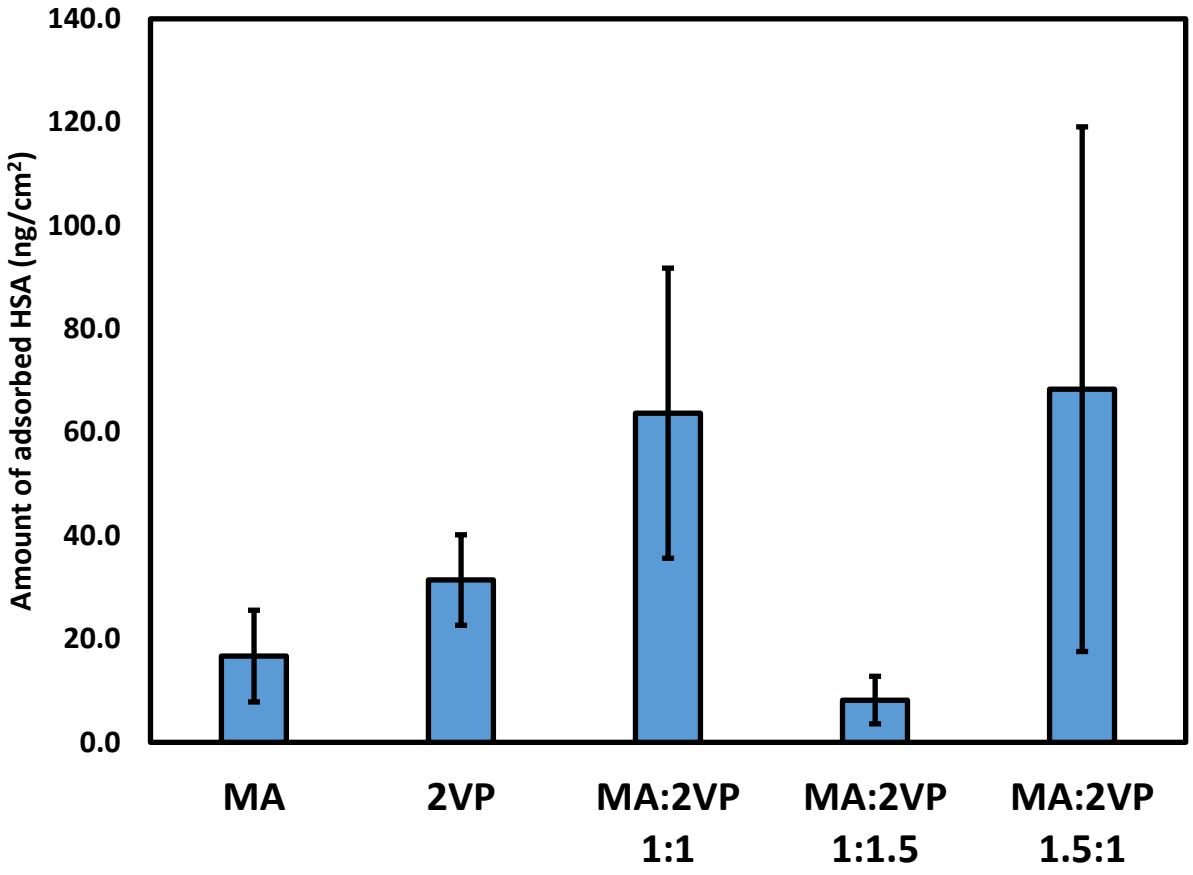

Figure 2.7. Amount of HSA competitively adsorbed to plasma polymerized MA, 2VP, MA:2VP 1:1, MA:2VP 1:1.5 and MA:2VP 1.5:1 after 2 h in a binary solution of HSA: 0.3 mg/mL and Fg: 0.03 mg/mL in cPBSzI as determined by I-125 radiolabeling method.

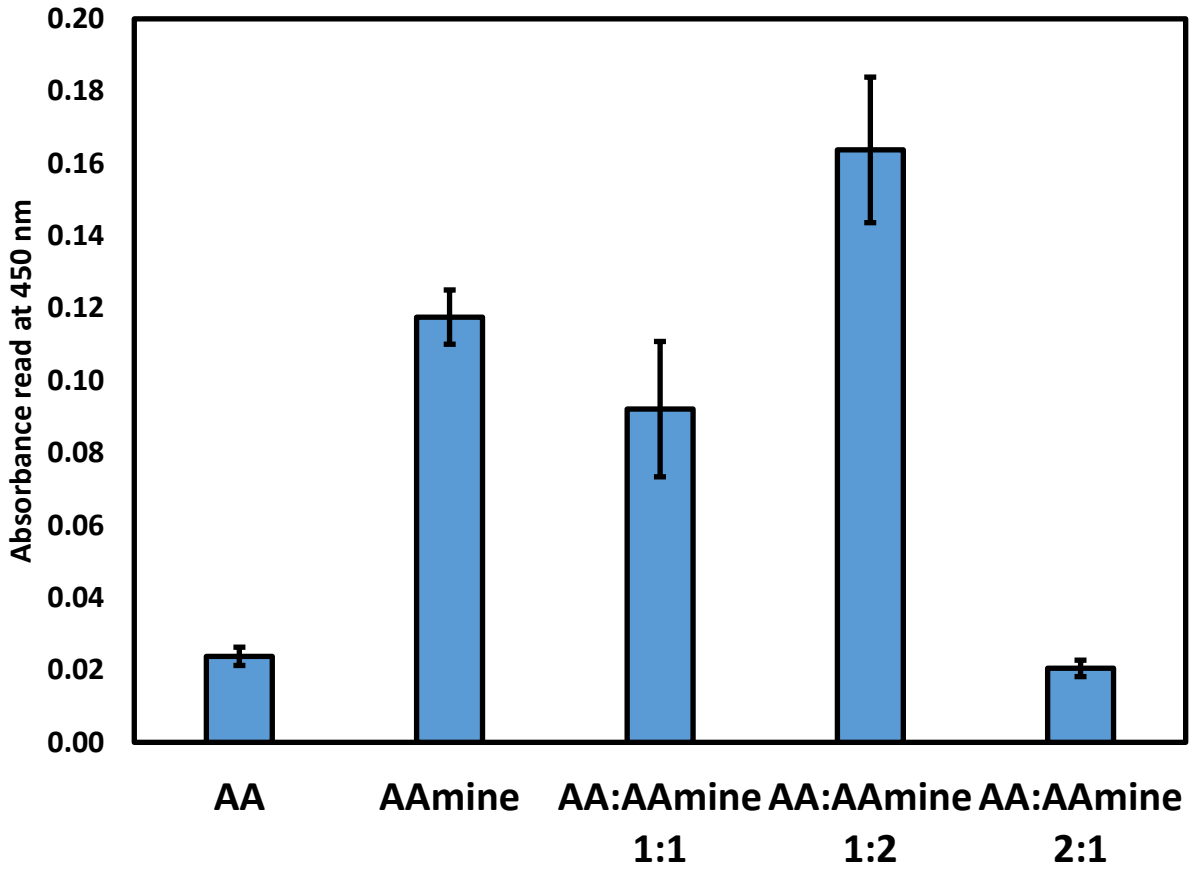

Figure 2.8. Amount of active IgG adsorbed to plasma polymerized AA, AAmine, AA:AAmine 1:1, AA:AAmine 1:2 and AA:AAmine 2:1 after 2 h in a 0.1 mg/mL bovine IgG solution in cPBS as determined by substrate-based ELISA.

This led us to delve deeper into the surface composition and chemical bonding environment of these quasi-zwitterionic surface coatings via XPS. In order to speculate the surface charge of these mixed-charge surface coatings we took the ratio of the bulk COO peak at ~289 eV to the bulk CN/CO peak at ~287 eV to give us the "ratio of charge" and sorted each family of quasi-zwitterionic surface coatings from low to high (Table 2.3). The higher ratios suggested a higher net negative charge contributed by the carboxyl groups relative to the net positive charge being contributed by the amine groups.

We also sorted the protein adsorption data for each family of quasi-zwitterionic surface coatings, and plotted the "ratio of charge" on a secondary axis (Figures 2.9-2.11). Immediately we notice a trend: as the "ratio of charge" increases among each family of quasi-zwitterionic surface coatings there is a decrease in protein adsorption observed uniformly. This trend is observed for each family regardless of the type of protein adsorption experiment. Thus, as we increase the amount of carboxyl groups in these mixed-charge surface coatings we notice a decrease in protein adsorption. This is significant as it provides researchers with a new tool to fine-tune the surface of mixed-charge plasma polymer coatings so that they can reduce protein adsorption and mimic the non-fouling properties of zwitterionic polymers.

It should be noted, however, that this "ratio of charge" is only a gross indication of the surface charge of these quasi-zwitterionic surface coatings since the peak at ~287 eV is from both CN (amine groups) and CO (carboxyl groups) and there is no proper way to distinguish between the two. Further experimentation will be required to determine the exact amount of carboxyl groups and amine groups on the surface using chemical derivatization experiments. Furthermore, dynamic atomic force microscopy can also be employed to determine the relative surface charge density of these mixed-charge surface coatings.

Table 2.3. Summary of chemical bonding environments of plasma polymerized quasi-zwitterionic surface coatings as determined by high-resolution C1s scans obtained from XPS. The ratio of bulk COO peak at ~289 eV to the bulk CN/CO peak at ~287 eV was used as a gross indication of surface charge. As the ratio increased the amount of negative charge on the surface also increased relative to the positive charge.

Quasi-zwitterionic surface coatings	Bonding components C1s (%)			
	CH Peak 1	CO/CN Peak 2	COO Peak 3	Ratio of charge (Peak 3/Peak 2)
MA:DMAAm 1:3	67.69	20.30	12.01	**0.59**
MA:DMAAm 1:2	63.39	21.74	14.87	**0.68**
MA:DMAAm 1:1	66.56	18.11	15.33	**0.85**
MA:DMAAm 2:1	72.33	14.77	12.90	**0.87**
MA:DMAAm 3:1	67.88	15.57	16.55	**1.06**
MA	73.70	14.70	11.60	-
DMAAm	74.40	25.60	0.00	-
MA:2VP 1.5:1	76.38	17.64	5.98	**0.34**
MA:2VP 1:1	77.04	16.28	6.68	**0.41**
MA:2VP 1:1.5	71.63	19.73	8.64	**0.44**
MA	73.70	14.70	11.60	-
2VP	83.00	17.00	0.00	-
AA:Aamine 1:1	66.95	22.38	10.67	**0.48**
AA:Aamine 1:2	60.92	25.77	13.31	**0.52**
AA:Aamine 2:1	70.57	15.38	14.05	**0.91**
AA	72.92	12.91	14.18	-
AAmine	75.06	24.94	0.00	-

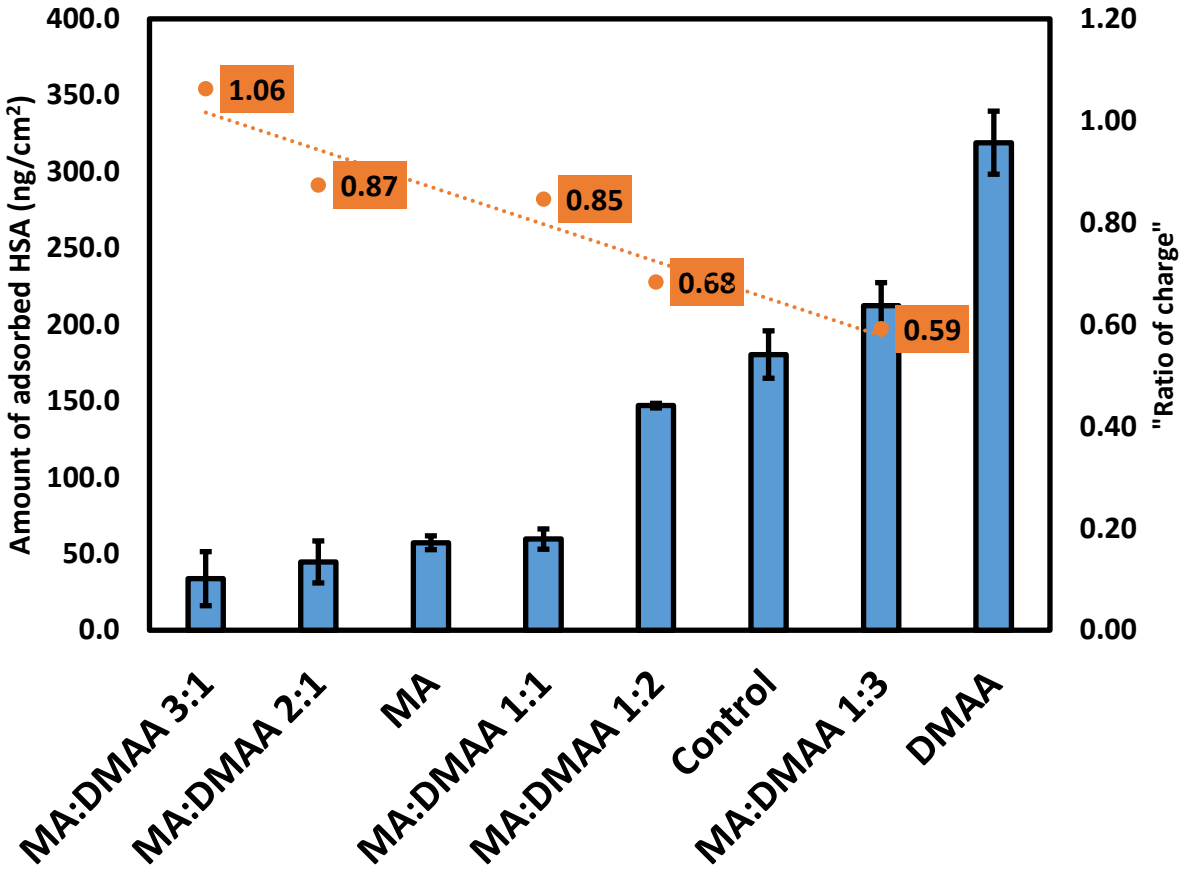

Figure 2.9. Amount of HSA adsorbed to plasma polymerized MA, DMAA, MA:DMAA 1:1, MA:DMAA 1:2, MA:DMAA 2:1, MA:DMAA 1:3, MA:DMAA 3:1 and glass control after 2 h in a 0.3 mg/mL HSA solution in CPBSzI as determined by I-125 radiolabeling method, sorted and plotted against the "ratio of charge."

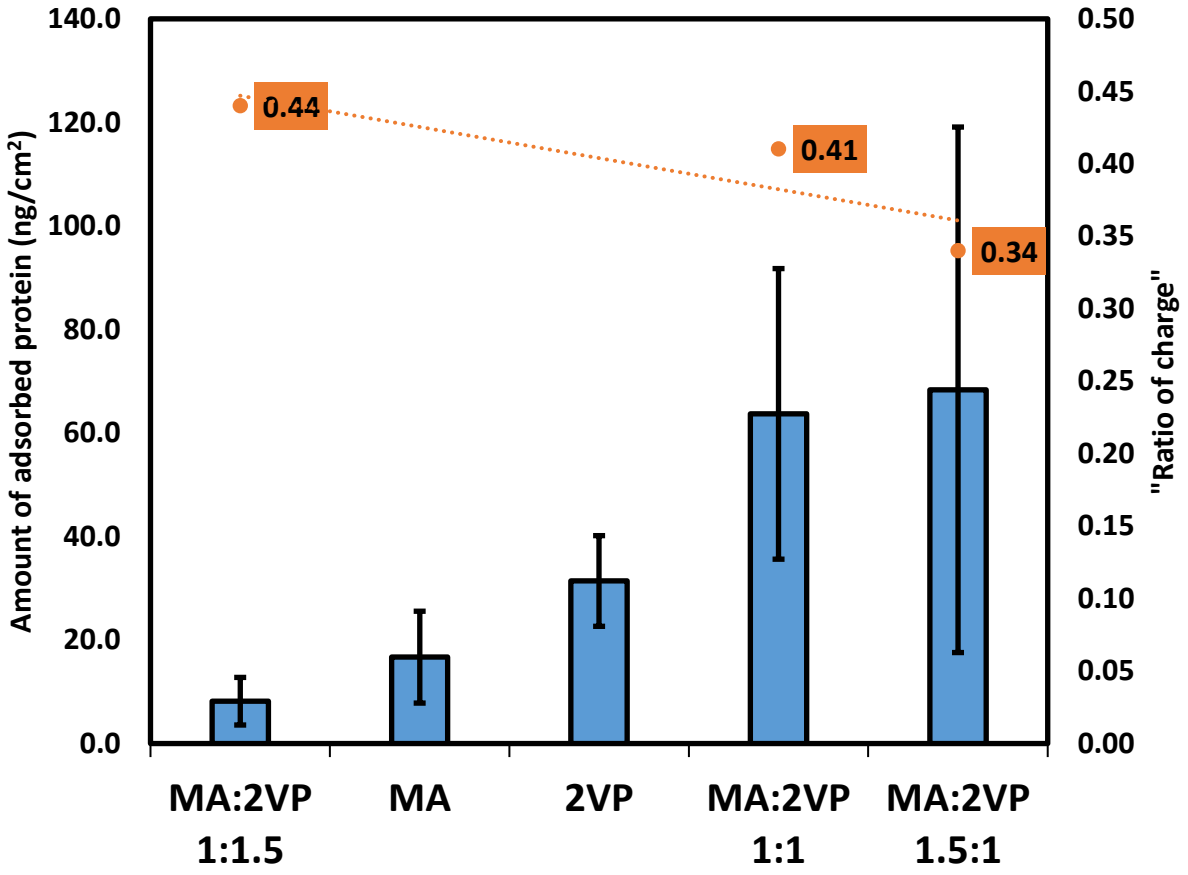

Figure 2.10. Amount of HSA competitively adsorbed to plasma polymerized MA, 2VP, MA:2VP 1:1, MA:2VP 1:1.5 and MA:2VP 1.5:1 after 2 h in a binary solution of HSA: 0.3 mg/mL and Fg: 0.03 mg/mL in cPBSzI as determined by I-125 radiolabeling method, sorted and plotted against the "ratio of charge."

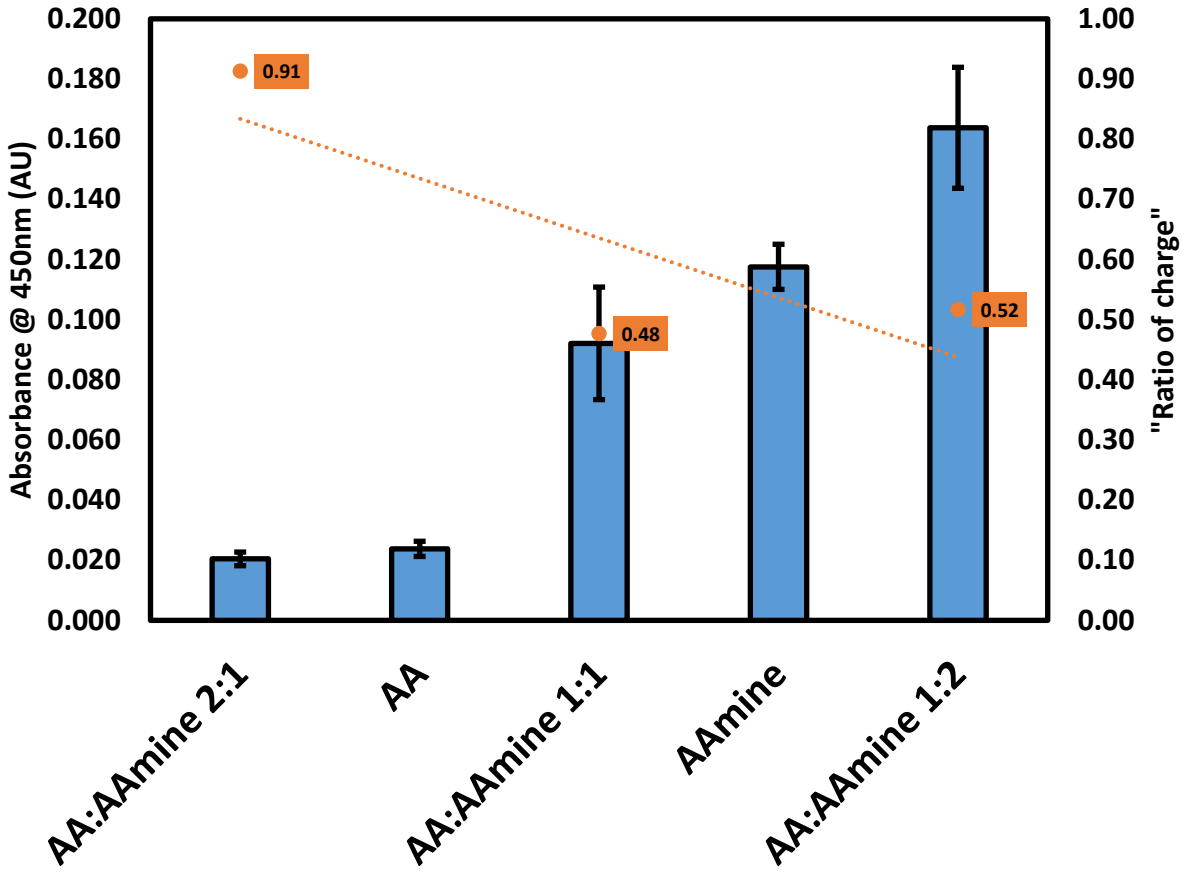

Figure 2.11. Amount of active IgG adsorbed to plasma polymerized AA, AAmine, AA:AAmine 1:1, AA:AAmine 1:2 and AA:AAmine 2:1 after 2 h in a 0.1 mg/mL bovine IgG solution in cPBS as determined by substrate-based ELISA, sorted and plotted against the "ratio of charge."

2.5 Conclusions

The goal of this research was to come up with new RF glow discharge plasma surface coatings that will be non-fouling and can potentially be used in AV vascular grafts to prevent blood clots in the long run. We have demonstrated that RF glow-discharge plasma can be used to copolymerize a positively charged and a negatively charged monomer to create a quasi-zwitterionic or mixed-charge surface coating. Furthermore, we have established that these quasi-zwitterionic surface coatings significantly reduce protein adsorption, and are non-cytotoxic.

Additionally, we have also provided researchers with a new tool ("ratio of charge") to fine-tune the surfaces of mixed-charge polymer coatings in order to reduce protein adsorption. Finally, due to the versatility of RF glow discharge plasma technology, this process is scalable and can be applied to the lumen of AV vascular grafts. We believe that these quasi-zwitterionic coatings are a step in the right direction and will help improve the quality of life hemodialysis patients while reducing financial burden associated with vascular access failure. Future studies will investigate protein adsorption and platelet adhesion and activation to these quasi-zwitterionic surface coatings using whole blood serum plasma to demonstrate their blood compatibility.

2.6 Acknowledgements

Funding was provided through the University of Washington Engineered Biomaterials program. Part of this work was conducted at the Molecular Analysis Facility, a National Nanotechnology Coordinated Infrastructure site at the University of Washington which is supported in part by the National Science Foundation (grant ECC-1542101), the University of Washington, the Molecular Engineering & Sciences Institute, the Clean Energy Institute, and the National Institutes of Health.

Chapter 3

STUDYING THE BIOLOGICAL ACTIVITIY OF ADSORBED PROTEIN ON BIOMATERIAL SURFACES USING A COMBINATION OF I-125 RADIOLABELED PROTEIN ADSORPTION, RADIOIMMUNOASSAY AND ELISA TECHNIQUES.

Marvin M. Mecwan[1] and Buddy D. Ratner[1,2]

1 Department of Bioengineering, University of Washington, Seattle, WA 98195

2 Department of Chemical Engineering, University of Washington, Seattle, WA 98195

3.1 ABSTRACT

All proteins rapidly adsorb to solid surfaces irreversibly and leads to protein conformational changes which results in denaturation and/or aggregation of the protein. The authors describe a variety of methods to assess the biological activity of protein adsorbed onto various biomaterial surfaces using a combination of I-125 radiolabeled protein adsorption, radioimmunoassay and substrate-based direct ELISA (enzyme linked immunosorbent assay). Hydrophilic and hydrophobic surface coatings were prepared by radio frequency (RF) glow-discharge plasma onto glass coverslips and stainless steel substrates. Bovine IgG was used as a model protein for the I-125 radiolabeled protein adsorption and retention studies, and goat anti-bovine IgG (unconjugated) was used as the secondary antibody for the radioimmunoassay while its HRP conjugate was used as the secondary antibody for ELISA. Bovine IgG was adsorbed onto the surfaces for 2 h and its biological activity was assessed at day 0 and at day 7. The results suggested that hydrophilic surfaces tend to have more active protein adsorbed onto its surface as compared to hydrophobic surfaces, and that increased residence time causes a reduction in activity of the protein. Since these

combination techniques allow us to monitor changes in protein activity over time together they can be used as valuable tools to help assess the biocompatibility of three-dimensional biomaterial surfaces.

3.2 INTRODUCTION

In recent years, protein and antibody-based drugs have assumed major importance to the pharmaceutical industry and to patients.[55] This is because small molecule drugs can only address a fraction of desired therapeutic targets because of the nature of recognition sites on cells and tissues. Protein and antibody-based drugs, on the other hand, can be specifically tuned for effective bio-recognition and can be made patient specific. However, protein-based pharmaceuticals present unique challenges when it comes to processing, packaging and delivery of these drugs. All proteins rapidly adsorb irreversibly to solid surfaces and undergo conformational changes upon adsorption.[56] The interactions of protein with surfaces impacts proteins unfavorably, usually reducing their bioactivity or leading to aggregation.

Surface protein interaction studies have been widely used to assess biocompatibility of biomedical materials and devices.[57–60] Particularly, at the University of Washington, a number of techniques have been previously employed to determine the amount of adsorbed protein to biomaterial surfaces, including techniques such as X-ray photoelectron spectroscopy (XPS),[61,62] time-of-flight secondary ion mass spectroscopy (ToF-SIMS),[63,64] surface plasmon resonance,[65,66] as well as radioactively labeled I-125 protein studies.[67,68] Sometimes, two or more of these techniques have been used in combination to help better understand protein adsorption to biomaterial surfaces and changes in protein conformation thereafter.[69–72]

In order to study the biological activity of adsorbed protein to biomaterial surfaces an antibody-based protein detection method such as ELISA needs to be employed. However, there are limitations when performing ELISA on three-dimensional surfaces since this method is qualitative and not quantitative; a reliable standard curve cannot be produced for the assay. Radioimmunoassays, on the other hand, uses a radioactively labeled secondary antibody which can be correlated to a radioactively labeled protein standard, and hence can be used to quantify the amount of secondary antibody attached to the adsorbed protein. However, there is a lack of literature with regard to using radioimmunoassays as a method to determine biological activity of adsorbed proteins to biomaterial surfaces.

In this paper, the authors propose a combination of various protein detection methods to assess the biological activity of adsorbed protein to biomaterial surfaces. To this end, we prepare polyether and fluoropolyether surface coatings onto glass coverslips and stainless steel substrates using RF glow-discharge plasma. This technology is commonly used to deposit a monomer from a gaseous state onto a substrate using two capacitively coupled electrodes and can create thin polymeric network films that are strongly bound to surfaces.[25–27] Our monomers of choice for the plasma polymerized surface coatings include: tetraglyme (TG) (hydrophilic), acrylic acid (AA) (hydrophilic), perfluoropropylene (C3F6) (hydrophobic), and perfluoromethyl vinyl ether (C3F6O) (hydrophobic). Following bovine IgG protein adsorption to these surfaces, the effect of surface wettability and residence time of the adsorbed protein is evaluated by a variety of protein detection and quantification techniques including I-125 radiolabeled protein adsorption studies, radioimmunoassay and substrate-based direct ELISA techniques. The authors propose the use of these techniques in combination to help researchers to better understand and evaluate the biological

activity of adsorbed protein to biomaterial surfaces which in turn would help to assess the biocompatibility of these surfaces better.

3.3 EXPERIMENT

3.3.1 Plasma deposition and characterization of biomaterial surfaces

3.3.1.1 Materials

8 mm glass coverslips were purchased from Knitell Glass (Cat. No. G401-08). Stainless steel sheets were generously donated by Eli Lilly and Company, Indianapolis, IN. Acrylic Acid (AA) (Cat. No. 147230) and tetraglyme (TG) (Cat. No. 172405) were purchased from Sigma-Aldrich. Perfluoropropylene (C3F6) (Cat. No. 1300-2-02) and perfluoromethyl vinyl ether (C3F6O) (Cat. No. 2307-2-01) were purchased from SynQuest Laboratories. All organic solvents were purchased from Fisher Scientific.

3.3.1.2 Plasma polymerization of TG, AA, C3F6 and C3F6O

Prior to plasma deposition, 8 mm glass coverslips were placed in a sample holder within a glass container and ultrasonicated in a water bath for two 10 min cycles each in methylene chloride, followed by acetone and then methanol. Stainless steel (SS) samples were cut into 7 mm x 7 mm squares, placed in a beaker and were cleaned using the same solvents as the glass coverslips. All samples were then air-dried in a fume hood.

Plasma polymerization of TG, AA, C3F6 and C3F6O were carried out in a custom-built plasma reactor setup based on the design reported in Lopez et al[34] (Figure 3.1). Cleaned glass coverslips and SS samples were loaded in the plasma and a mechanical pump was used evacuate

the reactor to the desired base pressure in the low 10^{-3} Torr range. A liquid nitrogen cooled cold trap between the vacuum pump and the reactor was used to condense organic materials. The powered electrode was connected to a 13.56 MHz radio frequency power source and an automatic impedance matching network. The coverslips were first etched in argon gas for 10 min at 40 W while maintaining a pressure of 250 mT. Following this, the glass coverslips and SS samples were coated with the monomer of choice (either TG, AA, C3F6 or C3F6O). The parameters used to plasma treat the substrates for each monomer is outlined in Table 3.1. Following plasma treatment, samples were quenched with the monomer vapor for 5 min before retrieving them. Upon retrieval, samples were flipped, and the plasma treatment process was repeated with the same parameters to ensure uniform coating on both sides of samples.

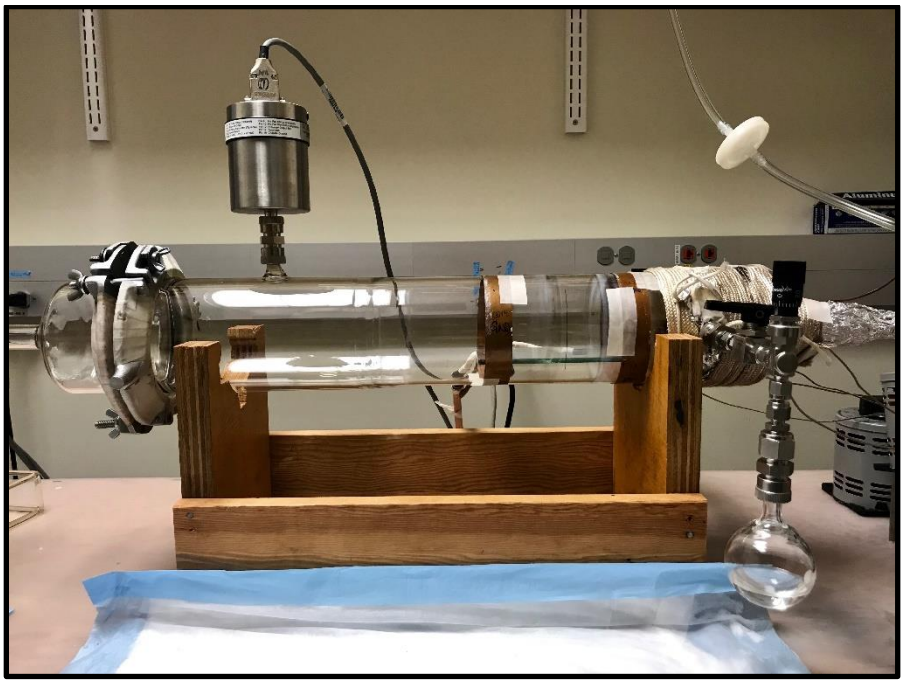

Figure 3.1. Custom-built plasma reactor setup for the plasma polymerization of monomers.

Table 3.1. Summary of the plasma treatment parameters used for the plasma deposition of AA, TG, C3F6 and C3F6O onto substrates.

	Monomers			
Parameters	**AA**	**TG**	**C3F6**	**C3F6O**
Flow Rate (SCCM)	4	1.33	10.2	10.3
Pressure (mT)	250	350	150	250
Treatment	80W/ 1min 10W/ 10min	80W/ 1min 10W/ 20min	60W/ 1min 20W/ 20min	60W/ 1min 5W/ 20min

3.3.1.3 Surface characterization

X-ray photoelectron spectroscopy (XPS) was performed on all plasma polymerized glass disc samples on a Surface Science Instruments S-Probe equipped with a monochromatic Al Kα source and a low energy electron flood gun for charge neutralization. X-ray analysis for these acquisitions was in a circle approximately 800 µm across. Pressure in the analytical chamber during spectral acquisition was less than 5×10^{-9} Torr. Low-resolution survey scans were obtained from 0 to 1100 eV with a 1 eV step size and pass energy of 150 eV. High resolution C 1s scans were obtained from 270 to 290 eV with a 0.065 eV step size and pass energy of 50 eV. The spectra were analyzed off line with Service Physics Hawk version 7 data analysis software to calculate the elemental compositions from peak areas and to peak fit high resolution spectra. All binding energies were calibrated with reference to the aliphatic carbon at C 1s = 285.0 eV. A Shirley background was used for all spectra.

3.3.2 I-125 radiolabeled protein adsorption and radioimmunoassay

3.3.2.1 Materials

Bovine IgG (Cat. No. I5506), sodium azide (Cat. No. S2002), and sodium iodide (NaI) (Cat. No. 383112) were purchased from Sigma-Aldrich. Boric acid (Cat. No. A73-500), sodium phosphate monobasic (Cat. No. S369-500), and sodium hydroxide (Cat. No. S399-500) were purchased from Fisher Scientific. Goat anti-bovine IgG antibody, unconjugated (Cat. No. A18753) and Goat IgG isotype control (Cat. No. 02-6062) were purchased from Invitrogen. Sodium chloride crystals (Cat. No. SX0420-3) was purchased from EMD Millipore. Citric Acid, Monohydrate (Cat. No. 0115-01) was purchased from J.T. Baker. Iodine-125 radionuclide (Specific Activity: ~17Ci/mg, 10^{-5}M NaOH (pH 8-11)) was purchased from Perkin-Elmer (Cat. No. NEZ033A).

3.3.2.2 Protein iodination using ICl method

Bovine IgG, goat anti-bovine IgG (unconjugated) and IgG isotype (unconjugated) were radiolabeled using the iodine monochloride (ICl) method modified by Horbett[54]. Briefly, 1mCi of Iodine-125 radionuclide was added to 0.5 mL 2x borate solution, to which 0.5 mL of ICl/NaCl mixture in a 2:1 ratio was added. Finally, either 0.5 mL of a 10 mg/mL bovine IgG or 2.5 mg/mL goat anti-bovine IgG or 5 mg/mL IgG isotype in a citrate phosphate buffered saline solution with sodium azide (cPBSz) was added and the iodination reaction was performed on ice for 20 min and then run through a size exclusion chromatography column. 40 fractions were collected to capture the labeled protein and free iodine peaks to evaluate iodination efficiency. The fractions from protein peaks were pooled together and run through a second chromatography column,

repeating fraction collection and peak identification. Purified radiolabeled protein fractions were pooled together, placed in a lead pig, and frozen in -80^0 C freezer until further use.

3.3.2.3 I-125 radiolabeled bovine IgG protein adsorption and retention.

Prior to the protein adsorption studies, plasma treated substrates (n = 4) were soaked in 0.5 mL cPBS solution with 10mM NaI (cPBSzI) for 30 min. For the adsorption, the radiolabeled bovine IgG was thawed and then added to a 0.2 mg/mL solution of bovine IgG in cPBSzI to create "hot IgG" protein with an activity ~200 CPM/ng. 0.5 mL of the "hot IgG" protein was then added to each sample and allowed to adsorb for 2 h before rinsing three times with cPBSzI using a rinsing system. The samples were then transferred to a gamma counter tube and the radioactivity of each sample was then measured for 1 min along with protein standards using a Perkin Elmer Wizard 2 Gamma Counter.

For the protein retention studies, samples with adsorbed IgG were placed in new tubes with 1 mL of 1% SDS and allowed to sit overnight. The samples were then rinsed three times using a rinsing system with cPBSzI placed in a gamma counter tube and measured for 1 min along with protein standards using a Packard Cobra gamma counter. Untreated glass and SS samples were used as controls. Adsorption and retention data were reported in ng/cm^2.

3.3.2.4 Radioimmunoassay using goat anti-bovine IgG (unconjugated)

For the radioimmunoassay, plasma treated substrates (n = 7) were soaked in 0.5 mL cPBS solution with 10mM NaI (cPBSzI) for 30 min. To this, 0.5 mL of a 0.2 mg/mL solution of bovine IgG in cPBSzI was added to each sample and allowed to adsorb for 2 h before rinsing three times with PBS containing 0.05% Tween20 (wash buffer). The samples were then blocked

using 1 mL of 1x assay diluent, followed by rinsing three times with the wash buffer. Samples were then transferred to a new sample cup.

The radiolabeled goat anti-bovine IgG was thawed and then added to a 25 µg/mL solution of goat anti-bovine IgG in 1x assay diluent respectively to create "hot 2^{o} Ab" protein with an activity ~200 CPM/ng. Similarly, radiolabeled IgG isotype was thawed and then added to a 25 µg/mL solution of IgG isotype in 1x assay diluent respectively to create "hot isotype" protein with an activity also ~200 CPM/ng. To one set of samples (n = 4) 1 mL of the "hot 2^{o} Ab" protein was added, and to another set of samples (n = 3) 1mL of the "hot isotype" protein was added, and both were allowed to bind to the adsorbed bovine IgG on the surface for 30 min before rinsing five times with wash buffer. The samples were then transferred to a gamma counter tube and the radioactivity of each sample was then measured for 1 min along with protein standards using a Perkin Elmer Wizard 2 Gamma Counter.

Untreated glass and SS samples were used as controls. The amount of goat anti-bovine IgG and IgG isotype on each surface were calculated in ng/cm^2, and the amount of tagged goat-anti-bovine IgG to tagged bovine IgG adsorbed was reported as a ratio.

3.3.3 Substrate-based direct ELISA

3.3.3.1 Materials.

Goat anti-bovine IgG antibody, HRP conjugate (Cat. No. A18751) was purchased from Invitrogen. 5X ELISA/ELISPOT Diluent (Cat. No. 00-4202-56) and 1X TMB Substrate Solution (Cat. No. 00-4201-56) were purchased from eBioscience.

3.3.3.2 Substrate-based direct ELISA using goat anti-bovine IgG (HRP conjugate)

The substrate-based direct ELISA followed a protocol similar to the method described in 3.3.2.4. Briefly, plasma treated substrates (n = 4) were soaked in 0.5mL cPBS solution with 10mM NaI (cPBSzI) for 30 min. To this, 0.5 mL a 0.2 mg/mL solution of bovine IgG in cPBSzI was added to each sample and allowed to adsorb for 2 h before rinsing three times with wash buffer. The samples were then blocked using 1 mL of 1x assay diluent, followed by rinsing three times with the wash buffer. Samples were transferred to new sample cups. 1 mg/mL solution of goat anti-bovine IgG conjugated with HRP was diluted 1:100 in 1x assay diluent, and 1 mL was then added to each sample and allowed to bind to the adsorbed bovine IgG on the surface for 30 min before rinsing five times with wash buffer. Samples were once again transferred to new sample cups and 1x TMB substrate was then added, allowed to incubate at room temperature for 2 min and the reaction was stopped using 0.5 mL of 1N phosphoric acid. 150 µL of the yellow colored solution was then transferred to a clear 96 well plate and the absorbance of each well was read at 450 nm and the absorbance at 570 nm was subtracted each well.

In order to understand the change in activity of adsorbed protein with increased residence time on the surface of biomaterials, a set of plasma treated substrates (n = 4) underwent protein adsorption for 2 h using a 0.1 mg/mL solution of bovine IgG in cPBSzI, rinsed with wash buffer three times and then allowed to sit in 1 mL of cPBSzI for 7 days at 4^{o} C. After the time had passed, the samples underwent the same direct ELISA protocol as described above. Untreated glass and SS samples were used as controls in all direct ELISA experiments.

3.4 Results and Discussion

The goal of this research was to develop better methods to assess biological activity of adsorbed antibody-based drugs onto biomaterial surfaces and to determine any change in activity due to protein residence time. To this end, we prepared hydrophilic and hydrophobic surfaces by plasma polymerizing polyether and fluoropolyether coatings onto glass coverslips and SS substrates which are relevant to the pharmaceutical industry.

XPS was used to assess the surface of all plasma-treated polyether and fluoropolyether substrates. The representative survey scans seen in Figure 3.2, and summarized in Table 3.2, provide information on the overall surface chemical composition. Survey scans of the various treatment groups from XPS on both glass coverslips and SS substrates were identical, indicating that there were no differences in plasma coatings between substrates. Furthermore, no peaks associated with the substrates (such as, Si for glass coverslips, and Fe and Cr for SS substrates) were seen in the survey scans, which indicate that the plasma coatings were greater than 10nm in thickness, as this is the depth to which XPS is able to analyze a surface. However, further experiments will need to be conducted in order to determine the thickness of the plasma coatings using either ellipsometry or profilometry. Moreover, plasma coatings did not delaminate after being soaked in water overnight. This indicates that the coatings are tightly bound to the glass coverslips and SS substrates and would withstand the washing procedures performed during protein adsorption and radioimmunoassay studies.

Table 3.2. Summary of surface elemental composition of plasma polymerized AA, TG, C3F6 and C3F6O surface coatings as determined by survey scans obtained from XPS.

Plasma coating		Elemental Composition (%)		
		C	**O**	**F**
AA	Observed	**64.5**	**35.5**	**-**
	Expected	60	40	-
TG	Observed	**68.2**	**31.8**	**-**
	Expected	66.7	33.3	-
C3F6	Observed	**35.2**	**-**	**64.8**
	Expected	33.3	-	66.7
C3F6O	Observed	**36.1**	**3.1**	**60.8**
	Expected	30.0	10.0	60.0

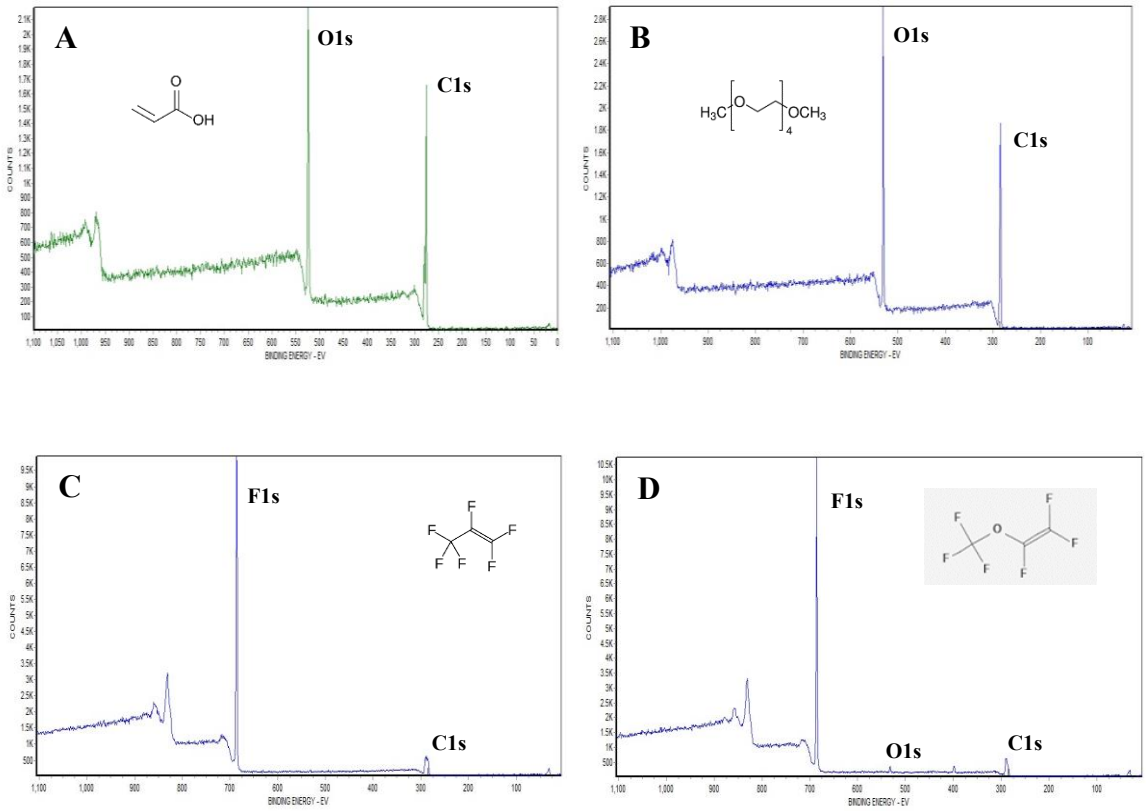

Figure 3.2. Representative XPS survey scans and corresponding monomer chemical structures (inset) of plasma polymerized (A) AA (B) TG (C) C3F6 and (D) C3F6O. Major elemental peaks are labeled in each survey scan.

High resolution C 1s spectra (Figure 3.3) provide insight into the chemical bonding environment of carbon. All plasma coatings showed characteristic shifts in the carbon peaks based on the chemical structure of the monomer. The C1s peak associated with AA was a doublet, with a characteristic peak at 285 eV associated with C-H bond, and another, smaller peak at ~288.5 eV associated with COO bond from the carboxyl group of acrylic acid. The high-resolution C1s from TG plasma coating is a singlet at ~286.5 eV and is characteristic of CO ether bonds. As seen from Figure 3.3, the shape and features of the high-resolution C1s peak of all plasma polymerized fluoropolyether coatings allowed us to fit four width-constrained peaks

corresponding to four different bonding environments: C—O (~287eV), C—F (~290eV), C—F2 (~292eV), and C—F3 (~294eV). It should be noted that all XPS spectra were shifted so that the hydrocarbon peak could align at 285.0 eV (charging binding energy correction).

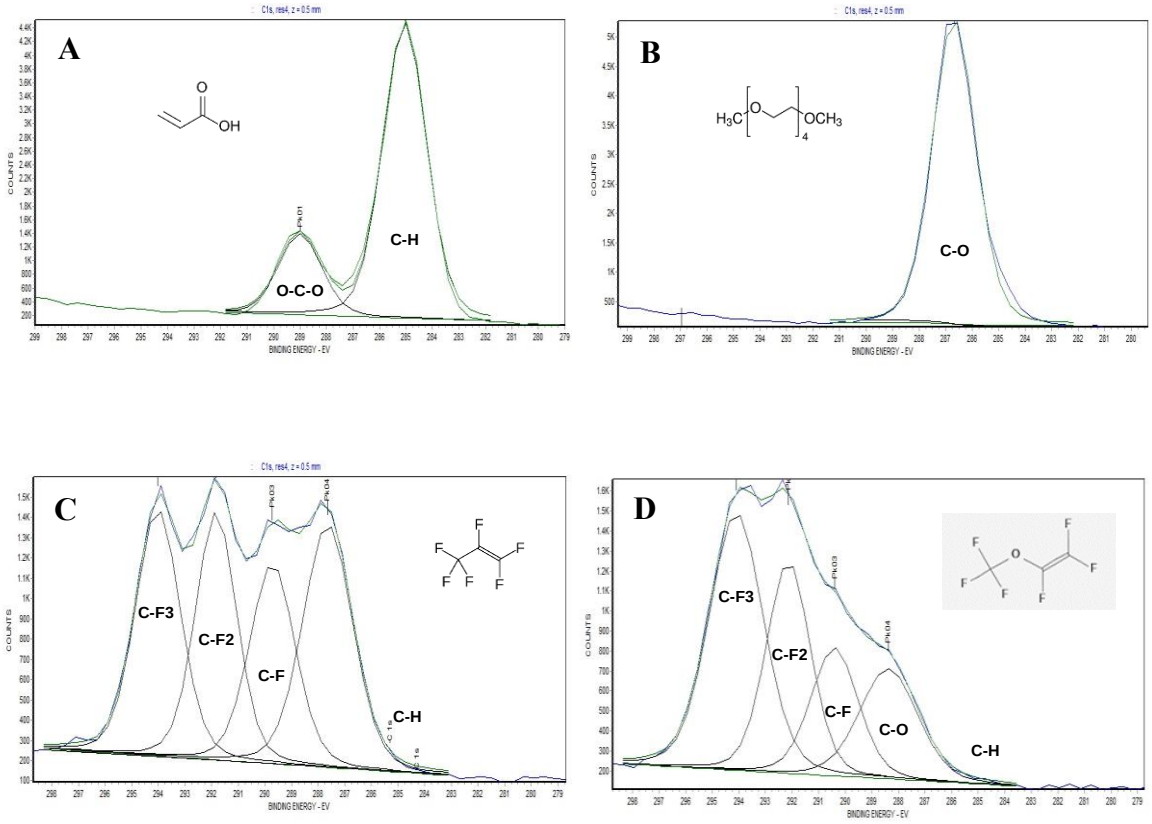

Figure 3.3. Representative high-resolution spectra of the C1s peak and corresponding monomer chemical structure (inset) of plasma polymerized (A) AA (B) TG (C) C3F6 and (D) C3F6O. Fitted peaks are labeled to correspond to different bonding environments within each chemical structure.

For this research, bovine IgG was selected as a model protein to examine the interaction between antibody-based drugs and biomaterial surfaces. Figure 3.4 depicts the results from the IgG protein adsorption study using I-125 radiolabeled bovine IgG. TG and AA showed the least

amount of adsorbed IgG on the surface as compared to C3F6 and C3F6O on both glass coverslips and SS substrates. Since AA and TG are hydrophilic surfaces it was expected that proteins would not adsorb to such surfaces.[73] On the other hand, C3F6 and C3F6O had higher protein adsorption and is comparable to what we would expect of fluoropolymers which are reported to be in the range of 100-150 ng/cm^2.[74,75]

Retention studies help understand the strength of bonding between the adsorbed protein and the biomaterial surface. Figure 3.5 illustrates the results from the IgG protein retention study after an overnight elution in 2% SDS. As seen, C3F6 and C3F6O, retain the most amount of IgG on the surface, while TG and AA retain the least amount of IgG on the surface (<5 ng/cm^2). These results indicate that bovine IgG is not as strongly bound to the surface of hydrophilic surfaces as compared to hydrophobic surfaces.

The radioimmunoassay method allows us to quantitatively determine how much of the secondary antibody non-specifically binds to the adsorbed protein on the surface. Since the secondary antibody used in this study is polyclonal it can attach to multiple sites (either the Fab or Fc segment) of bovine IgG. Therefore, by taking a ratio of the amount of non-specifically bound secondary antibody to the amount of adsorbed bovine IgG to the surface, we can evaluate the biological activity of the adsorbed bovine IgG—the higher the number, the more active the adsorbed protein. As seen in Figure 3.6, it is interesting to note, that despite TG only adsorbing a small amount of bovine IgG, a larger fraction of the adsorbed protein remains active as compared to the other treatment groups.

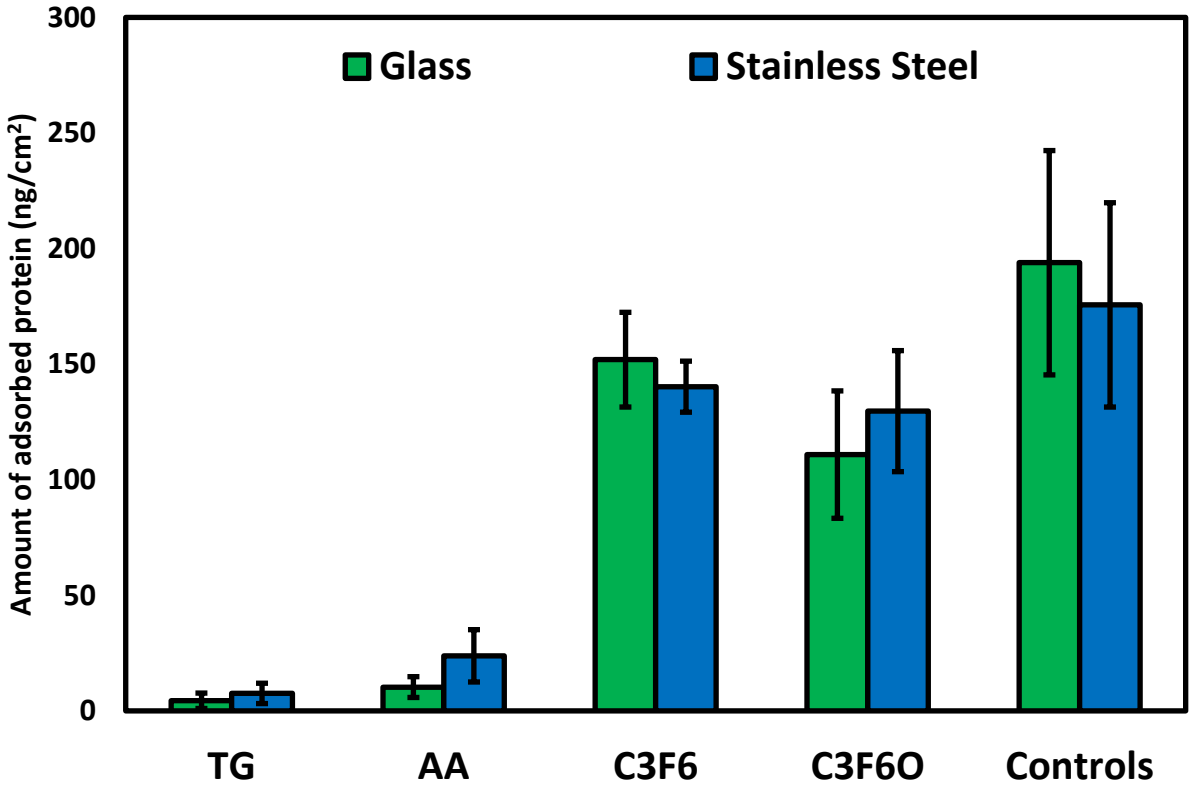

Figure 3.4. Amount of IgG adsorbed to plasma polymerized AA, TG, C3F6 and C3F6O on glass coverslips and SS substrate after 2 h in a 0.1 mg/mL bovine IgG solution as determine I-125 radiolabeling method.

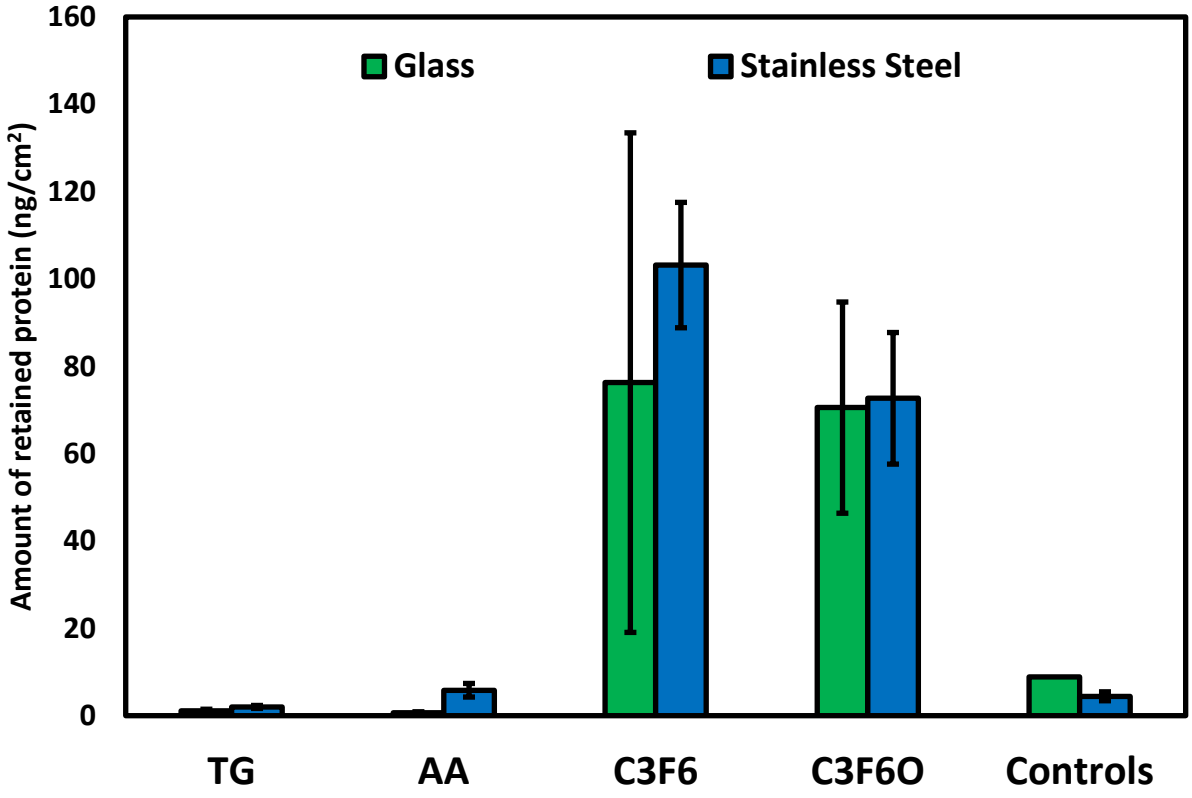

Figure 3.5. Amount of IgG retained on plasma polymerized AA, TG, C3F6 and C3F6O on glass coverslips and SS substrate after overnight elution with 2% SDS as determined by I-125 radiolabeling method.

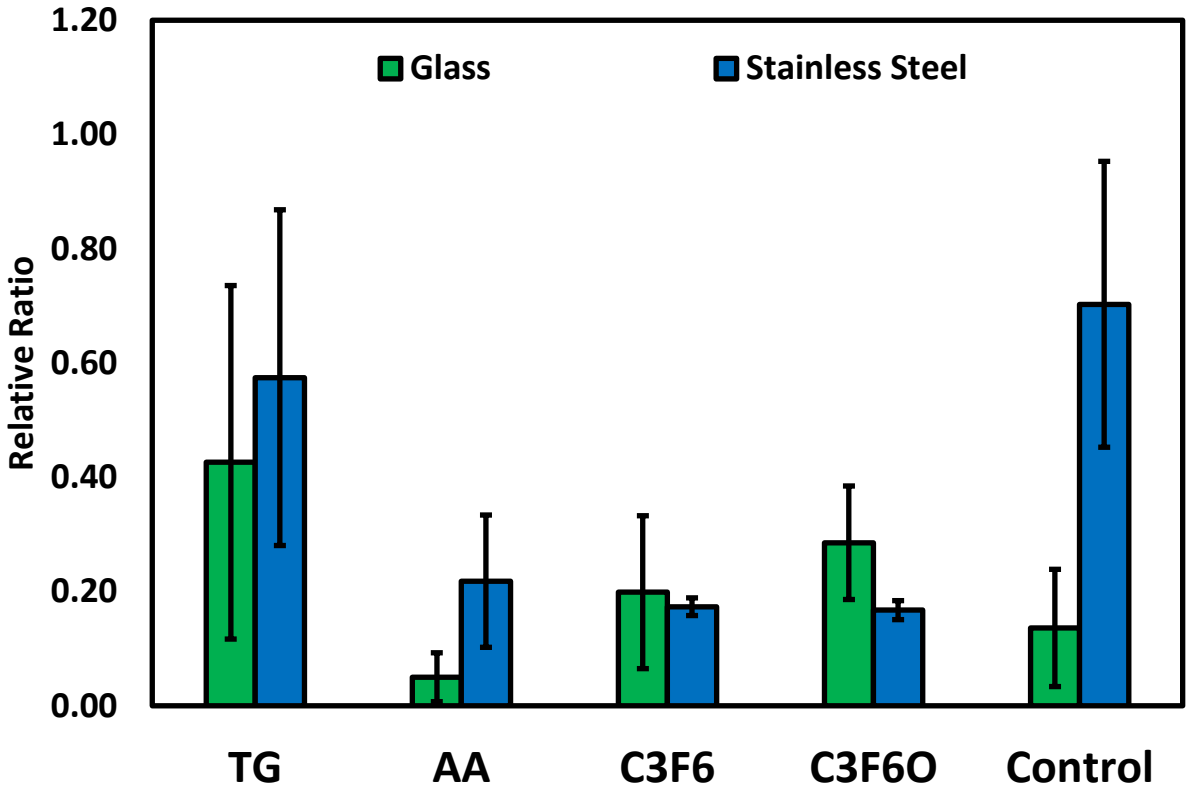

Figure 3.6. The ratio of tagged goat anti-bovine IgG to tagged bovine IgG adsorbed to the surface of plasma polymerized TG, AA, C3F6 and C3F6O on glass coverslips and SS substrates as determined by radioimmunoassay.

We also propose the use of substrate-based direct ELISA in combination with I-125 radiolabeled protein adsorption studies as another methodology to determine the biological activity of adsorbed protein to biomaterial surfaces. Similar to the radioimmunoassay, the secondary antibody for the direct ELISA method used in this study is also polyclonal. Hence, by taking a ratio of the absorbance values obtained from direct ELISA to the amount of adsorbed bovine IgG determined by I-125 radiolabeled protein adsorption studies we can evaluate the activity of the adsorbed bovine IgG. Once again, the higher the ratio, the more active the

adsorbed protein on the surface. Figure 3.7 depicts the absorbance read at 450 nm using direct ELISA normalized to the amount of adsorbed bovine IgG to the surface. By comparing the results in Figure 3.6 and 3.7 it is easy to notice a similar trend between the two—TG has relatively more active adsorbed bovine IgG as compared to AA, C3F6 or C3F6O.

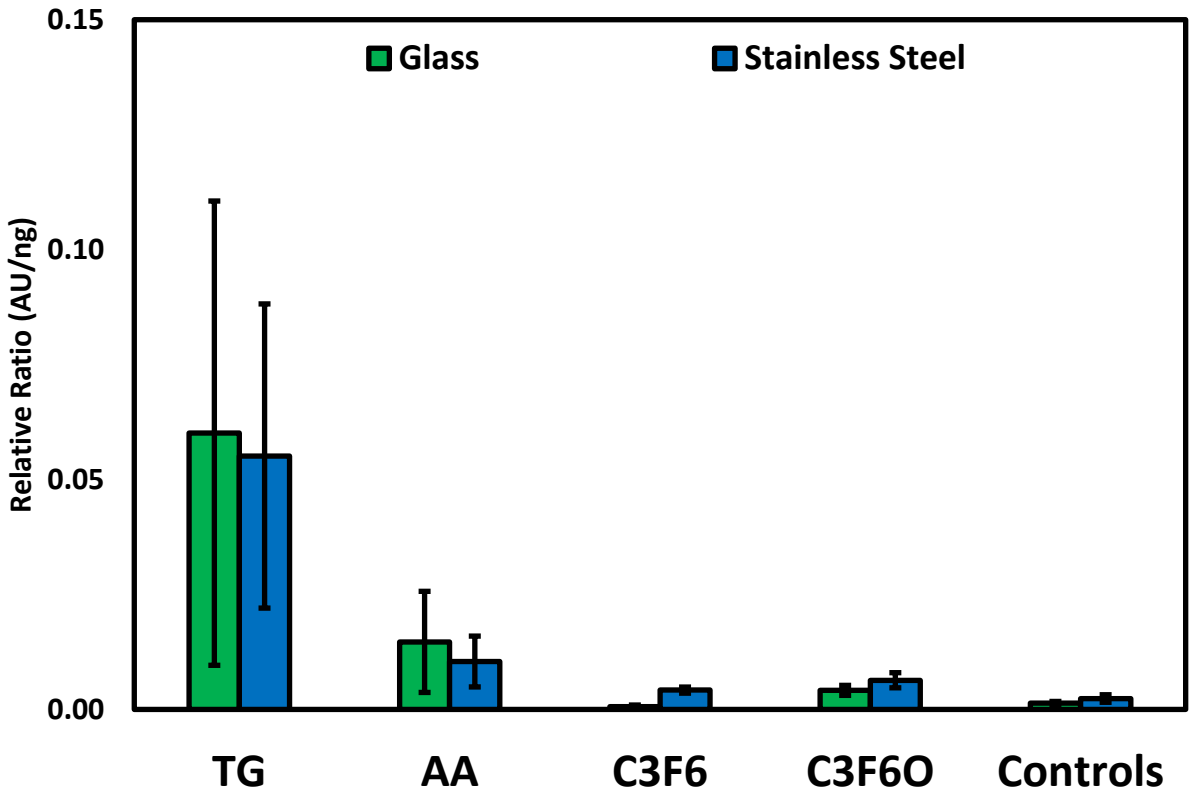

Figure 3.7. The ratio of absorbance read at 450 nm using substrate-based direct ELISA to the amount of tagged bovine IgG adsorbed determined by radioimmunoassay to the surface of plasma polymerized TG, AA, C3F6 and C3F6O on glass coverslips and SS substrates.

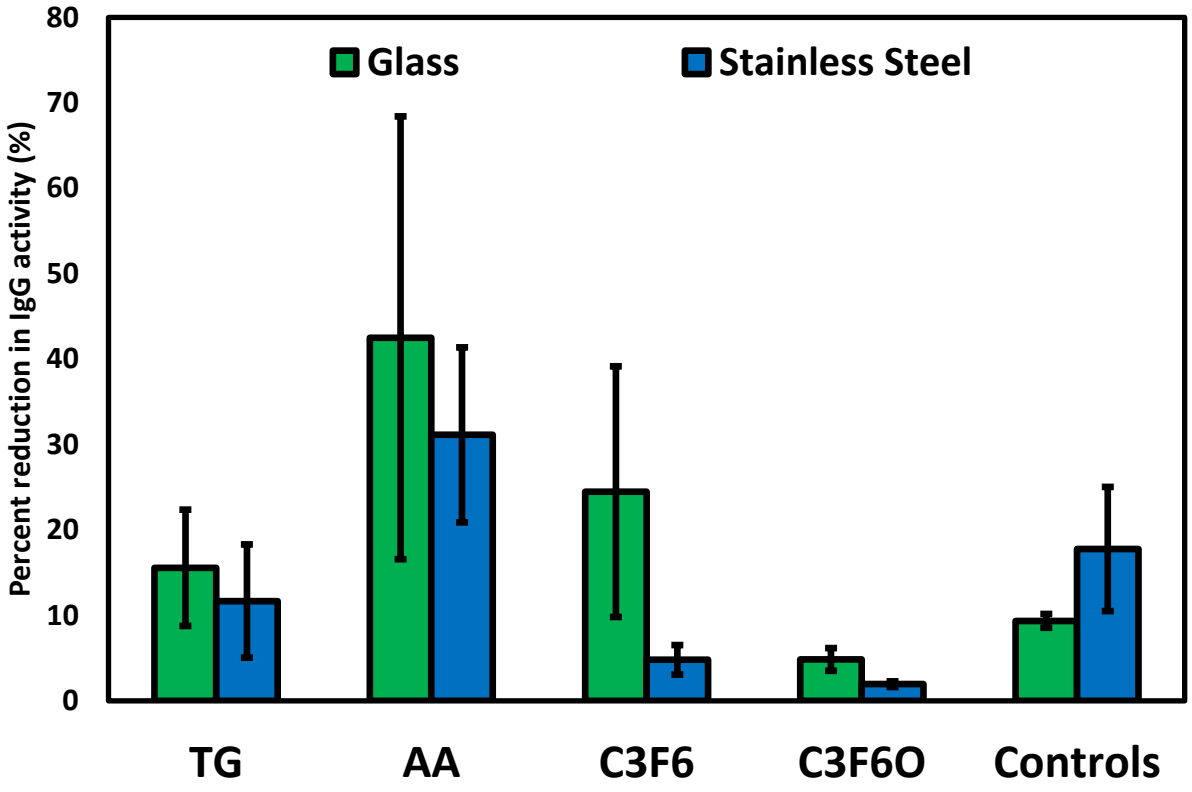

Figure 3.8. The percentage reduction in bovine IgG protein activity after a residence time of 7 d on the surface of plasma polymerized TG, AA, C3F6 and C3F6O on glass coverslips and SS substrates as determined by substrate-based direct ELISA.

We can also use substrate-based direct ELISA to study the resident-time dependent changes in adsorbed protein to biomaterial surfaces. Figure 3.8 illustrates the percent reduction in the biological activity of adsorbed IgG after being adsorbed to the surface of plasma polymerized TG, AA, C3F6 and C3F6O for 7 d. Interestingly, AA greatly reduces protein activity of adsorbed bovine IgG, whereas C3F6O has the least reduction in protein activity of the adsorbed bovine IgG as compared to the other treatment groups.

3.5 CONCLUSIONS

The goal of this research was to develop new methodologies for assessing the biological activity of adsorbed protein to biomaterial surfaces and to study the changes in activity of the protein with residence time. To this end, we successfully prepared hydrophilic and hydrophobic surface coatings by RF glow-discharge plasma on both glass coverslips and SS substrates. We were able to determine that the hydrophilic surface TG adsorbed and retained the least amount of bovine IgG, had the highest relative amount of active adsorbed bovine IgG, about only 15% of which lost their biological activity after a residence time of 7 d. In comparison, the hydrophilic surface C3F6O adsorbed and retained the highest amount of bovine IgG, had a relatively small amount of active bovine IgG adsorbed to the surface, about 95% of which continued to stay active after a residence time of 7 d. Hence, by combining radiolabeled protein adsorption and retention studies, radioimmunoassay and substrate-based ELISA techniques we were able to show that plasma polymerized TG surface coatings are more biocompatible compared to plasma polymerized AA, C3F6 and C3F6O surface coatings. Future studies will investigate different proteins such as albumin and fibrinogen as well as the effect of longer residence times on the activity of adsorbed protein to the biomaterial surfaces using the same combination of techniques.

3.6 ACKNOWLEDGEMENTS

Funding was provided through the University of Washington Engineered Biomaterials program. Part of this work was conducted at the Molecular Analysis Facility, a National Nanotechnology Coordinated Infrastructure site at the University of Washington which is supported in part by the National Science Foundation (grant ECC-1542101), the University of Washington, the

Molecular Engineering & Sciences Institute, the Clean Energy Institute, and the National Institutes of Health.

Chapter 4

PLASMA POLYMERIZED HMDSO COATINGS FOR SYRINGES PREVENTS PROTEIN ADSORPTION WHILE MAINTAINING SYRINGE LUBRICITY

Marvin M. Mecwan,[1] Xia Dong[2] and Buddy D. Ratner[1,3]

1 Department of Bioengineering, University of Washington, Seattle, WA 98195

2 Eli Lilly and Company, Indianapolis, Indiana 46285

3 Department of Chemical Engineering, University of Washington, Seattle, WA 98195

4.1 ABSTRACT

Current glass containers, both cartridges and syringes, contain silicone oil which seeps into the protein solution and results in adsorption, aggregation and denaturation of the protein. The authors describe new surfaces for the storage and delivery of antibody-based therapeutics prepared by radio frequency (RF) glow-discharge plasma polymerization. Using this robust technique, we plasma polymerize methacrylic acid (MA) (hydrophilic, -ve charge), hexamethyldisiloxane (HMDSO) (hydrophobic, neutral), tetraglyme (hydrophilic, neutral), as well as copolymerize HMDSO and MA to create a plasma polymerized HMDSO-MA (hydrophobic, -ve charge) surface. Untreated glass coverslips and glass coverslips dip-coated in PDMS were used as controls. Of all the plasma polymerized surface coatings, TG and MA adsorbed the least amount of protein in all pH conditions. Interestingly HMDSO-MA retained significantly lesser protein compared to HMDSO and dip-coated PDMS samples. In the presence of Polysorbate 80 (PS80) all plasma polymerized coatings adsorbed (<10ng/cm^2) and retained (<1ng/cm^2) negligible amounts of protein, compared to dip-coated PDMS and uncoated glass coverslips. Due to the versatility of RF

glow-discharge plasma, this process is scalable and can be used for the treatment of hypodermic syringes used for the storage and delivery of protein-based therapeutics.

4.2 INTRODUCTION

Current primary containers, including cartridges and syringes, used for storage and delivery of protein based drugs are dominated by silicone oil lubricated glass containers. Due to the high mobility of silicone oil there remains a major challenge for both reliable device performance and drug stability. Numerous studies have focused on understanding protein-silicone interactions.[76–80] Silicone oil which is commonly used as a lubricant in hypodermic syringes promote protein aggregation[78] which is due to the result of sloughing of silicone oil into the bulk over time or under agitation.[79] One study suggests that only at solution concentrations greater than 5 mg/mL does silicone oil cause aggregation in proteins,[80] whereas another study suggests that silicone oil only induces aggregation in the presence of another stressor like agitation.[81] Due to these challenges, significant efforts have been made in the pharmaceutical industry to develop alternative containers that have less mobile lubricants.

Furthermore, there is not enough fundamental understanding of critical attributes of surface-protein interactions, including the effects of surface properties, protein structures and formulation composition. Therefore, making it difficult to evaluate new containers that are being developed for storage and delivery of protein and antibody-based drugs. This paper addresses the nature of the surfaces that antibody-based protein drugs may contact, and their interactions with these proteins. An understanding of their impact on device performance will lead to the identification of new surfaces that will be best for contact with protein therapeutic agents while maintaining syringe lubricity.

RF glow-discharge plasma treatment is a method commonly used in microelectronics and biomaterials industry to deposit a monomer from a gaseous state onto a substrate. It has been well acknowledged that plasma polymerization is a very complex process, and the structure of plasma deposited films depends on many factors, including monomer structure, monomer pressure, monomer flow rate, substrate temperature, power level, and frequency.[25–27] Our lab has previously used RFGD technology to prepare a variety of surface coatings such as tetraethylene glycol dimethyl ether or tetraglyme (TG),[34] 2-hydroxyethylmethacrylate (HEMA),[50] and hexafluoropropylene (C3F6),[43] among others, for various applications.

Hexamethyldisiloxane (HMDSO) has a chemical structure quite similar to polydimethylsiloxane (PDMS) or silicone oil. Therefore, for this research, we propose to plasma polymerize hexamethyldisiloxane (HMDSO) and add a net negative charge to the surface coating by copolymerizing methacrylic acid (MA) in a 1:1 vapor pressure ratio (HMDSO-MA) as an alternative to using PDMS. Furthermore, Polysorbate 80 (PS80) in very low concentrations is currently used in the pharmaceutical industry to prevent proteins from aggregating in solution. Bovine IgG was used as a model antibody and the adsorption and retention of bovine IgG to these surface coatings were studied with and without the presence of PS80. In addition, the authors also examine the effect of pH (acidic, neutral and basic) on protein adsorption. Since most proteins and antibodies have a net negative charge in a neutral solution, we hypothesize that the net negative charge of the copolymer HMDSO-MA will help prevent proteins from adsorbing to the surface while maintaining syringe lubricity. To this end, we will be assessing the chemical composition, the fouling properties and lubricity of these newly prepared surface coatings by RF glow-discharge plasma. Moreover, since plasma technology can be used to coat almost any type of surface at an industrial scale, including glass containers and syringes, this technology would be easily

translatable to meet pharmaceutical industry needs for commercialization purposes. This would not only allow for more reliable delivery of protein drugs but also enhancing their stability and shelf life.

4.3 EXPERIMENT

4.3.1 Plasma deposition and characterization of HMDSO, MA, HMDSO-MA and TG surface coatings

4.3.1.1 Materials

8mm glass coverslips were purchased from Knitell Glass (Cat. No. G401-08). Hexamethyldisiloxane (HMDSO) (Cat. No. 205389), methacrylic acid (MA) (Cat. No. 395374) and tetraglyme (TG) (Cat. No. 172405) were purchased from Sigma-Aldrich. Silicone oil was graciously donated by Eli Lilly and Company. All organic solvents were purchased from Fisher Scientific.

4.3.1.2 Plasma polymerization

Prior to plasma deposition, 8 mm glass coverslips were placed in a sample holder within a glass container and ultrasonicated in a water bath for two 10 min cycles each in methylene chloride, followed by acetone and then methanol. All samples were air-dried in a fume hood before use.

Plasma polymerization was carried out in a custom-built plasma reactor setup based on the design reported in Lopez et al[34] and was modified to have two inlets which allowed for the flow of two monomers into the plasma chamber (Figure 4.1). Cleaned glass coverslips were

loaded in the plasma reactor and positioned in between the powered and grounded electrodes (100 mm apart), and a mechanical pump was used evacuate the reactor to the desired base pressure in the low 10^{-3} Torr range. A liquid nitrogen cooled cold trap between the vacuum pump and the reactor was used to condense organic materials. The powered electrode was connected to a 13.56 MHz radio frequency power source and an automatic impedance matching network.

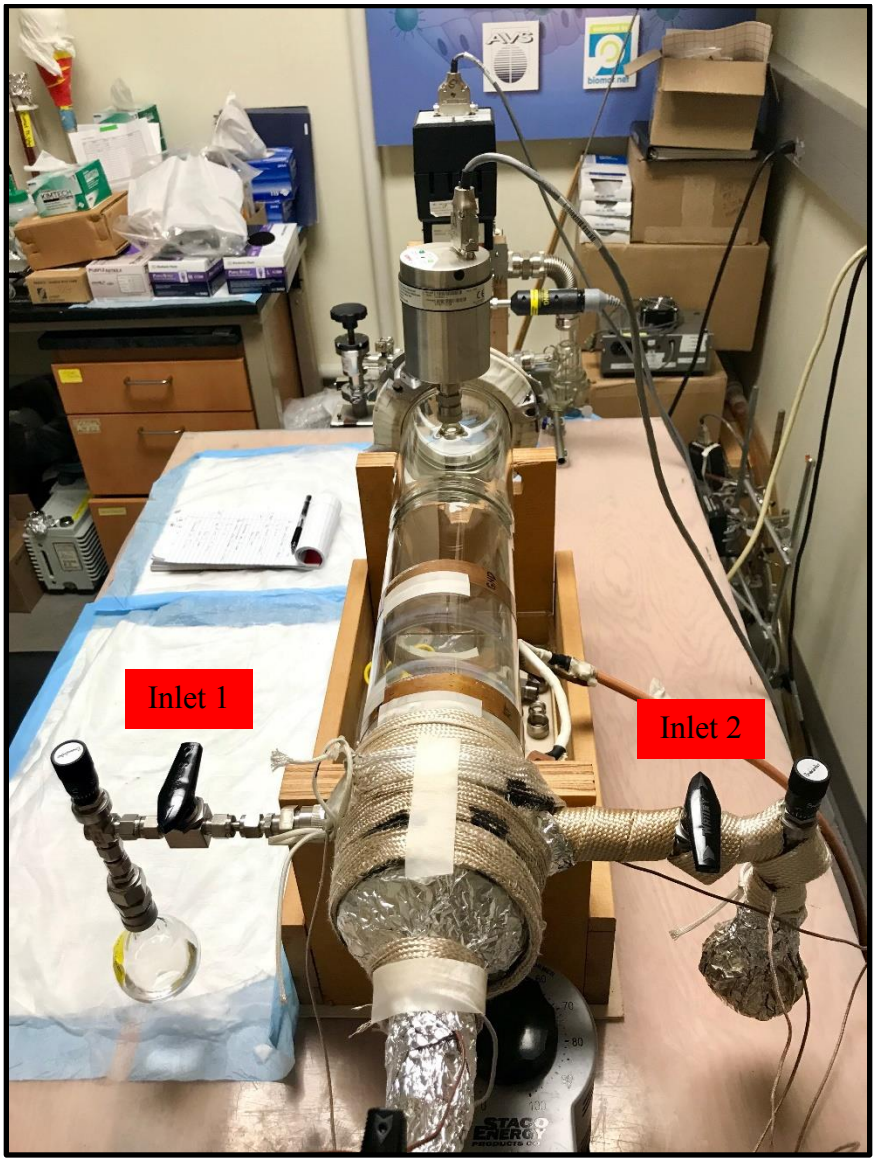

Figure 4.1. Custom-built plasma reactor setup with two inlets which allows for the controlled flow of two monomers into the plasma chamber using vernier caliper valves.

Cleaned glass coverslips used for the deposition of plasma polymerized MA were first etched in argon for 10 min at 40 W while maintaining a pressure of 150mT. Following that, substrates were coated with MA for 1 min at 80 W in order to form an adhesion layer, after which the power was lowered to 10 W for 10 min, while maintaining a pressure of 150 mT for the monomer throughout the plasma deposition process. Finally, samples were quenched for 5 min before retrieving them. Upon retrieval, samples were flipped, and the plasma treatment process was repeated with the same parameters to ensure uniform coatings on both sides of samples. The monomer was maintained at ambient room temperature during the plasma polymerization process

For plasma polymerized HMDSO samples, the monomer had to be heated to 40^{o} C using a water bath. Similarly, cleaned glass coverslips were first etched in argon for 10 min at 40W. Following that, substrates were coated with HMDSO for 1 min at 80 W, followed by 10W for 10 min. A pressure of 150 mT for the monomer as maintained throughout the plasma deposition process. Finally, samples were quenched for 5 min before retrieving them. Upon retrieval, samples were flipped, and the process was repeated to ensure uniform coatings.

In order to copolymerize MA and HMDSO, MA was connected to one inlet and maintained at room temperature, while HMDSO was connected to the other inlet and heated to 40^{o} C using a water bath. Cleaned glass coverslips were first etched in argon for 10 min at 40W. Both monomers were then introduced into the chamber at a 1:1 vapor pressure ratio and the pressure was maintained at 150 mT. The plasma polymerization parameters were exactly the same: 80 W for 1 min, and 10W for 10 min, followed by quenching for 5 min. Samples were then flipped and the process was repeated on the opposite side.

Previous research in our lab has shown that plasma polymerized tetraethylene glycol dimethyl ether coatings or TG have low fouling characteristics.[34,49] Therefore, the authors included TG as a potential candidate and control. For plasma polymerized TG samples, we followed a protocol as previously described in Chapter 3. Briefly, following the argon etching process, the TG monomer was heated to 110^{o} C and allowed to enter into the plasma chamber using a mass flow controller at a flow rate of 1.33 SCM. The glass coverslips were then coated with TG for 1 min at 80 W, followed by 20 min at 10 W, quenched for 5 min in the chamber and then retrieved. A pressure of 350 mT was maintained for the monomer during the plasma deposition process. After retrieving the samples, they were flipped and the process was repeated to ensure even coatings on both sides.

As another control we dip-coated glass coverslips in PDMS. Briefly, glass coverslips were cleaned using piranha solution (2 parts sulfuric acid and 1-part hydrogen peroxide) and then dip-coated in 1% PDMS in xylene and dried in an oven overnight at 60^{o} C, and repeated three times.

4.3.1.3 Surface characterization

X-ray photoelectron spectroscopy (XPS) was performed on all plasma polymerized glass disc samples on a Surface Science Instruments S-Probe equipped with a monochromatic Al Kα source and a low energy electron flood gun for charge neutralization. X-ray analysis for these acquisitions was in a circle approximately 800 μm across. Pressure in the analytical chamber during spectral acquisition was less than 5 x 10^{-9} Torr. Low-resolution survey scans were obtained from 0 to 1100 eV with a 1 eV step size and pass energy of 150 eV. High resolution C 1s scans were obtained from 270 to 290 eV with a 0.065 eV step size and pass energy of 50 eV.

The spectra were analyzed off line with Service Physics Hawk version 7 data analysis software to calculate the elemental compositions from peak areas and to peak fit high resolution spectra. All binding energies were calibrated with reference to the aliphatic carbon at C 1s = 285.0 eV. A Shirley background was used for all spectra.

4.3.1.4 Water contact angle

Water contact angles were measured for each plasma polymerized sample (n = 3) in a custom goniometer consisting of a syringe, digital microscope, light source, and a specimen platform. A 5 μL aliquot of deionized water was dropped onto the sample, brought into focus with the digital microscope, an image was captured, and the contact angle measured. The water contact angle was reported in degrees.

4.3.2 I-125 radiolabeled protein studies

4.3.2.1 Materials

Bovine IgG (Cat. No. I5506), sodium azide (Cat. No. S2002), and sodium iodide (Cat. No. 383112) were purchased from Sigma-Aldrich. Boric acid (Cat. No. A73-500), sodium phosphate monobasic (Cat# S369-500), and sodium hydroxide (Cat. No. S399-500) were purchased from Fisher Scientific. Sodium chloride crystals (Cat. No. SX0420-3) was purchased from EMD Millipore. Citric Acid, Monohydrate (Cat. No. 0115-01) was purchased from J.T. Baker. Iodine-125 radionuclide (Specific Activity: ~17Ci/mg, 10^{-5}M NaOH (pH 8-11)) was purchased from Perkin-Elmer (Cat. No. NEZ033A).

4.3.2.2 Protein iodination using ICl method

Bovine IgG was radiolabeled using the iodine monochloride (ICl) method modified by Horbett.[54] Briefly, 1mCi of Iodine-125 radionuclide was added to 0.5 mL 2x borate solution, to which 0.5mL of ICl/NaCl mixture in a 2:1 ratio was added. Finally, 0.5mL of a 10 mg/mL bovine IgG in a citrate phosphate buffered saline solution with sodium azide (cPBSz) was added and the iodination reaction was performed on ice for 20 min and then run through a size exclusion chromatography column. 40 fractions were collected to capture the labeled protein and free iodine peaks to evaluate iodination efficiency. The fractions from protein peaks were pooled together and run through a second chromatography column, repeating fraction collection and peak identification. Purified radiolabeled protein fractions were pooled together, placed in a lead pig, and frozen in -80^0 C freezer until further use.

4.3.2.3 I-125 radiolabeled bovine IgG protein adsorption and retention

Prior to the protein adsorption studies, plasma treated substrates (n = 4) were soaked in 0.75 mL cPBS solution with sodium iodide for 2 h in either acidic pH (~4), neutral pH (~7.4) or basic pH (~10). For the adsorption, the radiolabeled bovine IgG was thawed and then added to a 0.2 mg/mL solution of bovine IgG in cPBSzI in either acidic, neutral or basic pH to create “hot” protein with an acitivity of ~100 CPM/ng. 0.75mL of the “hot IgG” protein was then added to each plasma treated substrate sample, and allowed to adsorb for 2 h, before washing three times with cPBSzI using a rinsing system. The samples were then transferred to a gamma counter tube and the radioactivity of each sample was then measured for 1 min along with protein standards using a Packard Cobra 2 Gamma Counter. To understand the effect of PS80 on bovine IgG protein adsorption, the above protein adsorption experiment was repeated in buffer solutions

with different pH (acidic, neutral and basic) with 0.04 mg/mL PS80. For the protein retention studies, samples with adsorbed bovine IgG protein in the various conditions (different pH, and with or without PS80) were placed in new tubes with 1mL of 1% SDS and allowed to sit overnight. The samples were then rinsed three times using a rinsing system with cPBSzI, placed in a gamma counter tube and measured for 1 min along with protein standards using a Packard Cobra Gamma Counter. Uncoated glass disc samples were used as controls. Adsorption and retention data were reported in ng/cm^2.

4.3.3 Syringe glide force testing

4.3.3.1 Plasma polymerization

3 mL syringe barrels (without the plunger) were placed in a rack holder right in between the electrodes of the plasma reactor. The syringe barrels were placed in the direction of flow of gasses in the reactor such that the gases flowed from the barrel flange end to the adaptor end of the syringe barrel. The syringe barrels were then plasma polymerized similar to the methods described in Section 4.3.1.2. This process was repeated for the syringe plungers. The syringe plungers were also placed in the direction of flow of gases in the reactor such that the gases flowed from the plunger seal end to the plunger flange end.

4.3.3.2 Glide force measurements using INSTRON

BD Luer-Lok^{TM} Tip 3mL syringes (Cat. No. 309657) were purchased from Fisher Scientific. The syringe glide force was measured using an INSTRON with a custom built syringe testing fixture (Figure 4.2) and analyzed using the Bluehill testing software. For testing, we followed a protocol similar to the one laid out by Yoshino et al.[82] Briefly, syringe barrels with

plunger were placed in the syringe testing fixture and the plunger was moved downward at room temperature using a 10N load cell and the force required for gliding the plunger stopper and plunger were recorded. The stroke distance and the crosshead speed were set at 30 mm and 200 mm/min, respectively. The maximum gliding force between 0 and 5 mm of stroke distance was defined as the syringe peak glide force and was reported in N.

Each syringe plasma coated with either MA, HMDSO, HMDSO-MA and TG were tested dry as well as wet (soaked in cPBS buffer for 3 h). Untreated syringes were used as controls.

Figure 4.2. Custom-built syringe testing fixture for use with the INSTRON to measure the syringe glide force.

4.4 Results and Discussion

The goal of this research was to identify new surface coatings prepared by RF glow-discharge plasma for the treatment of hypodermic syringes that would be best for contact with protein therapeutic agents while maintaining syringe lubricity. To this end, we prepared a plasma polymerized HMDSO surface and added a net negative charge to the surface by copolymerizing HMDSO with MA. We then assessed the chemical composition, stability, protein adsorption and safety (toxicology) of these plasma polymerized surface coatings so that we can make appropriate surface recommendations for the storage and delivery of antibody-based drugs.

XPS was used to assess the surface of all plasma polymerized samples. The survey scans seen in Figure 4.2, and summarized in Table 4.1, provide information on the overall surface chemical composition. For all plasma polymerized coatings we found that the overall chemical composition matched the expected composition reasonably well (Table 4.1). Furthermore, no Si peaks associated with the glass coverslips were seen in the survey scans, which indicate that the plasma coatings were greater than 10nm in thickness, as this is the depth to which XPS is able to analyze a surface. However, further experiments will need to be conducted in order to determine the thickness of the plasma coatings using either ellipsometry or profilometry. It should be noted that XPS was not done on the PDMS dip-coated glass coverslips due to potential PDMS contamination to the XPS instrument.

High resolution C 1s spectra (Figure 4.3) provide insight into the chemical bonding environment of carbon. All plasma coatings showed characteristic shifts in the carbon peaks based on the chemical structure of the monomer. The carbon peak associated with MA was a

doublet, with a characteristic peak at ~285 eV associated with the hydrocarbon bond, and another, smaller peak at ~289 eV associated with COOR bond from the carboxyl group of MA. The high-resolution carbon peak from HMDSO is a singlet at ~285 eV which is characteristic of CH bond, and the high-resolution carbon peak from TG plasma coating is also a singlet at ~286.5 eV and is characteristic of CO bond (Figure 3.3 B). Similar to MA, two width-constrained peaks were used to fit the high-resolution C1s peaks of the copolymer HMDSO-MA: CH at ~285.0 eV and COO at ~289 eV. It should be noted that all XPS spectra were shifted so that the hydrocarbon peak could align at 285.0 eV (charging binding energy correction).

Water contact angle experiments was used to assess the surface wettability of plasma treated substrates. Cleaned glass coverslips had a water contact angle of $32.3^{o} \pm 2.8^{o}$. Plasma polymerized MA samples were hydrophilic with a water contact angle of $39.7^{o} \pm 1.8^{o}$. As expected, dip-coated PDMS surfaces was hydrophobic with water contact angles at $89.1^{o} \pm 1.8^{o}$. Copolymer HMDSO-MA surface coatings were also slightly hydrophobic at $87.0^{o} \pm 3.1^{o}$ but less than plasma polymerized HDMSO surfaces which is at $103.0^{o} \pm 1.1^{o}$. Since HMDSO-MA is slightly less hydrophobic that HMDSO, these results are in accordance with the fact that we copolymerized MA with HMDSO.

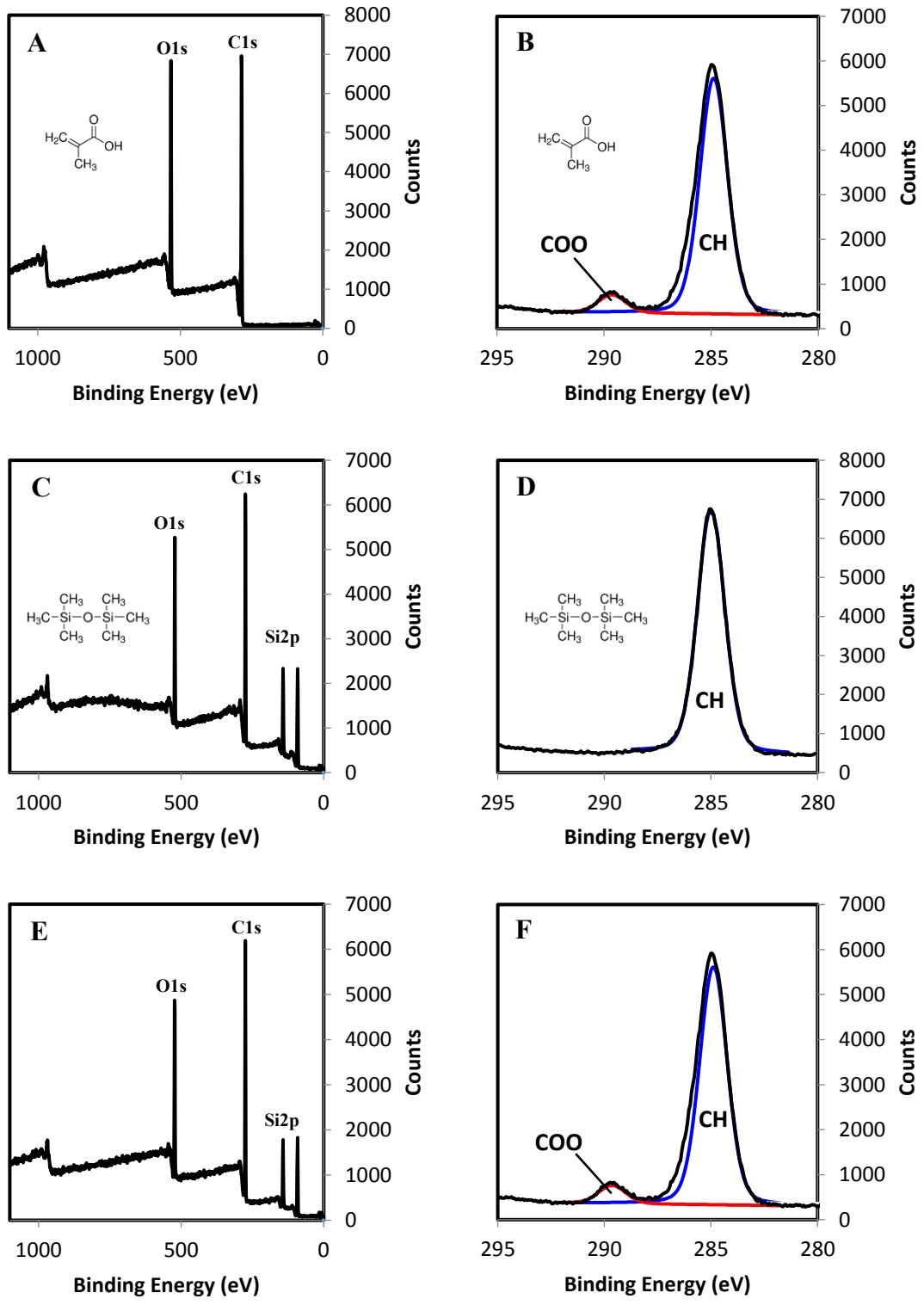

Figure 4.3. Representative XPS survey scans and high-resolution spectra of the C1s peak (black envelope) and corresponding monomer chemical structure (inset) of plasma polymerized (A) and (B) MA; (C) and (D) HMDSO; and (E) and (F) HMDSO-MA on glass coverslips. Fitted peaks are colored to correspond to carbons in different chemical environments.

Table 4.1. Summary of surface elemental composition of plasma polymerized MA, HMDSO, HMDSO-MA and TG surface coatings as determined by survey and hi-res scans obtained from XPS (n = 3).

Plasma coating		Elemental Composition (%)			Bonding Components of C 1s (%)		
		C	O	Si	1 (CH)	2 (CO)	3 (COO)
MA	Observed	**81.2 ± 0.7**	**18.8 ± 0.7**	-	**76.5 ± 0.3**	**11.5 ± 0.3**	**12.0 ± 0.5**
	Expected	66.7	33.3	-	50	25	25
HMDSO	Observed	**51.5 ± 0.7**	**18.8 ± 0.9**	**29.6 ± 0.7**	**100**	-	-
	Expected	66.7	11.1	22.2	100	-	-
HMDSO-MA	Observed	**59.8 ± 0.3**	**19.1 ± 0.2**	**21.1 ± 0.2**	**80.9 ± 2.8**	**13.6 ± 2.4**	**5.5 ± 0.4**
	Expected	66.7	20	13.3	40	20	20
TG	Observed	**67.3 ± 1.7**	**32.7 ± 1.7**	-	-	**100**	-
	Expected	66.7	33.3	-	-	100	-

For this research, bovine IgG was used as a model protein to examine the interaction between antibody-based drugs and our plasma polymerized surface coatings. Figure 4.4 depicts the results from the bovine IgG protein adsorption study in different pH environments. As expected, hydrophilic surfaces, TG and MA, adsorb protein less than the hydrophobic surfaces, dip-coated PDMS and plasma polymerized HMDSO and HMDSO-MA. Furthermore, within each treatment group, it is clear that bovine IgG adsorbs the least amount in basic pH conditions. Since the isoelectronic point of most immunoglobulins is around pH 7, we would expect bovine IgG to have a net negative charge in a basic pH solution and a net positive charge in acidic solution of pH 4 respectively. This would cause the bovine IgG to repel from a negatively charged surface in a basic pH, and attract to a negatively charged surface in an acidic pH, which is evident from Figure 4.4.

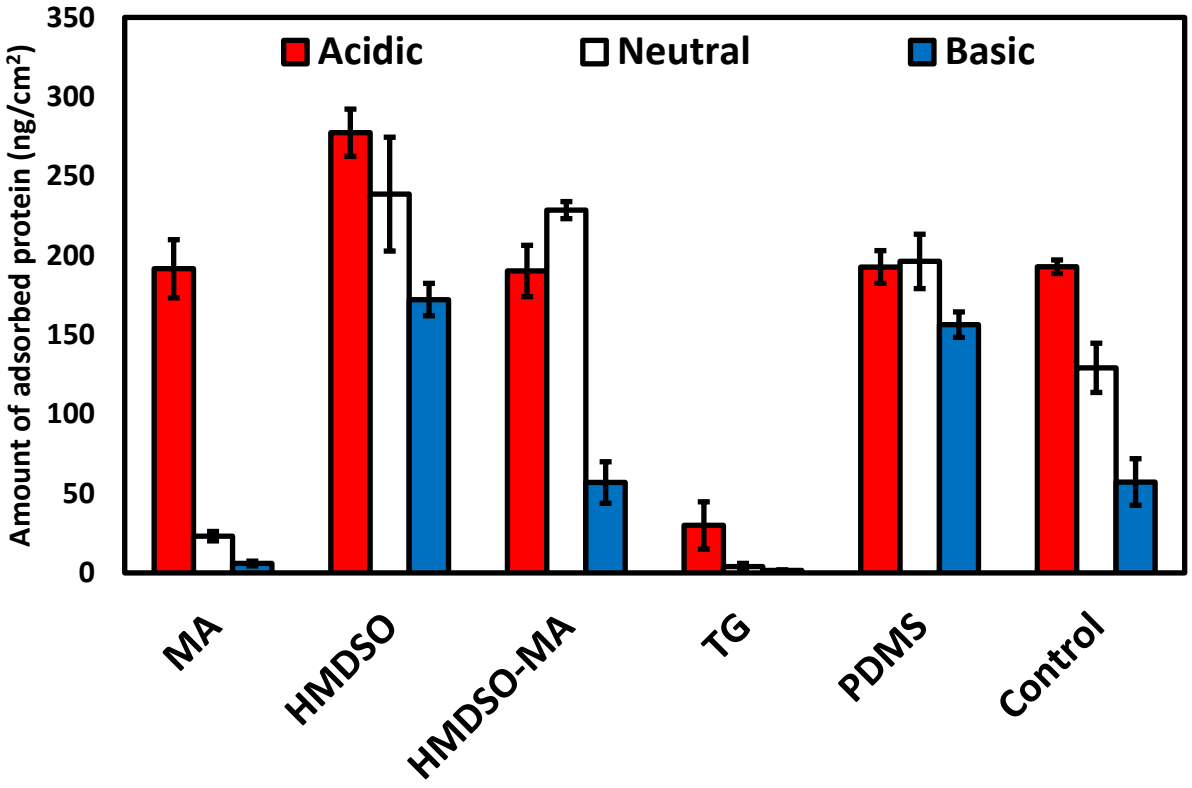

Figure 4.4. Amount of bovine IgG adsorbed onto plasma polymerized MA, HMDSO, HMDSO-MA, TG and dip-coated PDMS samples after 2 h in a 0.1 mg/mL bovine IgG solution in different pH conditions (acidic, neutral and basic) as determined by I-125 radiolabeling method.

Retention studies help understand the strength of bonding between the adsorbed protein and the surface. Figure 4.5 illustrates the results from the bovine IgG retention study in different pH environments. As expected, hydrophobic surfaces, dip-coated PDMS and plasma polymerized HMDSO, retain the most amount of protein on the surface, while the hydrophilic surfaces, TG and MA, retain the least amount of protein on the surface (<1 ng/cm^2) in all pH solutions. Interestingly, plasma polymerized HMDSO-MA did not retain as much bovine IgG as compared to the other hydrophobic surfaces (<5 ng/cm^2). These results indicate that

copolymerized HMDSO-MA surface coatings do not strongly bind to the adsorbed bovine IgG as compared to plasma polymerized HMDSO and dip-coated PDMS.

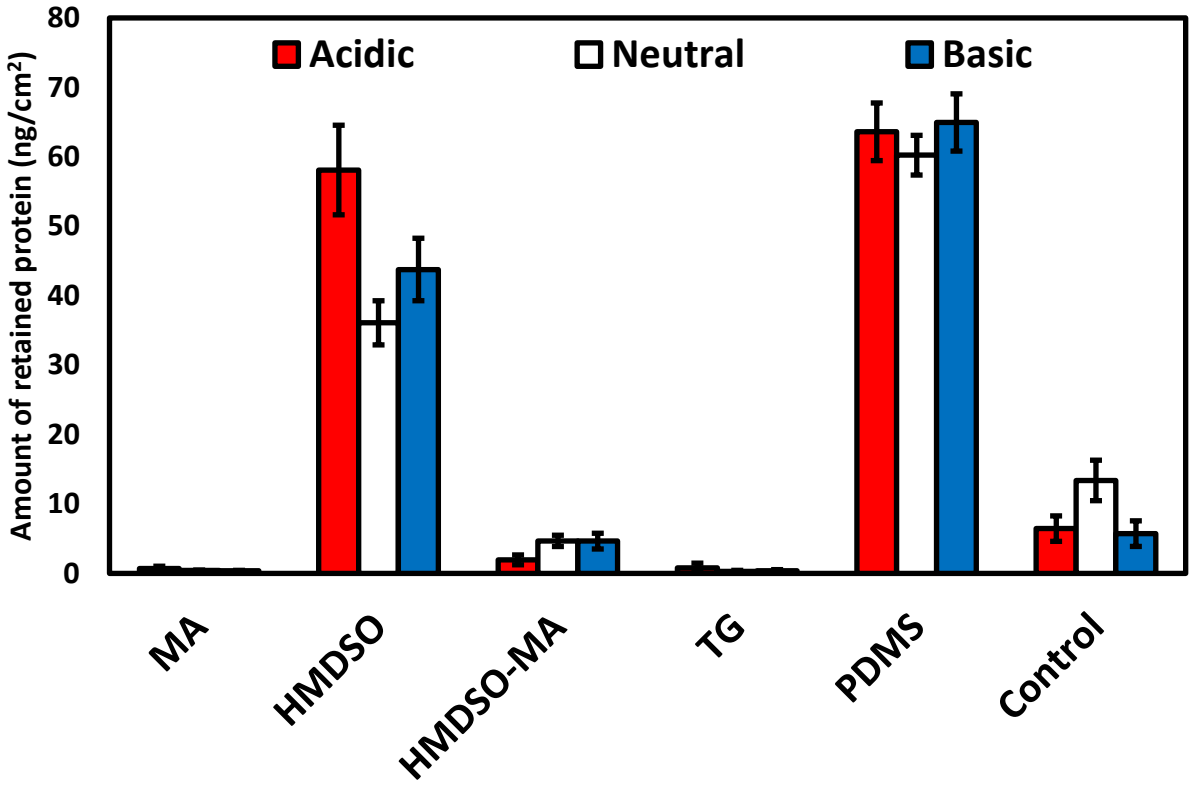

Figure 4.5. Amount of bovine IgG retained on plasma polymerized MA, HMDSO, HMDSO-MA, TG and dip-coated PDMS samples in different pH conditions (acidic, neutral and basic) after overnight elution with 2% SDS as determined by I-125 radiolabeling method.

PS80 in small concentrations have been shown to prevent protein adsorption and stabilize against protein aggregation in solution.[83] Therefore, a number of pharmaceutical companies use PS80 to increase the shelf life of protein-based therapeutics. Figure 4.6 depicts the results from the bovine IgG protein adsorption study in different pH environments in the presence of PS80.

As seen, all plasma polymerized surface, both hydrophilic and hydrophobic, adsorb <10 ng/cm^2 of protein on the surface in the presence of PS80. We also notice a reduction in the adsorption of bovine IgG to dip-coated PDMS surfaces in the presence of PS80, however, they are still higher compared to the other plasma polymerized surface coatings. For the dip-coated PDMS and control samples we see that more protein is adsorbed in acidic pH compared to neutral or basic pH. However, for the other plasma polymerized surface coatings in the presence of PS80 pH did not seem to have an effect on the amount of adsorbed.

Figure 4.7 depicts the results from the bovine IgG retention study in different pH environments in the presence of PS80. All plasma polymerized coatings retain almost no protein on the surface (<1 ng/cm^2), whereas dip-coated PDMS retains the most amount of protein in all pH conditions. These results indicate that in the presence of PS80 bovine IgG does not strongly bind to the surface of plasma polymerized MA, HMDSO, HMDSO-MA, or TG surface coatings.

Finally, we tested whether our plasma polymerized surface coatings had any effect in syringe lubricity. Figure 4.8 depicts the results of the syringe peak glide force measurements of the plasma polymerized syringes in dry and wet conditions. We observe that the plasma coatings have no effect on syringe peak glide force as compared to untreated syringe controls in both dry and wet conditions. Therefore, these plasma coatings can be used to coat syringes without affecting the syringe lubricity.

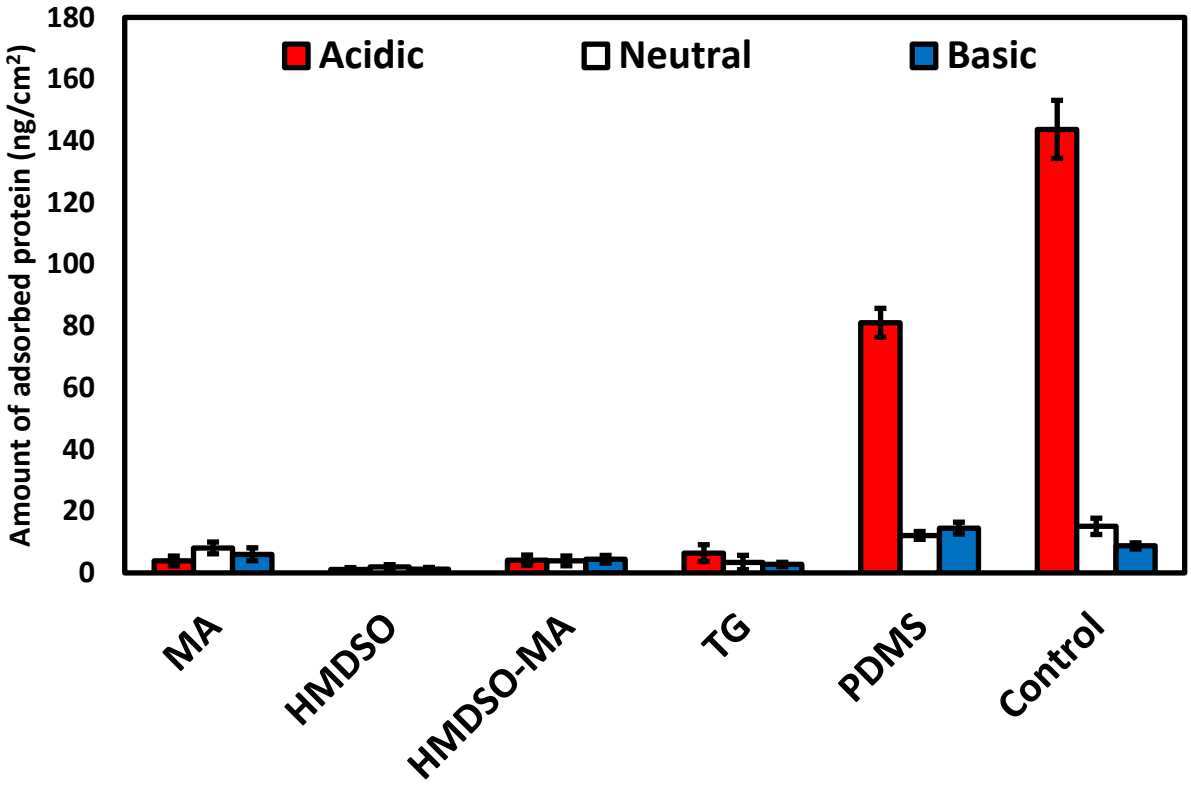

Figure 4.6. Amount of bovine IgG adsorbed onto plasma polymerized MA, HMDSO, HMDSO-MA, TG and dip-coated PDMS samples after 2 h in a 0.1 mg/mL bovine IgG solution in different pH conditions (acidic, neutral and basic) in the presence of PS80 as determined by I-125 radiolabeling method.

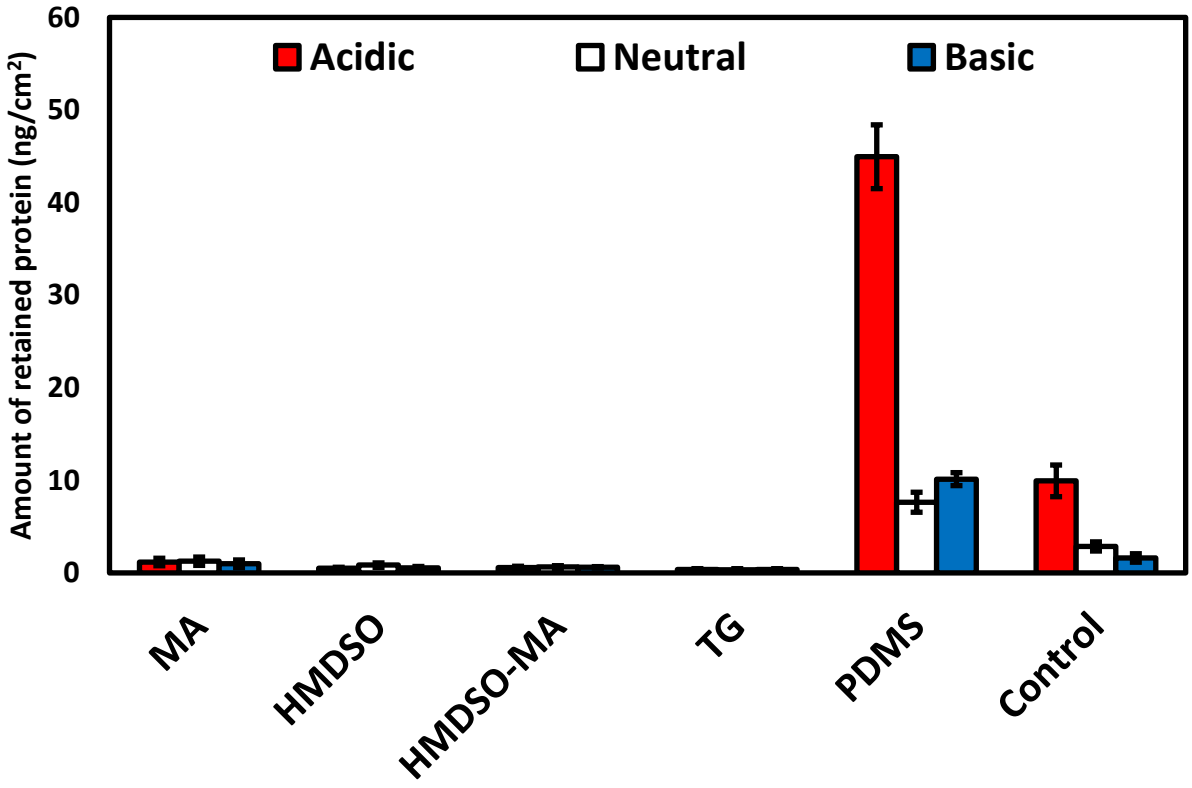

Figure 4.7. Amount of bovine IgG retained onto plasma polymerized MA, HMDSO, HMDSO-MA, TG and dip-coated PDMS samples in different pH conditions (acidic, neutral and basic) in the presence of PS80 after overnight elution with 2% SDS as determined by I-125 radiolabeling method.

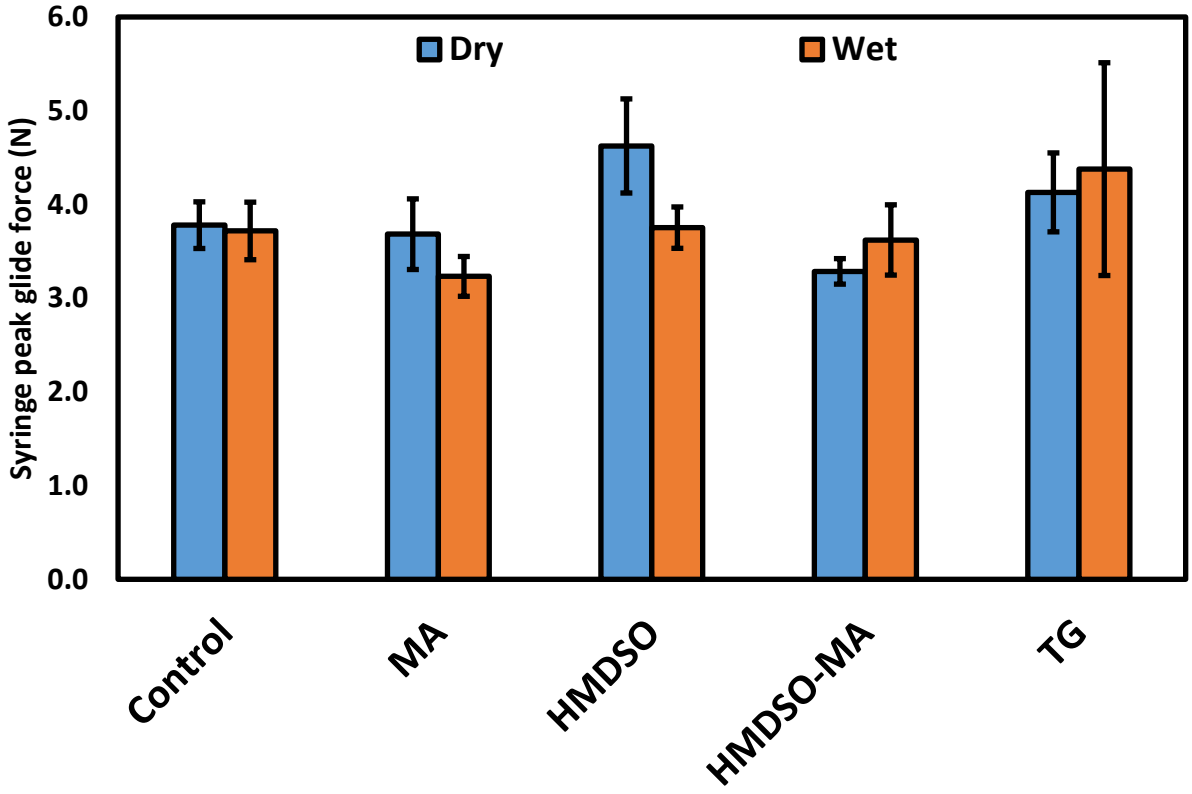

Figure 4.8. Syringe peak glide force measurements of plasma polymerized MA, HMDSO, HMDSO-MA, TG and untreated control syringes at room temperature in both dry and wet conditions.

4.5 Conclusions

The goal of this research was to create new surface coatings that will allow more reliable delivery of protein drugs while enhancing their stability and shelf life. We have demonstrated that plasma polymerized MA, HMDSO, HMDSO-MA and TG adsorb and retain less protein in different pH conditions, both with and without PS80, as compared to dip-coated PDMS and untreated glass controls making them good recommendations for hypodermic syringe treatments

which will allow more reliable delivery of protein drugs while enhancing their stability and shelf life. Due to the versatility of RF glow-discharge plasma technology, this process is scalable and can be applied to hypodermic syringes, for the delivery and storage of protein therapeutics. We have also demonstrated that these plasma coatings can be easily applied to syringe barrels and plungers while not affecting syringe lubricity, and thus provide better alternatives to using silicone oil. Future studies will examine syringe lubricity of these plasma polymerized coatings a) before and after protein adsorption in different pH solutions; and b) with and without PS80. Furthermore, we will also investigate the toxicology profile of these surface treatments via cell culture.

4.6 Acknowledgements

Part of this work was conducted at the Molecular Analysis Facility, a National Nanotechnology Coordinated Infrastructure site at the University of Washington which is supported in part by the National Science Foundation (grant ECC-1542101), the University of Washington, the Molecular Engineering & Sciences Institute, the Clean Energy Institute, and the National Institutes of Health.

BIBLIOGRAPHY

1. He, X., Yang, W. & Pei, X. Preparation, characterization, and tunable wettability of poly(ionic liquid) brushes via surface-initiated atom transfer radical polymerization. *Macromolecules* (2008). doi:10.1021/ma702389y

2. Yue, W. W. *et al.* Grafting of zwitterion from polysulfone membrane via surface-initiated ATRP with enhanced antifouling property and biocompatibility. *J. Memb. Sci.* (2013). doi:10.1016/j.memsci.2013.06.029

3. Huang, J., Murata, H., Koepsel, R. R., Russell, A. J. & Matyjaszewski, K. Antibacterial polypropylene via surface-initiated atom transfer radical polymerization. *Biomacromolecules* (2007). doi:10.1021/bm061236j

4. Jones, D. M., Smith, J. R., Huck, W. T. S. & Alexander, C. Variable Adhesion of Micropatterned Thermoresponsive Polymer Brushes: AFM Investigations of Poly(N-isopropylacrylamide) Brushes Prepared by Surface-Initiated Polymerizations. *Adv. Mater.* (2002). doi:10.1002/1521-4095(20020816)14:16<1130::aid-adma1130>3.0.co;2-7

5. Ma, H., Hyun, J., Stiller, P. & Chilkoti, A. 'Non-Fouling' Oligo(ethylene glycol)-Functionalized Polymer Brushes Synthesized by Surface-Initiated Atom Transfer Radical Polymerization. *Adv. Mater.* (2004). doi:10.1002/adma.200305830

6. Siegwart, D. J., Oh, J. K. & Matyjaszewski, K. ATRP in the design of functional materials for biomedical applications. *Progress in Polymer Science (Oxford)* (2012). doi:10.1016/j.progpolymsci.2011.08.001

7. Morandi, G., Heath, L. & Thielemans, W. Cellulose nanocrystals grafted with polystyrene chains through Surface-Initiated Atom Transfer Radical Polymerization (SI-ATRP). *Langmuir* (2009). doi:10.1021/la900452a

8. Huang, C., Tassone, T., Woodberry, K., Sunday, D. & Green, D. L. Impact of ATRP initiator spacer length on grafting poly(methyl methacrylate) from Silica nanoparticles. *Langmuir* (2009). doi:10.1021/la901918v

9. Lee, B. S., Chi, Y. S., Lee, K. B., Kim, Y. G. & Choi, I. S. Functionalization of poly(oligo(ethylene glycol) methacrylate) films on gold and Si/SiO2 for immobilization of proteins and cells: SPR and QCM studies. *Biomacromolecules* (2007). doi:10.1021/bm7009043

10. Mrabet, B. *et al.* Anti-fouling poly(2-hydoxyethyl methacrylate) surface coatings with specific bacteria recognition capabilities. *Surf. Sci.* (2009). doi:10.1016/j.susc.2009.05.020

11. Kim, D. J. *et al.* Formation of thermoresponsive gold nanoparticle/PNIPAAm hybrids by surface-initiated, atom transfer radical polymerization in aqueous media. *Macromol. Chem. Phys.* (2005). doi:10.1002/macp.200500268

12. Zhang, Z., Chao, T., Chen, S. & Jiang, S. Superlow fouling sulfobetaine and carboxybetaine polymers on glass slides. *Langmuir* (2006). doi:10.1021/la062175d

13. Ladd, J., Zhang, Z., Chen, S., Hower, J. C. & Jiang, S. Zwitterionic polymers exhibiting high resistance to nonspecific protein adsorption from human serum and plasma. *Biomacromolecules* (2008). doi:10.1021/bm701301s

14. Zhang, Z., Chen, S., Chang, Y. & Jiang, S. Surface grafted sulfobetaine polymers via atom transfer radical polymerization as superlow fouling coatings. *J. Phys. Chem. B* (2006). doi:10.1021/jp057266i

15. Yang, W. & Zhou, F. Polymer brushes for antibiofouling and lubrication. *Biosurface and Biotribology* **3**, 97–114 (2017).

16. Matyjaszewski, K., Patten, T. E. & Xia, J. Controlled/'living' radical polymerization. Kinetics of the homogeneous atom transfer radical polymerization of styrene. *J. Am. Chem. Soc.* (1997). doi:10.1021/ja963361g

17. Min, K., Gao, H. & Matyjaszewski, K. Use of Ascorbic Acid as Reducing Agent for Synthesis of Well-Defined Polymers by ARGET ATRP. *Macromolecules* (2007). doi:10.1021/ma0702041

18. Kwak, Y. & Matyjaszewski, K. ARGET ATRP of methyl methacrylate in the presence of nitrogen-based ligands as reducing agents. *Polym. Int.* (2009). doi:10.1002/pi.2530

19. Paterson, S. M. *et al.* The synthesis of water-soluble PHEMA via ARGET ATRP in protic media. *J. Polym. Sci. Part A Polym. Chem.* (2010). doi:10.1002/pola.24194

20. Jones, D. M., Brown, A. A. & Huck, W. T. S. Surface-initiated polymerizations in aqueous media: Effect of initiator density. *Langmuir* (2002). doi:10.1021/la011365f

21. Zhu, B. & Edmondson, S. Polydopamine-melanin initiators for Surface-initiated ATRP. *Polymer (Guildf).* (2011). doi:10.1016/j.polymer.2011.03.027

22. Yang, W. J. *et al.* Biomimetic anchors for antifouling and antibacterial polymer brushes on stainless steel. *Langmuir* (2011). doi:10.1021/la200620s

23. Mühlebach, A., Gaynor, S. G. & Matyjaszewski, K. Synthesis of amphiphilic block copolymers by atom transfer radical polymerization (ATRP). *Macromolecules* (1998). doi:10.1021/ma9804747

24. Mignard, E. *et al.* Kinetics and molar mass evolution during atom transfer radical polymerization of n-Butyl acrylate using automatic continuous online monitoring. *Macromolecules* (2005). doi:10.1021/ma050590r

25. Yasuda, H. Glow discharge polymerization. *J. Polym. Sci. Macromol. Rev.* (2003). doi:10.1002/pol.1981.230160104

26. Biederman, H. & Slavínská, D. Plasma polymer films and their future prospects. *Surf. Coatings Technol.* (2000). doi:10.1016/S0257-8972(99)00578-2

27. Hoffman, A. S. Ionizing radiation and gas plasma (or glow) discharge treatments for preparation of novel polymeric biomaterials. in (2012). doi:10.1007/3-540-12796-8_12

28. Teare, D. O. H. *et al.* Substrate-independent approach for polymer brush growth by surface atom transfer radical polymerization. *Langmuir* (2005). doi:10.1021/la051772h

29. Morsch, S., Schofield, W. C. E. & Badyal, J. P. S. Tailoring the density of surface-tethered bottlebrushes. *Langmuir* (2011). doi:10.1021/la201967f

30. Shi, Y. *et al.* A versatile and rapid coating method via a combination of plasma polymerization and surface-initiated SET-LRP for the fabrication of low-fouling surfaces. *J. Polym. Sci. Part A Polym. Chem.* (2017). doi:10.1002/pola.28646

31. Coad, B. R., Styan, K. E. & Meagher, L. One step ATRP initiator immobilization on surfaces leading to gradient-grafted polymer brushes. *ACS Appl. Mater. Interfaces* (2014). doi:10.1021/am501052d

32. Saboohi, S., Coad, B. R., Michelmore, A., Short, R. D. & Griesser, H. J. Hyperthermal Intact Molecular Ions Play Key Role in Retention of ATRP Surface Initiation Capability of Plasma Polymer Films from Ethyl α-Bromoisobutyrate. *ACS Appl. Mater. Interfaces* (2016). doi:10.1021/acsami.6b04477

33. Hucknall, A. *et al.* Versatile synthesis and micropatterning of nonfouling polymer brushes on the wafer scale. *Biointerphases* (2009). doi:10.1116/1.3151968

34. Löpez, G. P. *et al.* Glow discharge plasma deposition of tetraethylene glycol dimethyl ether for fouling-resistant biomaterial surfaces. *J. Biomed. Mater. Res.* (1992). doi:10.1002/jbm.820260402

35. Olivier, A., Meyer, F., Raquez, J. M., Damman, P. & Dubois, P. Surface-initiated controlled polymerization as a convenient method for designing functional polymer brushes: From self-assembled monolayers to patterned surfaces. *Progress in Polymer Science (Oxford)* (2012). doi:10.1016/j.progpolymsci.2011.06.002

36. Senaratne, W., Andruzzi, L. & Ober, C. K. Self-assembled monolayers and polymer brushes in biotechnology: Current applications and future perspectives. *Biomacromolecules* (2005). doi:10.1021/bm050180a

37. Vickerman, J. C. & Gilmore, I. S. *Surface Analysis - The Principal Techniques: Second Edition*. *Surface Analysis - The Principal Techniques: Second Edition* (2009). doi:10.1002/9780470721582

38. Alvarez, S., Mota, F. & Novoa, J. Structure and Stability of Br4 and Br42_ and Their Interaction with Cations and Transition Metals. *J. Am. Chem. Soc.* (1987). doi:10.1021/ja00256a003

39. Yaya, A. *et al.* A study of polybromide chain formation using carbon nanomaterials via density functional theory approach. *Cogent Eng.* (2016). doi:10.1080/23311916.2016.1261509

40. Easton, M. E. *et al.* The formation of high-order polybromides in a room-temperature ionic liquid: From monoanions ([Br5]-to [Br11]-) to the isolation of [PC16H36]2[Br24] as Determined by van der Waals Bonding Radii. *Chem. - A Eur. J.* (2015).

doi:10.1002/chem.201404505

41. Taylor, M. *et al.* 3D chemical characterization of frozen hydrated hydrogels using ToF-SIMS with argon cluster sputter depth profiling. *Biointerphases* (2016). doi:10.1116/1.4928209

42. Lanzalaco, S. *et al.* Atom transfer radical polymerization with different halides (F, Cl, Br, and I): Is the process 'living' in the presence of fluorinated initiators? *Macromolecules* (2016). doi:10.1021/acs.macromol.6b02286

43. Garrison, M. D., Luginbühl, R., Overney, R. M. & Ratner, B. D. Glow discharge plasma deposited hexafluoropropylene films: Surface chemistry and interfacial materials properties. *Thin Solid Films* (1999). doi:10.1016/S0040-6090(98)01733-7

44. Liyanage, T. *et al.* Worldwide access to treatment for end-stage kidney disease: A systematic review. *Lancet* (2015). doi:10.1016/S0140-6736(14)61601-9

45. Robinson, B. M. *et al.* Factors affecting outcomes in patients reaching end-stage kidney disease worldwide: differences in access to renal replacement therapy, modality use, and haemodialysis practices. *The Lancet* (2016). doi:10.1016/S0140-6736(16)30448-2

46. 2018 USRDS Annual Data Report: Executive Summary. *Am. J. Kidney Dis.* (2019). doi:10.1053/j.ajkd.2019.01.002

47. Kakkos, S. K. *et al.* Equivalent secondary patency rates of upper extremity Vectra Vascular Access Grafts and transposed brachial-basilic fistulas with aggressive access surveillance and endovascular treatment. *J. Vasc. Surg.* (2008). doi:10.1016/j.jvs.2007.09.061

48. Snyder, D. C., Clericuzio, C. P., Stringer, A. & May, W. Comparison of outcomes of arteriovenous grafts and fistulas at a single Veterans' Affairs medical center. *Am. J. Surg.* (2008). doi:10.1016/j.amjsurg.2008.07.013

49. Cao, L. *et al.* Plasma-deposited tetraglyme surfaces greatly reduce total blood protein adsorption, contact activation, platelet adhesion, platelet procoagulant activity, and in vitro thrombus deposition. *J. Biomed. Mater. Res. - Part A* (2007). doi:10.1002/jbm.a.31091

50. López, G. P., Ratner, B. D., Rapoza, R. J. & Horbett, T. A. Plasma Deposition of Ultrathin Films of Poly(2-hydroxyethyl methacrylate): Surface Analysis and Protein Adsorption Measurements. *Macromolecules* (1993). doi:10.1021/ma00065a001

51. Cao, L., Sukavaneshvar, S., Ratner, B. D. & Horbett, T. A. Glow discharge plasma treatment of polyethylene tubing with tetraglyme results in ultralow fibrinogen adsorption and greatly reduced platelet adhesion. *J. Biomed. Mater. Res. - Part A* (2006). doi:10.1002/jbm.a.30908

52. Jiang, S. & Cao, Z. Ultralow-fouling, functionalizable, and hydrolyzable zwitterionic materials and their derivatives for biological applications. *Adv. Mater.* (2010). doi:10.1002/adma.200901407

53. Zhang, L. *et al.* Zwitterionic hydrogels implanted in mice resist the foreign-body reaction.

Nat. Biotechnol. (2013). doi:10.1038/nbt.2580

54. Horbett, T. A. Adsorption of proteins from plasma to a series of hydrophilic-hydrophobic copolymers. II. Compositional analysis with the prelabeled protein technique. *J. Biomed. Mater. Res.* (1981). doi:10.1002/jbm.820150506

55. Chames, P., Van Regenmortel, M., Weiss, E. & Baty, D. Therapeutic antibodies: Successes, limitations and hopes for the future. *British Journal of Pharmacology* (2009). doi:10.1111/j.1476-5381.2009.00190.x

56. Balasubramanian, V., Grusin, N. K., Bucher, R. W., Turitto, V. T. & Slack, S. M. Residence-time dependent changes in fibrinogen adsorbed to polymeric biomaterials. *J. Biomed. Mater. Res.* (1999). doi:10.1002/(SICI)1097-4636(19990305)44:3<253::AID-JBM3>3.0.CO;2-K

57. Chen, H., Yuan, L., Song, W., Wu, Z. & Li, D. Biocompatible polymer materials: Role of protein-surface interactions. *Progress in Polymer Science (Oxford)* (2008). doi:10.1016/j.progpolymsci.2008.07.006

58. Andrade, J. D. & Hlady, V. Protein adsorption and materials biocompatibility: A tutorial review and suggested hypotheses. in (1986). doi:10.1007/3-540-16422-7_6

59. Elbert, D. L. & Hubbell, J. A. Surface Treatments of Polymers for Biocompatibility. *Annu. Rev. Mater. Sci.* (1996). doi:10.1146/annurev.ms.26.080196.002053

60. Roach, P., Farrar, D. & Perry, C. C. Interpretation of protein adsorption: Surface-induced conformational changes. *J. Am. Chem. Soc.* (2005). doi:10.1021/ja042898o

61. Sofia, S. J., Premnath, V. & Merrill, E. W. Poly(ethylene oxide) grafted to silicon surfaces: Grafting density and protein adsorption. *Macromolecules* (1998). doi:10.1021/ma971016l

62. Paynter, R. W., Ratner, B. D., Horbett, T. A. & Thomas, H. R. XPS studies on the organization of adsorbed protein films on fluoropolymers. *J. Colloid Interface Sci.* (1984). doi:10.1016/0021-9797(84)90023-7

63. Lhoest, J. B., Wagner, M. S., Tidwell, C. D. & Castner, D. G. Characterization of adsorbed protein films by time of flight secondary ion mass spectrometry. *J. Biomed. Mater. Res.* (2001). doi:10.1002/1097-4636(20011205)57:3<432::AID-JBM1186>3.0.CO;2-G

64. Wagner, M. S. & Castner, D. G. Characterization of adsorbed protein films by time-of-flight secondary ion mass spectrometry with principal component analysis. *Langmuir* (2001). doi:10.1021/la001209t

65. Zhang, Z. *et al.* Blood compatibility of surfaces with superlow protein adsorption. *Biomaterials* (2008). doi:10.1016/j.biomaterials.2008.07.039

66. Li, L., Chen, S., Zheng, J., Ratner, B. D. & Jiang, S. Protein adsorption on oligo(ethylene glycol)-terminated alkanethiolate self-assembled monolayers: The molecular basis for nonfouling behavior. *J. Phys. Chem. B* (2005). doi:10.1021/jp0473321

67. Shen, M. & Horbett, T. A. The effects of surface chemistry and adsorbed proteins on monocyte/macrophage adhesion to chemically modified polystyrene surfaces. *J. Biomed. Mater. Res.* (2001). doi:10.1002/1097-4636(20011205)57:3<336::AID-JBM1176>3.0.CO;2-E

68. Gombotz, W. R., Guanghui, W., Horbett, T. A. & Hoffman, A. S. Protein adsorption to poly(ethylene oxide) surfaces. *J. Biomed. Mater. Res.* (1991). doi:10.1002/jbm.820251211

69. Ferrari, S. & Ratner, B. D. ToF-SIMS quantification of albumin adsorbed on plasma-deposited fluoropolymers by partial least-squares regression. *Surf. Interface Anal.* (2000). doi:10.1002/1096-9918(200012)29:12<837::AID-SIA937>3.0.CO;2-O

70. Wagner, M. S., McArthur, S. L., Shen, M., Horbett, T. A. & Castner, D. G. Limits of detection for time of flight secondary ion mass spectrometry (ToF-SIMS) and X-ray photoelectron spectroscopy (XPS): Detection of low amounts of adsorbed protein. *J. Biomater. Sci. Polym. Ed.* (2002). doi:10.1163/156856202320253938

71. Tidwell, C. D. *et al.* Static time-of-flight secondary ion mass spectrometry and x-ray photoelectron spectroscopy characterization of adsorbed albumin and fibronectin films. *Surf. Interface Anal.* (2001). doi:10.1002/sia.1101

72. Baio, J. E., Cheng, F., Ratner, D. M., Stayton, P. S. & Castner, D. G. Probing orientation of immobilized humanized anti-lysozyme variable fragment by time-of-flight secondary-ion mass spectrometry. *J. Biomed. Mater. Res. - Part A* (2011). doi:10.1002/jbm.a.33025

73. Nakanishi, K., Sakiyama, T. & Imamura, K. On the adsorption of proteins on solid surfaces, a common but very complicated phenomenon. *Journal of Bioscience and Bioengineering* (2001). doi:10.1016/S1389-1723(01)80127-4

74. Favia, P., Perez-Luna, V. H., Boland, T., Castner, D. G. & Ratner, B. D. Surface chemical composition and fibrinogen adsorption-retention of fluoropolymer films deposited from an RF glow discharge. *Plasmas Polym.* (1996). doi:10.1007/BF02532828

75. Khalifehzadeh, R., Ciridon, W. & Ratner, B. D. Surface fluorination of polylactide as a path to improve platelet associated hemocompatibility. *Acta Biomater.* (2018). doi:10.1016/j.actbio.2018.07.042

76. Dixit, N., Maloney, K. M. & Kalonia, D. S. Protein-silicone oil interactions: Comparative effect of nonionic surfactants on the interfacial behavior of a fusion protein. *Pharm. Res.* (2013). doi:10.1007/s11095-013-1028-1

77. Dixit, N., Maloney, K. M. & Kalonia, D. S. The effect of Tween® 20 on silicone oil-fusion protein interactions. *Int. J. Pharm.* (2012). doi:10.1016/j.ijpharm.2012.03.005

78. Sun, L. *et al.* Protein denaturation induced by cyclic silicone. *Biomaterials* (1997). doi:10.1016/S0142-9612(97)00105-1

79. Thirumangalathu, R. *et al.* Silicone oil- and agitation-induced aggregation of a monoclonal antibody in aqueous solution. *J. Pharm. Sci.* (2009). doi:10.1002/jps.21719

80. Li, J. *et al.* Mechanistic understanding of protein-silicone oil interactions. *Pharm. Res.* (2012). doi:10.1007/s11095-012-0696-6

81. Love, P. Guidance for Industry and FDA Staff : Early Development Considerations for Innovative Combination Products. *Fda* (2006).

82. Yoshino, K. *et al.* Functional evaluation and characterization of a newly developed silicone oil-free prefillable syringe system. *J. Pharm. Sci.* (2014). doi:10.1002/jps.23945

83. Kerwin, B. A. Polysorbates 20 and 80 used in the formulation of protein biotherapeutics: Structure and degradation pathways. *Journal of Pharmaceutical Sciences* (2008). doi:10.1002/jps.21190

APPENDIX A

IgG Protein Iodination Protocol

Materials:

Qty	Item
2	Biorad Econo-Pac 10DG chromatography columns
5	Falcon 2054 tubes w/ caps
86	gamma tubes & racks (2x40 for columns, 6 for activity standards)
5	plastic transfer pipets
4	50 ml centrifuge tubes for buffers
1	50 ml centrifuge tube for biowaste
1	15 ml centrifuge tube for NaCl/ICl mixture
1	15 ml centrifuge tube for protein solution
80	2 oz. sample cups
	100mg IgG from bovine serum (Sigma-Aldrich I5506-100MG)
	Iodine-125 radionuclide, 2mCi; Specific activity: ~17Ci/mg; Concentration: 100mCi/mL (Perkin Elmer NEZ033A002MC)
	ice from 3rd floor Foege
	latex and PP gloves
	lead pig
	0.02 M ICl solution (Foege 351C)
	P20 & P1000 "hot" Pipetmans
	50 & 1000 µl "hot" pipet tips

Prep (day before):

a) 50 mL– 2x Borate

100 mL	
Chemical	**Amt. in grams**
NaCl	1.87
H_3BO_3	2.47
pH to 7.75	

b) 50 ml – 2M NaCl

100 mL	
Chemical	**Amt. in grams**
NaCl	11.70

c) 1L – 1X cPBSz

1L of 10x	
Chemical	**nt. in grams**
NaCl	70.08
citric acid, monohydrate	21.02
Na phosphate, monobasic	13.80
pH to 6.93 using approx. 15.75 g solid NaOH Add azide to solution after pHing.	
Na azide	2.00
A 1:10 dilution yields 1X CPBSz at pH=7.4	

Prep (day of):

a) Degas 1x cPBSz for ~ 1hr
b) Get ice from 3rd floor Foege
c) Place degassed 1X cPBSz over ice.

Iodination:

1. Make 1ml of 10 mg/mL bovine IgG w/ 1X cPBSz and store in 15ml centrifuge tube: weigh out 10 mg bovine IgG, place in 1.5ml centrifuge tube, add 1 mL 1X cPBSz and place in water bath until dissolved

2. Make ICl/NaCl mixture: 1ml 2M NaCl + 6.67 µl 0.02M stock ICl (2:1 ratio)

3. Fill radioactive ice bucket in the iodination hood

4. Prepare the following 3 falcon 2054 tubes and place on ice.

   TUBE 1……. 0.5 ml of 2X Borate

   TUBE 2……. 0.5 ml of ICl/NaCl mixture

   TUBE 3……. 0.5 ml of 10mg/ml bovine IgG in 1X cPBSz

5. Calculate volume of ^{125}I to give activity of 1mCi. Original solution is 100mCi/ml on reference date.

   Decay factor = exp (-0.01153 x ___ days) = _____

   1mCi = 10 µl/decay factor = _____ µl ^{125}I to add.

6. Add ^{125}I to 0.5ml 2X borate (**TUBE 1**) using hot pipet. Place pipet tip into empty waste container.

   NOTE: Never take objects through the arm holes of the iodination hood as this will lead to contamination of the arm holes.

7. Add ICl/NaCl mixture to 2X borate (**TUBE 2 to TUBE 1**) using transfer pipet and re-pipet gently to mix. Place used pipet into the waste container.

8. Add 0.5 ml of 10mg/ml bovine IgG to 2X borate (**TUBE 3 to TUBE 1**).

   NOTE: Be careful not to create any bubbles as this can denature the protein.

9. Keep TUBE 1 on ice for 20 mins to allow for protein labeling reaction. ^{125}I binds to the tyrosine amino acid residues in the protein.

10. During the 20 minute waiting period

    a) place 40 cups into rotating fractionation table. 40 cups allows one to capture the labeled protein peak and the unlabeled free iodine peak, both are useful to evaluate iodination efficiency.

    b) set up gamma tubes for 2 columns and activity standards

11. Take cap off 1st column, pour off excess buffer and fill w/ cPBSz buffer to rinse. Repeat twice.

12. Once the column has stopped dripping the excess rinse buffer, align the colmn with the first cup and add 1.5ml labeled protein to column along the side. Be careful to avoid creating bubbles. Let protein drip through advancing the table after 0.5ml has been collected in each cup (~10 drops/cup). NOTE: Do NOT add buffer until all protein solution has passed into the column.

13. Once drops stop, add cPBSz to the column; collect 0.5ml in each cup, advance table, and repeat until 40 fractions have been collected. NOTE: Be sure to maintain the height of the cPBSz within the column to maintain constant pressure.

14. Take 5µl samples from each of the 40 cups collected from column 1 and count for 0.1 min to identify protein and iodine peaks.

15. Drain and rinse 2nd column with cPBSz.

16. Pool samples from protein peaks (3-4 cups) and run through the second column repeating fraction collection and peak identification (steps 12-14).

17. Collect purified labeled protein (~3 cups) and run six 5µl activity standards for 0.1 min counts.

    Activity = $\frac{\text{(Ave \# counts for 0.1 min.) x 10}}{(5\times10^{-3}\ \text{ml})}$ = _____ cpm/ml

18. Aliquot labeled protein (if necessary), place in lead pig, and freeze in -80ºC freezer.

19. Dispose of all radioactive waste in LSA box or liquid waste bucket, and complete radiation survey of lab.

APPENDIX B

^{125}I-IgG Protein Adsorption Protocol

Materials:

Qty	Item
# samples	2oz. PS cups and racks
	buffer chemicals
# samples + 6	gamma tubes and racks
	250 mL PS bottle or 50 mL centrifuge tube
	50µl 1000µl pipet tips
	iodinated protein
	aluminum foil
	latex and PP gloves
	lead apron
	safety glasses
	lab coat
	P50 & P1000 "hot" Pipetman
	P1000 Pipetman
	timer

Prep (day before):

a) 4L 1X cPBSzI

4L of 1x	
Chemical	**Amt. in grams**
NaCl	25.72
NaI	6.00
citric acid, monohydrate	8.41
Na phosphate, monobasic	5.52
pH to 7.4 using approx. 6.3 g solid NaOH. Add azide to solution after pHing.	
Na azide	0.80

Prep (day of):

a) Degas 1L of 1X cPBSzI for a minimum of 2 hours

b) Get ice from 3rd floor Foege

c) Presoak samples for 2 hrs in 0.75ml degassed buffer. Cover samples with aluminum foil.

Protein Adsorption:

1. Thaw iodinated protein in hood in Foege 351C 30 mins to an hour before the adsorption.
2. Fill rinse system with 3L 1X CPBSzI and check that it is working properly.
3. Prepare 2x IgG w/ degassed 1X cPBSI in 50ml centrifuge tube. Rock gently to mix:

   (# of samples)(0.75ml/sample) = _____ ml of 2x protein to make

   NOTE: round up number; must account for 0.6 mL for two sets of activity standards

4. Calculate minimum signal needed from standards:

   (CPM desired)/(ng protein)(2x protein concentration, mg/mL)(Standard volume, uL)(1000) = (**minimum CPM needed)** for adequate sample measurement.

5. Calculate the amount of iodinated protein to add:

   (mL of 2x protein)(mg/mL of 2x protein)(CPM/ng desired)(10^6 ng/mg)/ (CPM/mL from iodination standards) = _____ **mL of hot protein to add**

6. Add iodinated protein to 2x protein in cPBSzI buffer and mix gently
7. Take ten 10 µl activity standards of "hot" 2x protein and count for 1 min.

   NOTE: If large variability, repeat activity standards.

   If not hot enough, based on calculations from step 3, calculate the necessary amount of iodinated protein to add, add it to the 2x protein, and repeat the activity standards.

8. Start timer and add 0.75ml of "hot" 2x protein to the first sample. Reaspirate 3 times to insure adequate mixing. Do subsequent samples at 1 minute intervals until all samples are completed.

   NOTE: Change pipet tips between samples

9. During the adsorption period, set up gamma tubes and racks.
10. Wait until 2 hours have expired since first sample was started, and rinse each sample at the same time interval of 1 minute as the "hot" protein solution was added.

    Rinse in three steps: 1st rinse of 6 secs for hot rinse [1-2-3-4-5-6], and

    2nd and 3rd rinse of 3 secs for cold rinse [1-2-3-1-2-3].

NOTE: 1st rinse goes into the radioactive liquid waste bucket. 2nd and 3rd rinse is poured down the sink and flushed with lots of water.

11. Each sample is placed in an individual gamma counter tube and counted for 10 minutes each. Standards are placed at the front and back of the samples.

12. Dispose of all radioactive waste in LSA box or liquid waste bucket and record waste values on sheets.

13. Complete radiation survey of lab and sign log-book.

VITA

Marvin Magan Mecwan was born in Dubai, United Arab Emirates on October 5th, 1987 to Indian expatriate parents Magan Madhav Mecwan and Selvarani Nagamani Magan Mecwan. Marvin's interest in scientific inquiry began in elementary school and was solidified in high school when he learned about xenografts and regenerative medicine. Soon after high school, he moved to the United States in May 2007 to pursue his higher education. Marvin earned his BS with honors in biomedical engineering and mathematics at the University of Memphis in May 2010 and continued to pursue his MS in biomedical engineering at the University of Tennessee Health Science Center under the mentorship of Dr. Joel Bumgardner where he studied chitosan based 3D scaffolds for bone tissue engineering. In the fall of 2012 he joined the bioengineering PhD program at the University of Washington and worked under the tutelage of Dr. Buddy Ratner. While there his research focused on non-fouling surfaces and materials and their use in clinical as well as industrial applications. Marvin earned his PhD in August 2019 and now plans to begin a career as a scientific researcher in the field. His current research interests lie at the interface of biology, medicine, materials science and tissue engineering, specifically with regard to improving host-biomaterial cell and tissue interaction.